



SAPIENZA
UNIVERSITÀ DI ROMA

Facoltà di Scienze Matematiche Fisiche e Naturali
Corso di Dottorato di Ricerca in Scienze Chimiche
XXIII Ciclo

***Oxidoreductases-based electrochemical biosensors:
general aspects, characterisation and applications***

PhD Student: Massimo Di Fusco

Supervisor: Prof. F. Mazzei

ID number: 694781

Coexaminer: Prof. T. Ferri

Anno Accademico 2009/2010

“...non ci si deve arrendere alla materia incomprensibile, non ci si deve sedere. Siamo qui per questo, per sbagliare e correggerci, per incassare colpi e renderli. Non ci si deve mai sentire disarmati: la natura è immensa e complessa, ma non è impermeabile all’intelligenza; devi girarle intorno, pungere, sondare, cercare il varco o fartelo”

Primo Levi, “Il sistema periodico”

Index

Preface	1
Chapter 1	
Biosensors	
1.1 General Features.....	2
1.2 Amperometric Biosensors.....	4
1.3 Enzyme Immobilization Techniques.....	9
1.4 Electrochemical Mediators.....	12
Chapter 2	
Characterization of a Polyazetidine Polymer Film	
2.1 Introduction.....	16
2.2 Experimental Section.....	20
2.2.1 Materials.....	20
2.2.2 Apparatus.....	20
2.2.3 Preparation of Polyazetidine-Coated Electrodes.....	21
2.2.4 Measurement of Diffusion Coefficients and Standard Heterogeneous Rate Constants.....	21
2.3 Results and Discussion.....	22
2.3.1 Theoretical Background.....	22
2.3.2 Determination at Different Temperatures of Diffusion Coefficient and Electron Exchange Constant Using Naked Microelectrode.....	25
2.3.3 Determination at Different Temperatures of Diffusion Coefficient and Electron Exchange Constant Using PAP-Covered Microelectrode.....	30
2.3.4 Calculation of Activation Energies for Diffusion and Heterogeneous Electron Exchange.....	37
2.4 Conclusions.....	40
Chapter 3	
Electrokinetic Characterisation of Different Laccases	
3.1 Introduction.....	41

3.1.1 Laccases.....	41
3.1.2 Laccase Structure and Catalytic Mechanism.....	43
3.1.3 Laccases Applications.....	48
3.2 Experimental Section.....	52
3.2.1 Materials.....	52
3.2.2 Apparatus.....	53
3.2.3 Electrochemical Measurements with Laccase from <i>Lentinus edodes</i> and <i>Panus tigrinus</i>	53
3.2.4 Electrochemical Measurements with Laccase from <i>Trametes versicolor</i> and <i>Trametes hirsuta</i>	54
3.3 Results and Discussion.....	55
3.3.1 Laccases from <i>Panus tigrinus</i> and <i>Lentinus edodes</i>	55
3.3.2 Laccases from <i>Trametes versicolor</i> and <i>Trametes hirsuta</i>	62
3.4 Conclusions.....	68

Chapter 4

Electrokinetic Characterisation of Amine Oxidase from *Lathyrus sativus* (LSAO)

4.1 Introduction.....	69
4.1.1 Amine Oxidases.....	69
4.1.2 Amine Oxidases Structure and Catalytic Mechanism	71
4.2 Experimental Section.....	80
4.2.1 Materials.....	80
4.2.2 Apparatus.....	81
3.2.3 Electrochemical Measurements with Amine Oxidase from <i>Lathyrus sativus</i> (LSAO).....	81
4.3 Results and Discussion.....	82
4.4 Conclusions.....	88

Chapter 5

Development of Laccase-Based Biosensors for Real Samples Analysis

5.1 Introduction.....	89
5.2 Experimental Section.....	95

5.2.1 Materials.....	95
5.2.2 Apparatus.....	96
5.2.3 Biosensors Preparation	96
5.2.4 Polyphenol Content by Folin-Ciocalteu Method	97
5.2.5 Electrochemical Measurements.....	98
5.3 Results and Discussion.....	99
5.3.1 Laccase-Based Biosensor for the Determination of Polyphenols in Wine.....	99
5.3.2 Laccase-Based Biosensor for the Determination of Catecholamines in Pharmaceutical Preparations	108
5.4 Conclusions.....	111

Chapter 6

Development of a LSAO-Based Biosensor for the Detection of Biogenic Amines in Real Samples

6.1 Introduction.....	112
6.2 Experimental Section.....	116
6.2.1 Materials.....	116
6.2.2 Apparatus.....	116
6.2.3 Biosensors Preparation	117
6.2.4 Biogenic Amines Content by GC-MS.....	117
6.2.5 Electrochemical Measurements.....	118
6.3 Results and Discussion.....	119
6.4 Conclusions.....	123

Chapter 7

Soft Landed Modified Electrodes

7.1 Introduction.....	124
7.2 Experimental Section.....	129
7.2.1 Materials.....	129
7.2.2 Synthesis of Ferrocene Derivatives	129
7.2.3 Apparatus.....	131
7.2.4 Soft Landing Experiments	132

7.2.5 Electrochemical Measurements.....	132
7.3 Results and Discussion.....	133
7.4 Conclusions.....	144

Preface

Part of this research project was integrated in an European project denominated BIO-MEDNANO that had as goal the study of enzymes, mediators and nanostructures to provide bio-powered bio-electrochemical sensing systems. In this contest the aim of my work was to perform a set of experiments focused on the characterisation of redox enzymes and their mediators, as well as to evaluate different immobilisation procedures and different electrodic materials with the purpose to develop electrochemical biosensors.

In particular, in this PhD work, the development of first and second-generation biosensors, having analytical applications in various sectors, with particular regard to health and food quality monitoring, were taken into account. To reach this goal, a bioelectrochemical study of redox enzymes (Laccases and Amino Oxidases), to test their ability in the catalytic transformation of their substrates and on their use as biological materials in biosensing, were performed. In addition, the possible use of polyazetidine prepolymer as a tool for redox enzymes immobilisation, suitable for electron transfer, was taken into account.

Once selected the target enzymes and evaluated their bioelectrochemical properties in the immobilised form within PAP structure, different biosensors were constructed, optimised, characterised and used in the detection of either polyphenols (Laccase biosensor) or biogenic amines (Amino Oxidase biosensor) in real samples.

Finally, in view of a possible development of innovative biosensing devices or biochips an elegant modification procedure for electrodic surfaces, was studied. In particular, this new immobilisation procedure of custom-synthesised redox mediators, leads to chemically modified electrodes namely Soft Landed Modified Electrodes (SLaME), whose performances and stability were studied thoroughly.

Chapter 1

Biosensors

1.1 General Features

A biosensor is defined by the International Union of Pure and Applied Chemistry (IUPAC)¹ as a device that uses specific biochemical reactions mediated by isolated enzymes, immunosystems, tissues, organelles or whole cells to detect chemical compounds usually by electrical, thermal or optical signals. This system can be schematised as in Figure 1.1.

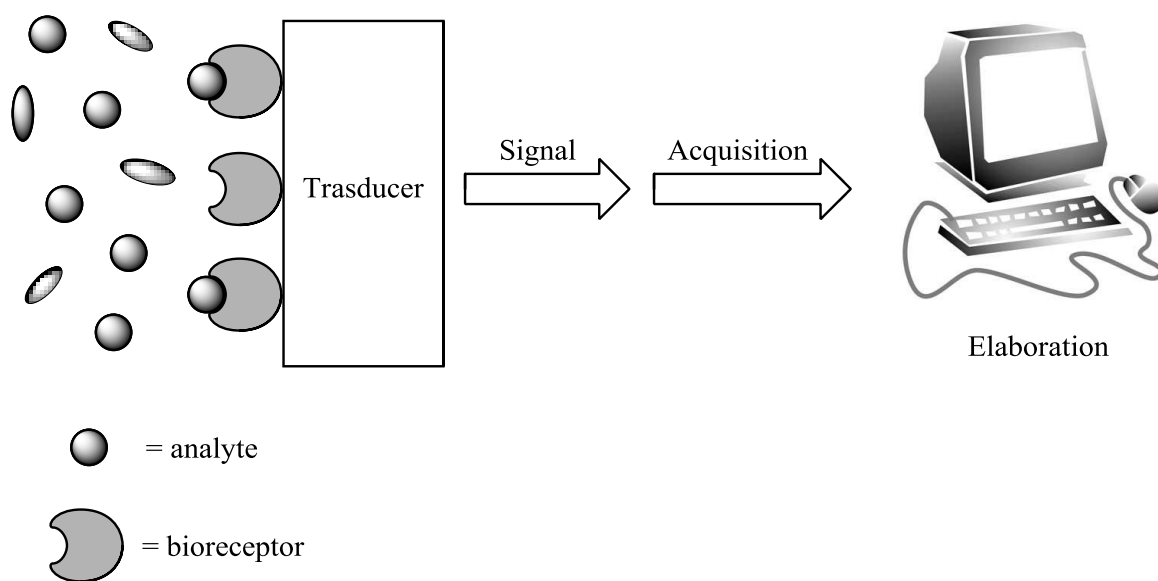


Figure 1.1 Main components of a biosensor.

¹ Nagel B., Dellwe H., Gierasch L. M. *Pure Appl. Chem.* **1992**, *64*, 143-168.

Nowadays there is an increasingly interest in improving those aspects affecting the quality of life that are closely connected to disease and environmental monitoring,² such as safety and quality of foodstuffs.³ In all these fields, continuous, fast and sensitive detection of chemical species playing the role of key parameters is required. The biosensors, combining a biological recognition element and a transducer, are very promising tools and play an increasingly important role in this context.⁴

The biological recognition element of a biosensor interacts selectively with the target analyte, thus ensuring the selectivity of the sensor. These items can be classified into two main categories: biocatalysts, such as enzymes, microorganisms, tissue or whole cells, and bioreceptors materials, such as antibodies or nucleic acids (DNA or aptamers).

Often, commercially available enzymes are used since they have the great advantage of being widely characterised in their biocatalytic properties and to be readily available . The disadvantages are that these proteins are not always sufficiently pure and often require the presence of cofactors to optimally perform their catalytic activity.

In some cases, the use of microorganisms and plant or animal tissues, has proven to be an excellent alternative to create a measurement system that has comparable and, in some cases, better features than those of enzymatic biosensors,⁵ not only because the enzyme is in its natural environment in the presence of its cofactors, but also because sometimes it is possibly to employ complex enzymatic patterns intrinsic of the whole cell.

On the other hand, as far as the use of bioreceptors is concerned, antigen-antibody reactions are generally exploited and the signal produced by the immunologic interaction

² (a) Munkittrick K. R., Arens C. J., Lowell R. B., Kaminski G. P. *Environ. Tox. Chem.* **2009**, 28, 1361-1371; (b) Jixin Q., Xiaolin H., Manuel M., Per R. *Anal. Chim. Acta* **2009**, 652, 66-84.

³ (a) Nicole B., Mark B., Michael R. *Sensors and Actuators, B: Chemical* **2006**, B114, 482-488; (b) Sheridan C., O'Farrell M., Lewis E., Lyons W. B., Flanagan C., Jackman N. *Measur. Sci. Technol.* **2006**, 17, 229-234.

⁴ (a) Jahir O., Cesar F.-S., Cecilia J.-J. *Sensors* **2010**, 10, 475-490; (b) Gayathri S., Braganca J. M. *Environmental Science: An Indian Journal* **2009**, 4, 297-305.

⁵ (a) Tag C., Hahn T., Riedel K., Kunze G. *Biosens. Bioassays Based Microorg.* **2006**, 211-228; (b) Bjerketorp J., Hakansson S., Belkin S., Jansson J. K. *Cur. Op. Biotechnol.* **2006**, 17, 43-49.

can be detected either by mass-sensitive systems or by “marking” the antigen or the antibody with an enzyme that catalyses the production of a chemical species detectable with other systems, such as optical and electrochemical.⁶ In this case the specificity of the method is usually very high being related to antigen-antibody reaction, while the sensitivity is not easily predictable since it is due to the affinity of the target molecule with the bioreceptor or to the enzymatic reaction that allows the detection of the signal.

The transducer converts the biological response, resulting from the interaction with the analyte, in a measurable signal and affects the sensitivity of the biosensor. These devices are typically of electrochemical, optical, thermal and piezoelectric type. Despite of the extremely large number of possible combinations between different types of bio-recognition elements and transducers, the coupling between the transducer and the biological element forming a self-consisting device, even if highly desirable it is limited to only a some cases.

Among all the different combinations, the most successful one is probably represented by the enzymatic electrochemical biosensors, that can be of amperometric,⁷ voltammetric,⁸ impedimetric⁹ and potentiometric type.¹⁰

1.2 Amperometric Biosensors

The most widely used biosensors are the amperometric ones,¹¹ which are based on the use of enzymes that catalyse redox reactions. These biosensors, according to the pathway

⁶ (a) Pohanka M., Skladal P. *J. Appl. Biomed.* **2008**, *6*, 57-64; (b) Yu H., Yan F., Dai Z., Ju H. *Anal. Biochem.* **2004**, *331*, 98-105; (c) Lu B., Iwuoha E., Smyth M. R., O’Kennedy R. *Anal. Chim. Acta* **1997**, *345*, 59-66; (d) Deasy B., Dempsey E., Smyth M. R., Egan D., Bogan D., O’Kennedy R. *Anal. Chim. Acta* **1994**, *294*, 291-297; (e) Baldrich E., Munoz F. X. *Analyst (Cambridge, UK)* **2008**, *133*, 1009-1012.

⁷ Mamas I. P., Miltiades I. K. *Electroanalysis* **2002**, *14*, 241-261.

⁸ Zhang D., Zhao J., Li G. *Protein Pept. Lett.* **2008**, *15*, 764-771.

⁹ Guan J.-C., Miao Y.-Q., Zhang Q.-J. *J. Biosc. Bioeng.* **2004**, *97*, 219-226.

¹⁰ Koncki R. *Anal. Chim. Acta* **2007**, *599*, 7-15.

¹¹ (a) Mraz B., Abel P. U. *Encyclopedia of Sensors* **2006**, *1*, 169-194; (b) Chen H.-Y., Xu J.-J. *Encyclopedia of Sensors* **2006**, *1*, 145-167; (c) Zayats M., Willner B., Willner I. *Electroanalysis* **2008**, *20*, 583-601; (d) Belluzo M. S., Ribone M. E., Lagier C. M. *Sensors* **2008**, *8*, 1366-1399.

followed by electrons in the functioning scheme, can be classified into first, second and third generation biosensors.

The first generation electrochemical biosensors, consist only of the enzyme and the transducer that measures the electrical discharge of a redox compound belonging to the natural scheme of enzymatic reaction. Namely, with these devices the electrochemical signal, related either to the formation or the consumption of one among the substrate, the product and the cofactor of an enzymatic reaction, is monitored. An Oxidase-based biosensor, where the measurement relies on the decrease of oxygen or the appearance of hydrogen peroxide, is a typical example of first-generation biosensor (Figure 1.2). The most common Oxidase enzyme type used in biosensing, is the Glucose Oxidase (GOx).¹² The catalytic activity of this enzyme is expressed by the oxidation of glucose and the simultaneous transition of the enzyme in its inactive reduced state. Subsequently, the enzyme returns to the active oxidised state by transferring electrons to molecular oxygen, resulting in the production of hydrogen peroxide. The course of the reaction may be followed by determining electrochemically the consumption of oxygen or the production of hydrogen peroxide.

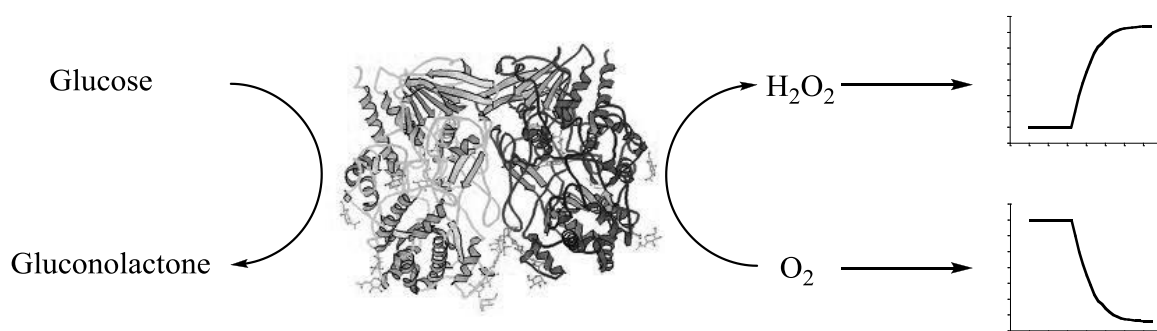


Figure 1.2 Schematic representation of a first generation biosensor that uses Glucose Oxidase (GOx) as biorecognition element.

¹² (a) Perez J. P. H., Lopez-Cabarcos E., Lopez-Ruiz B. *Talanta* **2010**, *81*, 1197-1202; (b) German N., Ramanaviciene A., Voronovic J., Ramanavicius A. *Microchimica Acta* **2010**, *168*, 221-229; (c) Guascito M. R., Malitesta C., Mazzotta E., Turco A. *Sensor Letters* **2009**, *7*, 153-159.

The current response is proportional to the concentration of the substrate in a given range so that is possible to determine the concentration of glucose in a solution. In the case of the systems based on the measurement of H_2O_2 produced, by means of its oxidation onto a Pt anode, the main disadvantage is the high applied voltage (generally 700 mV vs Ag/AgCl/ Cl^-) which could lead to the simultaneous discharge of oxidisable interfering compounds eventually present in the measuring solution. Conversely, in the case of the systems based on the measurement of O_2 consumption that involves the use of a Clark electrode, a variation of the amount of oxygen ascribable to microorganisms or convection in the buffer solution used for the measurement can be a limiting factor. In addition, this electrode has a limited sensitivity and operating range, because it is unable to detect oxygen concentration below a certain value.

Another example of first-generation biosensor is a device based on a Dehydrogenase enzyme type, for example the Alcohol Dehydrogenase (ADH).¹³ This enzyme catalyses the oxidation of an alcohol (ethanol) with the use of a cofactor, the NAD^+ , with the formation of the product (acetaldehyde) and NADH (Figure 1.3). In this case it is possible to measure the production of NADH or the disappearance of NAD^+ .

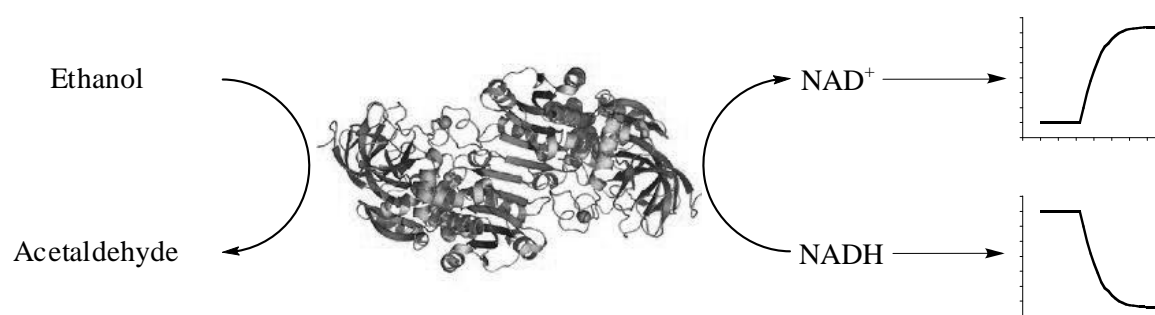


Figure 1.3 Schematic representation of a first generation biosensor that uses Alcohol Dehydrogenase (ADH) as biorecognition element.

¹³ (a) Wang J., Liu J. *Anal. Chim. Acta* **1993**, 284, 385-91; (b) Jiang X., Zhu L., Yang D., Mao X., Wu Y. *Electroanalysis* **2009**, 21, 1617-1623.

Even in this case there are significant disadvantages, such as very high potential required for the discharge of NADH and the need to modify the working electrode. In fact, the oxidation of NADH with the most common used electrodic materials produces a remarkable fouling, so that a chemical manipulation of the electrode surface is needed to achieve a stable electrochemical signal.¹⁴

In the second-generation biosensors the natural co-substrate is replaced by special redox compounds, called mediators, which have a redox potential adequate to regenerate the active state of the redox enzyme. This type of exchange is defined Mediated Electron Transfer (MET).

The medium in which the measurements are carried out must ensure the free diffusion of the mediator between the electrode and the enzyme, to allow its electrochemical regeneration (Figure 1.4).

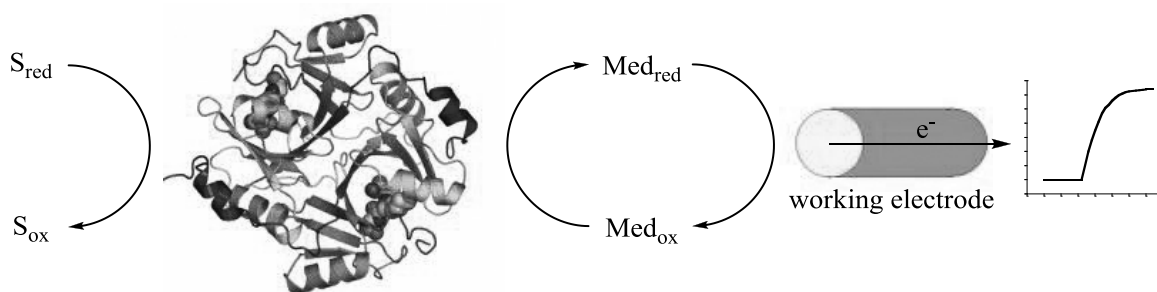


Figure 1.4 Schematic representation of the Mediated Electron Transfer (MET).

The redox potential of the mediator is extremely important because it is one factor that determines the choice of the potential applied to the electrode surface for the measurement allowing to operate at a potential value where the possible electrochemical interferences can be reduced or become completely negligible.

¹⁴ Tangkuaram T., Wang J., Rodriguez M. C., Laocharoensuk R., Veerasai W. *Sensors and Actuators, B: Chemical* **2007**, *B121*, 277-281.

Finally, the third-generation biosensors are characterised by the direct coupling between the electrode surface and the active site of the enzyme, therefore there is a Direct Electron Transfer (DET) between enzyme and electrode. In this case, since either mediator and any cofactor and cosubstrate are absent, the applied working potential is that of enzyme (Figure 1.5).

The third-generation biosensors have been developed in the recent years, but their use is limited only to certain proteins, for example several heme proteins, such as Horseradish Peroxidase (HRP).¹⁵ In fact, not all the enzymes are capable of transferring electrons directly to the electrode surface without denaturing and in this context plays a key role the orientation and the exposure of the active site.

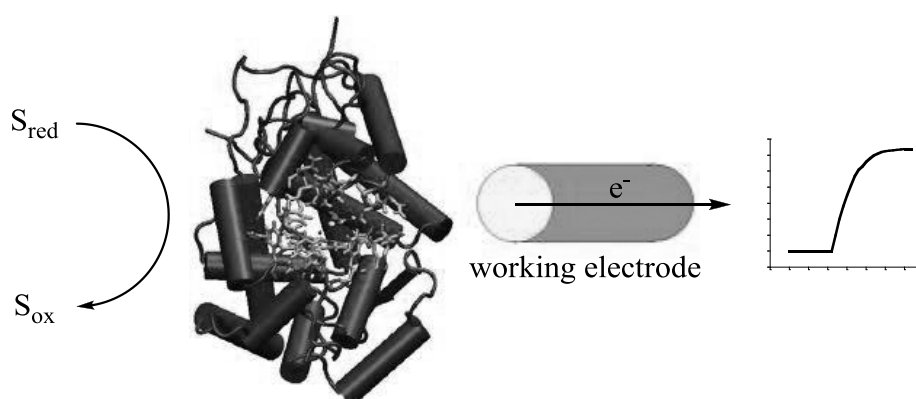


Figure 1.5 Schematic representation of the Direct Electron Transfer (DET).

Summarising, over the past years, three generation of biosensors have been developed and in Figure 1.6 is showed a summary scheme of the various types of amperometric biosensors.

¹⁵ (a) Zhou K., Zhu Y., Yang X., Luo J., Li C., Luan S. *Electrochim. Acta* **2010**, *55*, 3055-3060; (b) Teng Y. J., Zuo S. H., Lan M. B. *Biosens. Bioelectron.* **2009**, *24*, 1353-1357; (c) Wang B., Zhang J.-J., Pan Z.-Y., Tao X.-Q., Wang H.-S. *Biosens. Bioelectron.* **2009**, *24*, 1141-1145.

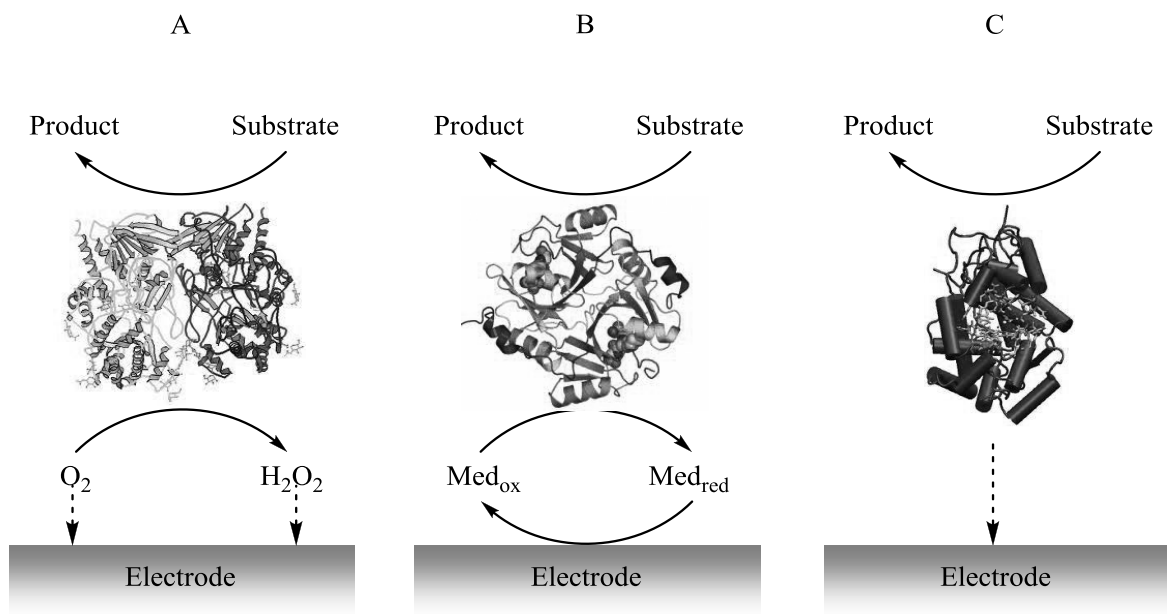


Figure 1.6 Summary scheme of the three generations of amperometric biosensors: first-generation (A) second-generation (B) and third-generation (C) biosensor.

1.3 Enzyme Immobilisation Techniques

In the construction of an electrochemical biosensor, the molecular recognition of the target analyte is ensured not only by a suitable choice of the biocatalytic material but also by a proper immobilisation of the latter on the transducer.

The immobilisation of the enzymatic material on the electrode surface produces a stability increase, an improving in the kinetic parameters, as well as economic advantages since it allows to perform multiple determinations with the same device without loss of performance using the same small amount of enzyme.¹⁶

Over the years, various immobilisation procedures have been developed for the construction of enzymatic biosensors that can be grouped in two main categories: physical and chemical immobilisation.

The physical entrapment can be either in or behind a membrane and this method has the advantage that it involves a minimal risk of loss of the catalytic activity, since it is not

¹⁶ Miletic N., Bos C., Loos K. *Polym. Mat.* **2009**, 131-153.

implied any kind of chemical linkage and consequently any disruption of enzymatic structure, but it has the limit to determine a weak interaction between the enzyme and the immobilising matrix, thus provoking the leakage of the protein and a little lifetime of the biosensor. This kind of immobilisation can be made in several ways: i) adsorption on solid supports; ii) entrapment within natural or synthetic gels; iii) micro-encapsulation into semipermeable polymers.

The physical immobilisation procedures most commonly used rely on the use of substances such as starch,¹⁷ polyacrylamide gel,¹⁸ dialysis membranes¹⁹ and acetyl cellulose²⁰ (Figure 1.7).

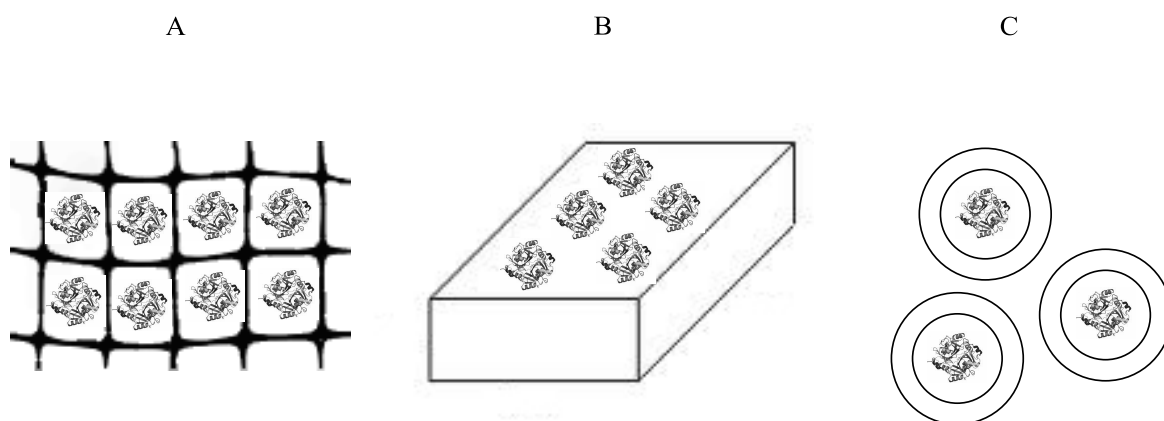


Figure 1.7 Physical immobilisation techniques: entrapment (A), adsorption (B) and microencapsulation (C).

On the other hand, the chemical immobilisation procedures exploit chemical reactions involving functional groups present in the enzyme protein (such as α - and ϵ -amino groups, β - and γ -carboxyl groups, the sulfhydryl group of cysteine and the histidine imidazole

¹⁷ Chen H., Liu L., Lv S., Liu X., Wang M., Song A., Jia X. *Appl. Biochem. Biotechnol.* **2010**, *162*, 24-32.

¹⁸ Tang J., Xiao P. *Biosens. Bioelectron.* **2009**, *24*, 1817-1824.

¹⁹ Hwang S., Cha W., Meyerhoff M. E. *Electroanalysis* **2008**, *20*, 270-279.

²⁰ Ren X., Chen D., Meng X., Tang F., Du A., Zhang L. *Colloids and Surfaces, B: Biointerfaces* **2009**, *72*, 188-192.

group). This immobilisation can occur through: i) covalent bond; ii) cross-linking bonds (Figure 1.8).

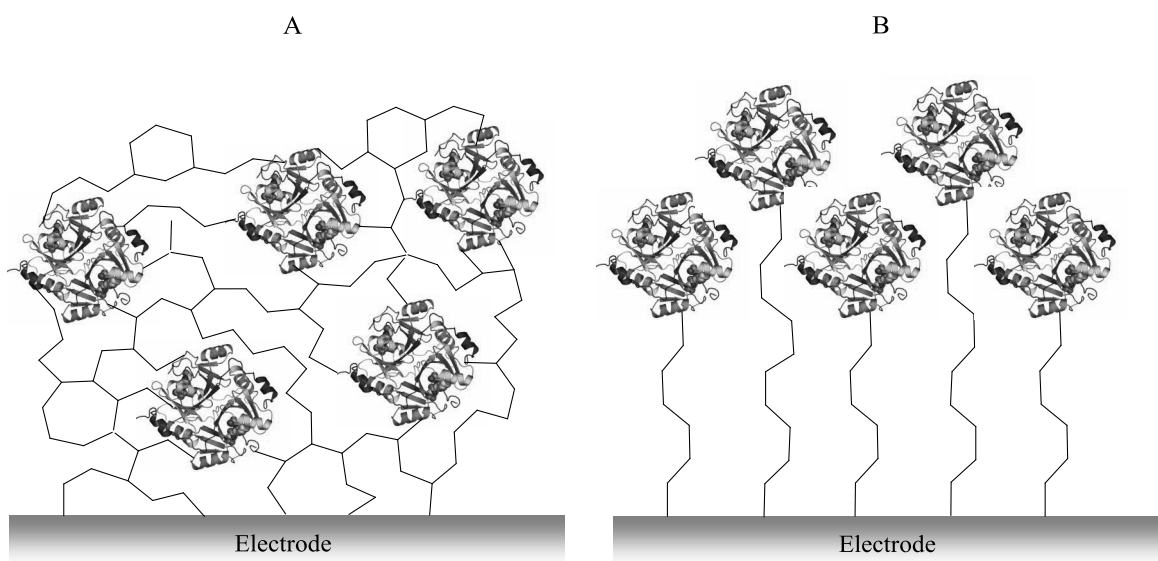


Figure 1.8 Chemical immobilisation techniques: cross-linking (A) and covalent bond (B).

Both the cross-linking strategy and the covalent bond formation can be employed to chemically immobilise enzymes onto either the electrodic surface or a suitable membrane to be overlapped on the electrode. Some examples of materials for supporting membranes used for the chemical immobilisation are nylon,²¹ cellulose²² and collagen.²³

A very versatile and extremely popular method, used to covalently bind molecules to a surface, involves the use of 1-ethyl-3-(3-dimethylaminopropyl) carbodiimide (EDC).²⁴ The EDC generates intermediate reactive carboxylic groups (eventually present) which can then react with appropriate nucleophiles (for example the amino groups of proteins). Since the intermediate in aqueous solution is very reactive, because of the hydrolysis of water, it is needed the presence of a competitive nucleophile. This shortcoming is overcome by using a mixture of EDC and *N*-hydroxysuccinimide (NHS), which generates an active ester derivative that retains its stability for longer time.

²¹ Caldwell S. R., Raushel F. M. *Appl. Biochem. Biotechnol.* **1991**, *31*, 59-73.

²² Pithawala K. A., Bahadur A. *Cellulose Chem. Technol.* **2003**, *36*, 265-273.

²³ Zong S., Cao Y., Ju H. *Anal. Lett.* **2007**, *40*, 1556-1568.

²⁴ Nien P.-C., Chen P.-Y., Ho K.-C. *Sensors* **2009**, *9*, 1794-1806.

Such chemical reactions can be carried out either on suitably modified polymeric membranes (e.g. nylon modified with carboxylic groups) or operating directly onto some electrodic materials such as pyrolytic graphite or after proper modification of the electrode surface with a Self Assembled Monolayer (SAM)²⁵. This latter strategy is often used to covalently bind enzymes onto gold electrode surface; the compounds most commonly used for this purpose are generally alkanethiols ending with a carboxyl group, such as the ω -mercaptopropionic acids (with $\omega = 3, 6, 11, \text{etc.}$), which react with the gold surface to form very strong Au-S bonds. Finally, the terminal carboxyl group is used to bind enzymes as described above with the mixture of EDC and NHS (Figure 1.9).

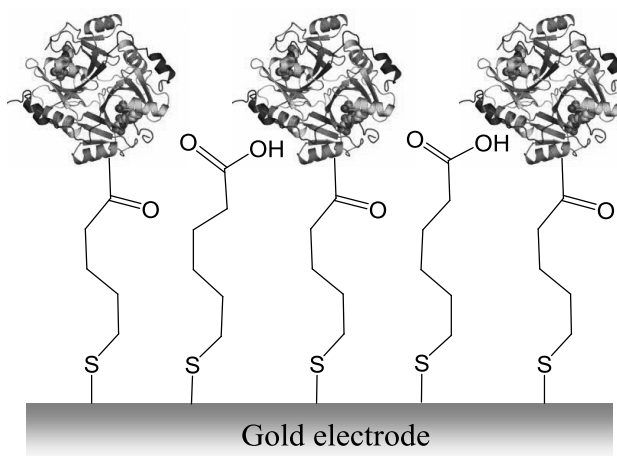


Figura 1.9 Schematisation of the enzyme immobilisation through the use of SAM.

1.4 Electrochemical Mediators

In the development of electrochemical biosensors, very often is required the presence of particular substances, called mediators, that are able to shuttle electrons between the electrode surface and the enzymatic active site, sometimes also increasing the redox

²⁵ Flink S., van Veggel F. C. J. M., Reinhoudt D. N. *Adv. Mat.* (Weinheim, Germany) **2000**, *12*, 1315-1328.

reaction rate. Really, a mediator is useful to facilitate an electronic transfer that, otherwise, would be kinetically disadvantaged.²⁶

As mentioned above, this kind of mechanism is defined Mediated Electron Transfer (MET).

A typical example is described above in Figure 1.4 for the oxidation of glucose by Glucose Oxidase. In this case M_{ox} and M_{red} are respectively the oxidised and the reduced form of the mediator and the production of M_{red} is estimated by amperometric measurement of the oxidation reaction that takes place at the electrode surface.

A good electrochemical mediator should fit the following features:

- it must be stable under the experimental conditions in its oxidised and reduced form;
- it must have a redox potential independent from pH to ensure reproducible measurements at a fix potential and lower than those of other electrochemically active substances present in the sample;
- it must be able to react rapidly with the enzyme;
- it must have a reversible heterogeneous kinetics.

For the development of second-generation biosensors, several organic compounds such as methylene blue,²⁷ phenazine,²⁸ prussian blue,²⁹ toluidine blue³⁰ have been extensively used; however, these compounds have some drawbacks, such as low stability and redox potential dependent on pH. On the other hand, the use of inorganic compounds is hindered because could be hard to modify their structure in order to modulate their solubility and redox potential. Other mediators used are ferrocene and its derivatives, which are among

²⁶ Brunetti B., Ugo P., Moretto L. M., Martin C. R. *J. Electroanal. Chem.* **2000**, *491*, 166-17.

²⁷ Zhang Y., Liu L., Xi F., Wu T., Lin X. *Electroanalysis* **2010**, *22*, 277-285.

²⁸ Pauliukaite R., Ghica M. E., Barsan M. M., Brett C. M. A. *Anal. Let.* **2010**, *43*, 1588-1608.

²⁹ Chu Z., Zhang Y., Dong X., Jin W., Xu N., Tiede B. *J. Mat. Chem.* **2010**, *20*, 7815-7820.

³⁰ Alpat S., Telefoncu A. *Sensors* **2010**, *10*, 748-764.

the most widely used substances for making stable biosensors.³¹ In fact, it has been demonstrated their great ability to transport the electronic charge from redox enzymes to the surface of the electrodes. These compounds have different interesting features that make them very suitable as mediators. For example, there are many ferrocene derivatives, thanks to the relative simplicity of their chemical synthesis, they have different solubility in various solvents and a standard redox potential that ranges between ca. -100 mV (decamethylferrocene) and ca. +700 mV (acetylferrocene) vs Ag/AgCl/Cl⁻. These compounds were tested with different redox enzymes of the class of the Oxidoreductases and showed good ability as electron donors.³²

Other typical redox mediators often used are tetracyanoquinodimethane (TCNQ),³³ 2,2,5,5-tetrathiofulvalene (TTF),³⁴ recognised as an alternative to ferrocene derivatives in the development of amperometric biosensors, conductors salts,³⁵ quinones³⁶ and ferricyanide,³⁷ one of the most common used inorganic mediator.

The electrochemical reaction of mediator regeneration occurs at its characteristic potential and, because its active redox state is reformed near the electrode surface, it hasn't to

³¹ (a) Colombari M., Ballarin B., Carpani I., Guadagnini L., Mignani A., Scavetta E., Tonelli D. *Electroanalysis* **2007**, *19*, 2321-2327; (b) Kajiya Y., Tsuda R., Yoneyama H. *J. Electroanal. Chem.* **1991**, *301*, 155-164; (c) Cass A. E. G., Davis G., Francis G. D., Hill H. A. O., Aston W. J., Higgins I. J., Plotkin E. V., Scott L. D. L., Turner A. P. F. *Anal. Chem.* **1984**, *56*, 667-671; (d) Turner A. P. F., Hendry S. P., Cardosi M. F. *The World Biotech. Report* **1987**, *1*, 125-137; (e) Luong J. H. T., Masson C., Brown R. S., Male K. B., Nguyen A. L. *Biosens. Bioelectron* **1994**, *9*, 577-584; (f) Hendry S. P., Cardosi M. F., Neuse E. W., Turner A. P. F. *Anal. Chim. Acta* **1995**, *281*, 453-459.

³² Frew J., Hill H. A. *Anal. Chem.* 1987, *59*, 933A-944A.

³³ (a) Dutra R. F., Moreira K. A., Oliveira M. I. P., Araujo A. N., Montenegro M. C. B. S., Filho J. L. L., Silva V. L. *Electroanalysis* **2005**, *17*, 701-705; (b) Cenas N. K., Kulys J. J. *J. Electroanal. Chem.* **1981**, *128*, 103-113; (c) Kulys J. J., Costa E. J. *Biosens. Bioelectron.* **1991**, *6*, 109-115; (d) Pandey P. C., Pandey V., Mehta S. *Indian. J. Chem.* **1993**, *32A*, 667-672; (e) Lima Filho J. L., Pandey P. C., Weetall H. H. *Biosens. Bioelectron.* **1996**, *11*, 719-723.

³⁴ (a) Bifulco L., Cammaroto C., Newman J. D., Turner A. P. F. *Anal. Let.* **1994**, *27*, 1443-52; (b) Murthy A. S. N., Anita *Biosens. Bioelectron.* **1996**, *11*, 191-193; (c) Palleschi G., Turner A. P. F. *Anal. Chim. Acta* **1990**, *234*, 459-463; (d) Mulchandani A., Bassi A. S., Nguyen A. *J. Food Sci.* **1995**, *60*, 74-78; (e) Qing J., Liu Y., Liu H., Yu T., Deng J. *Biosens. Bioelectron.* **1997**, *12*, 1213-1218.

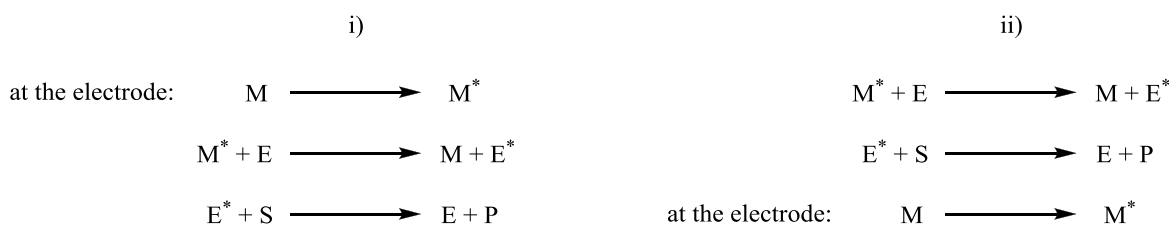
³⁵ (a) Pauliukaite R., Malinauskas A., Zhylyak G., Spichiger K., Ursula E. *Electroanalysis* **2007**, *19*, 2491-2498; (b) Ikeda T., Shibata T., Senda M. *J. Electroanal. Chem.* **1989**, *261*, 351-362; (c) Kulys J. J., Cenas N. K. *Biochem. Biophys. Acta* **1983**, *744*, 57-63; (d) Zhao S., Lennox K. B. *Anal. Chem.* **1991**, *63*, 1174-1187.

³⁶ Tseng T.-F., Yang Y.-L., Lin Y.-J., Lou S.-L. *Sensors* **2010**, *10*, 6347-6360.

³⁷ Saha S., Arya S. K., Singh S. P., Sreenivas K., Malhotra B. D., Gupta V. *Anal. Chim. Acta* **2009**, *653*, 212-216.

diffuse very far to shuttle electrons to the enzyme, provided that the latter is confined or immobilised onto the electrodic surface. Depending on this reaction, a current change, that can be put in relation with the concentration of the target analyte, is observed. However, since the electrochemical regeneration of the mediator is not specific, a special care must be taken to exclude that at the working potential other electroactive species could discharge at the electrode.

Mediated reactions can be divided into two categories: homogeneous and heterogeneous depending whether the mediator is in solution or not. This kind of mediation can follow two reaction schemes, showed below: i) the conversion of the mediator in the proper redox state by the electrode followed by the reaction with the enzyme to generate its active state able to react with the analyte; ii) the reaction of the mediator with the enzyme to generate its active state able to react with the analyte followed by the electroregeneration of the mediator.



in which M and E are respectively the inactive states of the mediator and enzyme, M^* and E^* are the active states of the mediator and enzyme, respectively, S is the substrate and P the product of the enzymatic reaction.

Chapter 2

Characterisation of a Polyazetidine Polymer Film

2.1 Introduction

The modification of electrodes with redox mediators for use as chemical sensors, transducers of biosensors, electrodes of biofuel cells and other devices has attracted much attention in the past years. To this end the application of polymeric films onto the electrode surface represents a simple yet an effective approach. Most of the films belong to two main categories: i) redox polymers in which the redox active sites are included in the polymer backbone or in the side chain and ii) ion-exchange polymers in which the redox sites are immobilised by electrostatic attractions.¹

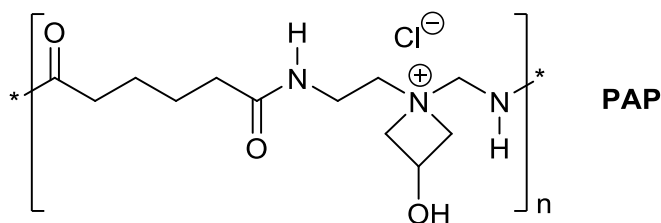
Much of the most recent researches in this field, have been focused onto the ion-exchange polymeric films: among them the most extensively studied is Nafion, a perfluorinated polysulfonate material.² Nevertheless, a problem associated with many ion-exchange polymers, including Nafion, is that they yield small diffusion coefficients for the

¹ (a) Rigla M., Hernando M.E., Gomez E.J., Brugues E., Garcia-Saez G., Capel I., Pons B., de Leiva A. *Diabetes Technol. Therapeut.* **2008**, *10*, 194-199; (b) Heller A. *Annu. Rev. Biomed. Eng.* **1999**, *1*, 153-175; (c) Barton C.S., Gallaway J., Atanassov P. *Chem. Rev.* **2004**, *104*, 4867-4886; (d) Heller A. *Phys. Chem. Chem. Phys.* **2004**, *6*, 209-216; (e) Willner I. *Biofuel Fuel Cells* **2009**, *9*, 5; (f) Suwansa-Ard S., Kanatharana P., Asawatreratanakul P., Limsakul C., Wongkittisuksa B., Thavarungkul P. *Biosens. Bioelectron.* **2005**, *21*, 445-454; (g) Tizzard A.C., Lloyd-Jones G. *Biosens. Bioelectron.* **2007**, *22*, 2400-2407; (h) Liu L.J., Chen Z.C., Yang S.N., Jin X., Lin X.F. *Sens. Actuators B: Chem.* **2008**, *129*, 218-224; (i) Liu Y., Dong S.J. *Biosens. Bioelectron.* **2007**, *23*, 593-597; (j) Cracknell J.A., Vincent K.A., Armstrong F.A. *Chem. Rev.* **2008**, *108*, 2439-2461; (k) Ramanavicius A., Kausaite A., Ramanaviciene A. *Biosens. Bioelectron.* **2005**, *20*, 1962-1967.

² (a) Rubinstein I., Bard A. J. *J. Am. Chem. Soc.* **1980**, *102*, 6641-6642; (b) Buttry D. A., Anson F. C. *J. Am. Chem. Soc.* **1982**, *104*, 4824-4829; (c) Martin C. R. *J. Chem. Soc., Faraday Trans. 1* **1986**, *82*, 1051-1070; (d) Fortier G., Beliveau R., Leblond E., Belanger D. *Anal. Lett.* **1990**, *23*, 1607-1619; (e) Pan S., Arnold M. A. *Talanta* **1996**, *43*, 1157-1162; (f) Gogol E. V., Evtugyn G. A., Marty J.-L., Budnikov H. C., Winter V. G. *Talanta* **2000**, *53*, 379-389; (g) Tsai Y.-C., Li S.-C., Chen J.-M. *Langmuir* **2005**, *21*, 3653-3658; (i) Castro S. S. L., Mortimer R. J., de Oliveira M. F., Stradiotto N. R. *Sensors* **2008**, *8*, 1950-1959; (j) Shie J.-W., Yogeswaran U., Chen S.-M. *Talanta* **2009**, *78*, 896-902; (k) George S., Lee H. K. *J. Phys. Chem. B* **2009**, *113*, 15445-15454; (l) Zain Z. M., O'Neill R. D., Lowry J. P., Pierce K. W., Tricklebank M., Dewa A., Ghani S. A. *Biosens. Bioelectron.* **2010**, *25*, 1454-1459.

immobilised species, particularly it is rather common a reduction up to 4 order of magnitude with respect to the same species free in solution. For certain applications, such as electrocatalysis, that requires a rapid charge transfer, these small diffusion coefficients are undesirable.

In this part of the work, the diffusion characteristics and electron transfer properties of a polymer film obtained from polyazetidinium prepolymer (PAP),³ that consisted in repeating units of 1-(aminomethyl)-1-{2-[(6-oxysesane)amino]ethyl}-3-hydroxyazetidinium chloride (Scheme 2.1), have been characterised.

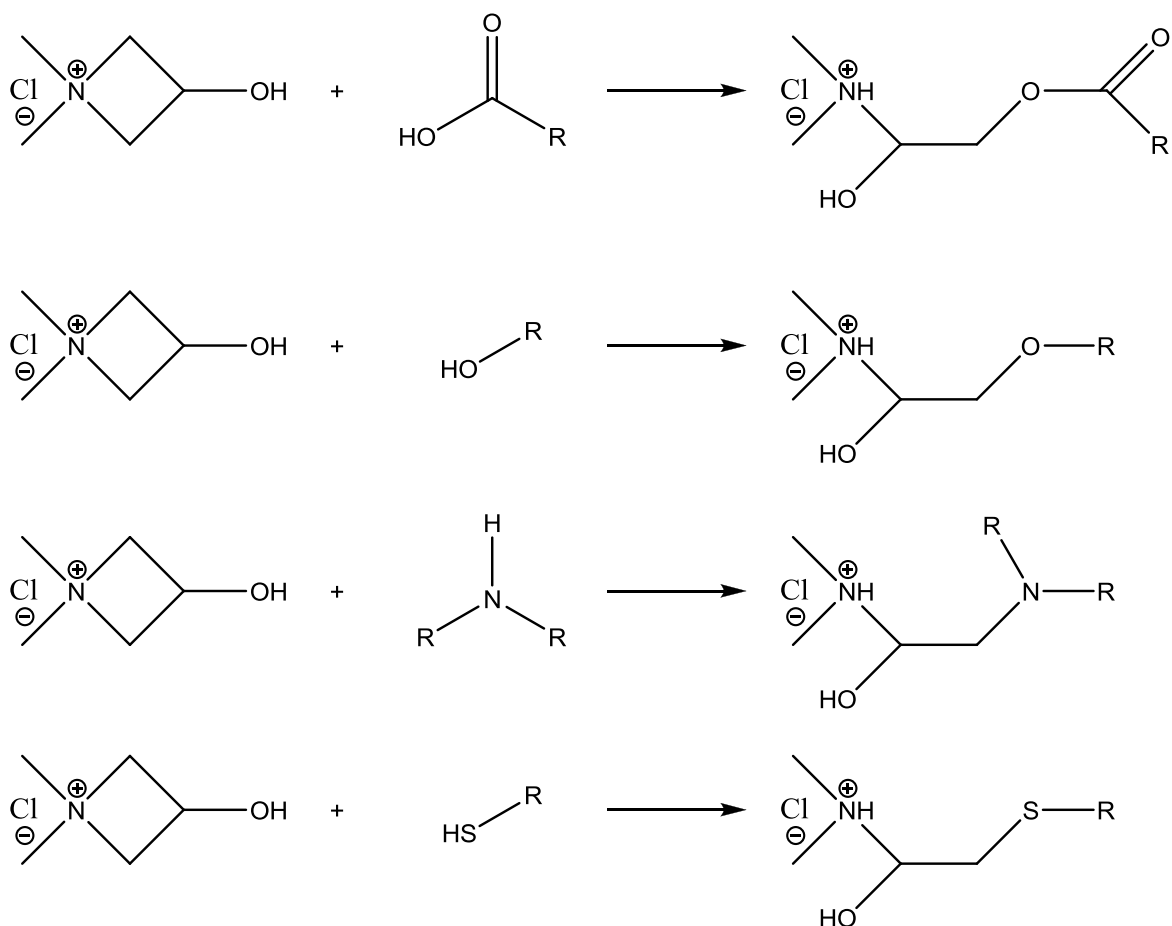


Scheme 2.1 PAP structure

PAP provides both a chemical and a physical entrapment^{3a,4} and the obtained immobilisation relies onto these peculiar features. In fact, PAP acts as a cross-linking agent being able to react with several different organic moieties (thiolic, oxydrilic, carboxylic, amino group) increasing the possibility to create chemical bonds with the enzyme, thus enhancing the immobilisation efficiency (Scheme 2.2).⁴

³ (a) Frasconi M., Favero G., Di Fusco M., Mazzei F. *Biosens. Bioelectron.* **2009**, *24*, 1424-1430; (b) Di Fusco M., Tortolini C., Deriu D., Mazzei F. *Talanta* **2010**, *81*, 235-240; (c) Tortolini C., Di Fusco M., Frasconi M., Favero G., Mazzei F. *Microchem. J.* **2010**, in press, doi:10.1016/j.microc.2010.05.004.

⁴ Mazzei F., Botrè F., Montilla S., Pilloton R., Podestà E., Botrè C. *J. Electroanal. Chem* **2004**, *574*, 95-100.



Scheme 2.2 PAP typical reactions.

This polymeric film has been used in the recent years as immobilising agent for enzymes in the construction of electrochemical biosensors. In those previous works,^{3,4} the efficiency of PAP as immobilising agent for proteins, coupled to its ability to preserve their native structure and as a consequence also their bioelectrochemical properties, has been established. On the other hand, a thorough investigation about the permeability of PAP towards redox mediators when used as immobilising agent in second-generation biosensors development, was still lacking so far. In this research PAP has been spread onto an electrodic surface without the addition of other compounds in order to form a pure polymeric film. This film acts as an hydrogel, so it may be described as a single-phase

“aqueous” matrix with excellent diffusional characteristics.⁵ Hydrogels have a number of characteristics that make them desirable electrode coatings especially for bioelectrochemical applications: high water content, biocompatibility, low interfacial tension between hydrogel surface and aqueous solution, excellent diffusion characteristics for small molecules and ions and optical transparency.⁶

For the characterisation of PAP, seven simple redox electroactive molecules have been considered as models; these species are widely used as enzyme mediators in the development of second generation biosensors: ABTS,⁷ catechol,^{7f,8} dopamine,⁹ ferrocenecarboxylic acid,¹⁰ ferricyanide,^{7f} ferrocyanide¹¹ and the complex osmium [bis(2,2-bipyridyl)-4-aminomethylpyridine chloride hexafluorophosphate] (Os[(bpy)₂ 4-AMP Cl]⁺).¹²

⁵ Wumpelmann M., Mollgaard H. *US Patent Number* 4892825, 9 Jan. **1990**.

⁶ Ratner B. D., Hoffman A. S. *Hydrogels for Medical and Related Applications* **1996**, 31, 1-36.

⁷ (a) Potthast A., Rosenau T., Chen C. L., Gratzl J. S. *J. Mol. Cat. A: Chem.* **1996**, 108, 5-9; (b) Majcherczyk A., Johannes C., Hüttermann A. *Appl. Microbiol. Biotechnol.* **1999**, 51, 267-276; (c) Muheim A., Fiechter A., Harvey P. J., Schoemaker H. E. *Holzforschung* **1992**, 46, 121-126; (d) Solís-Oba M., Ugalde-Saldívar V. M., González I., Viniegra-González G. *J. Electroanal. Chem.* **2005**, 579, 59-66; (e) Branchi B., Galli C., Gentili P. *Org. Biomol. Chem.* **2005**, 3, 2604-2614; (f) Baminger U., Ludwig R., Galhaup C., Leitner C., Kulbe K. D., Haltrich D. *J. Mol. Cat. B: Enzym.* **2001**, 11, 541-550.

⁸ (a) Solná R., Skládal P. *Electroanal.* **2005**, 23, 2137-2146; (b) Haghghi B., Gorton L., Ruzgas T., Jönsson L. *J. Anal. Chim. Acta* **2003**, 487, 3-14; (c) Portaccio M., Di Martino S., Maiuri P., Durante D., De Luca P., Lepore M., Bencivenga U., Rossi S., De Maio A., Mita D. G. *J. Mol. Cat. B: Enzym.* **2006**, 41, 97-102.

⁹ (a) Jarosz-Wilkolazka A., Ruzgas T., Gorton L. *Talanta* **2005**, 66, 1219-1224; (b) Xiang L., Lin Y., Yu P., Mao L. *Electrochim. Acta* **2007**, 52, 4144-4152; (c) Ferry Y., Leech D. *Electroanal.* **2005**, 17, 113-119; (d) Osina M. A., Bogdanovskaya V. A., Tarasevich M. R. *Russ. J. Electrochem.* **2003**, 39, 407-412.

¹⁰ Jusoh N., Abdul-Aziz A. *Proceedings of the 20th Symposium of Malaysian Chemical Engineers* **2006**, 29-34.

¹¹ (a) Liu Y., Liu H., Qian J., Deng J., Yu T. *Electrochim. Acta* **1996**, 41, 77-82; (b) Claus H., Faber G., König H. *Appl. Microbiol. Biotechnol.* **2002**, 59, 672-678.

¹² (a) Trudeau F., Daigle F., Leech D. *Anal. Chem.* **1997**, 69, 882-886; (b) Boland S., Foster K., Leech D. *Electrochim. Acta* **2009**, 54, 1986-1991; (c) Jenkins P. A., Boland S., Kavanagh P., Leech D. *Bioelectrochem.* **2009** 76, 162-168; (d) Boland S., Barrière F., Leech D. *Langmuir* **2008**, 24, 6351-6358.

2.2 Experimental Section

2.2.1 Materials

2,2'-azino-bis(3-ethylbenzothiazoline-6-sulfonic acid) diammonium salt (ABTS), catechol, dopamine, ferrocenecarboxylic acid (FcCOOH), potassium ferrocyanide (II) ($K_4[Fe(CN)_6]$), potassium ferricyanide (III) ($K_3[Fe(CN)_6]$) and osmium [bis(2,2-bipyridyl)-4-aminomethylpyridine chloride] hexafluorophosphate ($Os[(bpy)_2\text{-}4\text{-AMP Cl}]^+$) were used as received. The polymeric film employed was poly-1-(aminomethyl)-1-{2-[(6-oxysesane)amino]ethyl}-3-hydroxyazetidinium chloride (polyazetidine prepolymer, PAP®), donated by Hercules Inc. Wilmington DE (USA). Other chemicals were all of analytical grade. High purity deionised water (Resistance: $18.2\text{ M}\Omega \times \text{cm}$ at $25\text{ }^\circ\text{C}$; TOC < $10\text{ }\mu\text{g/L}$) obtained from Millipore (France) has been used to prepare all the solutions.

2.2.2 Apparatus

Electrochemical experiments were performed by using a μ -Autolab type III potentiostat (Eco Chemie, Netherlands) controlled by means of the GPES Manager program. The measurements were performed in a thermostated 10 ml glass cell with a conventional three-electrode configuration: $20\pm 1\text{ }\mu\text{m}$ diameter (determined experimentally, see section 2.2.3) platinum microdisk encased in glass (Amel, Italy) as working electrode, Ag/AgCl (KCl sat.) (Metrohm, Switzerland, 198 mV vs NHE) as reference and a graphite rod as counter electrode. All solutions were deaerated with nitrogen before every measurements and supporting electrolyte was 0.1 mol/L KCl. The temperature was controlled using a Julabo F10 thermostat (temperature error $\pm 0.5^\circ\text{C}$).

2.2.3 Preparation of Polyazetidine-Coated Electrodes

Platinum microdisk radius was measured before every experiment by chronoamperometric steady-state current using a 1.1 mmol L^{-1} of $\text{K}_3[\text{Fe}(\text{CN})_6]$ solution in 0.1 mol L^{-1} KCl (under this conditions, the diffusion coefficient of $\text{Fe}(\text{CN})_6^{3-}$ is $7.6 \cdot 10^{-6} \text{ cm}^2 \text{ s}^{-1}$).¹³ The electrode was first polished on alumina powder of different size (0.3 and 0.05 micron) and then ultrasonically cleaned in water for about 5 minutes. PAP-coated electrode was prepared depositing and leaving to dry overnight $3 \mu\text{l}$ of PAP. Before the measurements, the deposited matrix was left stabilising in the solution, scanning the potential between the reduced and oxidised form of the compound, until a stable voltammetric profile was reached in order to allow the selected mediator to fulfil the polymeric layer. All the measurements are the average of five or more replicate measurements.

2.2.4 Measurement of Diffusion Coefficients and Standard Heterogeneous Rate Constants

Diffusion coefficients were obtained by means of potential-step chronoamperometry on a 1.0 mol L^{-1} aqueous solution of the selected compound in presence of KCl 0.1 mol L^{-1} as supporting electrolyte. The experiments were performed using a sample time of 0.1 s. The system was pre-treated by holding the potential at a point corresponding to the passage of zero faradic current for 10 s, after that the experimental transient were obtained by stepping to a potential value greater, as absolute value, with respect to the reduction or oxidisation peak potential; after the application of the potential step the current was measured for 50 s. Anyway, in most cases, after 10 s the current reaches the steady state. Heterogeneous rate constants were obtained under the same experimental conditions, by means of steady-state voltammetry at a scan rate of 5 mV s^{-1} .

¹³ Von Stackelberg M. V., Pilgram M. Z. *Elektrochem.* **1953**, 57, 342-350.

2.3 Results and Discussion

2.3.1 Theoretical Background

The major problem to be addressed in measuring by chronoamperometric method the diffusion coefficient using a polymer film coated-electrode, is the unknown analyte concentration in the hydrogel; in order to overcome this obstacle the data should be treated in accordance with the normalised Cottrell equation.¹⁴ The latter consists of a rearrangement of the Cottrell equation (1) which describes the chronoamperometric response of an electroactive specie at a microdisk electrode:¹⁵

$$I = (\pi^{1/2}nFD^{1/2}Cr^2)/t^{1/2} + 4nFDCr \quad (1)$$

where n is the number of electrons exchanged in the redox reaction, F is Faraday's constant, D is the diffusion coefficient, C is the analyte concentration, t is the time elapsed after the application of an appropriate potential step and r is the radius of the microdisk electrode. Equation 1 contains both a time independent term and a time dependent term, the time independent term representing the steady-state behaviour (2):

$$I_d = 4nFDCr \quad (2)$$

At short experimental times, the time dependent term is large compared to the independent one, which becomes more important upon increasing experimental time. However, this effect is more evident using a microdisk electrode, in fact in this case the time dependent Cottrellian behaviour of the current response becomes negligible already after a few

¹⁴ Denuault G., Mirkin M. V., Bard A. J. *J. Electroanal. Chem.* **1991**, 308, 27-38.

¹⁵ (a) Bard A. J., Faulkner L. R. *Electrochemical Methods: Fundamentals and Applications*, 2nd Ed., Wiley, New York, 2001; (b) Cottrell F. G. *Z. Phys. Chem., Stoichiom. Verwandtschaftsl.* **1902**, 42, 385.

seconds from the application of the potential step;¹⁶ after this short time really, the time independent term becomes predominant and the faradic current generated at the microelectrode surface may be described by Equation 2. Normalisation of a chronoamperometric response I (in Eq. 1) by dividing the entire current-time curve by the steady-state current I_d leads to Equation 3 (Normalised Cottrell Equation):

$$I/I_d = (\pi^{1/2}r)/(4D^{1/2}t^{1/2}) + 1 \quad (3)$$

The plot of I/I_d vs $t^{1/2}$ has the form of a straight line with an intercept equal to unity and a slope $S = (\pi^{1/2}r)/(4D^{1/2})$, from which it is possible to evaluate D , if the radius r is known.

While on one hand the potential step chronoamperometry was employed to achieve a simple evaluation of the diffusion properties, on the other hand the scan voltammetry has been used to investigate the efficiency of the heterogeneous electron transfer. Because of the steady-state nature of the diffusion layer at a microdisk electrode, a sigmoidal voltammogram should be obtained at slow scan rate.¹⁷ Under this conditions, the half-wave potential $E_{1/2}$ can be obtained from the following equation:

$$E = E_{1/2} + (RT/nF) \ln[I / (I_d - I)] \quad (4)$$

where all the symbols have their usual meanings and I_d is the current expressed by Equation 2. $E_{1/2}$ can be easily extrapolated from a plot of E vs $\ln[I/(I_d-I)]$ and this value corresponds to E° value if we assume that the diffusion coefficient of the reduced and oxidised form are the same.

¹⁶ Petrovic S. C., Hammericksen R. H. *Electroanal.* **2002**, *14*, 599-604.

¹⁷ Howell J. O., Wightman R. M. *J. Phys. Chem.* **1984**, *88*, 3915-3918.

The equation for the voltammetric response of such a quasi-reversible redox reaction under steady-state conditions at a microdisk electrode was proposed by Galus et al.:¹⁸

$$(4D/\pi k_s r) \exp[-(1-\alpha)nf(E-E^\circ')] = (I_d - I / I) - (I_d - I' / I') \quad (5)$$

where k_s is the standard heterogeneous rate constant, α is the transfer coefficient of the cathodic reaction, $f = F/RT$, I_d is the steady-state current and I' is the calculated reversible current using Equation 6.¹⁹

$$\ln[(I_d - I') / I'] = nf(E^\circ' - E) \quad (6)$$

The logarithmic form of Equation 5 can be used to determine k_s :

$$E - E^\circ' = [1/(1-\alpha)nf] \ln(4D/\pi k_s r) - [1/(1-\alpha)nf] \ln[(I_d - I / I) - (I_d - I' / I')] \quad (7)$$

Using Equation 7, for a given value of the radius r , the first term on the right-hand side is constant. Therefore, a plot of $E - E^\circ'$ vs $\ln[(I_d - I / I) - (I_d - I' / I')]$ should be linear with slope $1/(1-\alpha)nf$ and intercept $[1/(1-\alpha)nf] \ln(4D/\pi k_s r)$ from which one may easily calculate the k_s value, provided that r and D are known.

¹⁸ Galus Z., Golas J., Osteryoung J. *J. Phys. Chem.* **1988**, 92, 1103-1107.

¹⁹ (a) Jun Z., Wang J., Tai Z., Ju H. *J. Electroanal. Chem.* **1995**, 381, 231-234; (b) Zhou H., Dong S. *J. Electroanal. Chem.* **1997**, 425, 55-59.

2.3.2 Determination at Different Temperatures of Diffusion Coefficient and Electron Exchange Constant Using Naked Microelectrode

The diffusion coefficients D of the seven considered redox molecules, at different temperatures, were determined using potential-step chronoamperometry. The data were fitted (using a non linear fit algorithm in SigmaPlot®) according to the Cottrell equation (Eq. 1) and the obtained diffusion current at the steady-state I_d was used to calculate D values. As an example, Figure 2.1 shows the potential-step chronoamperometry (time = 10 s) of FcCOOH in the range of temperature of 288-308 K. The averaged results of all compounds are listed in Table 2.1.

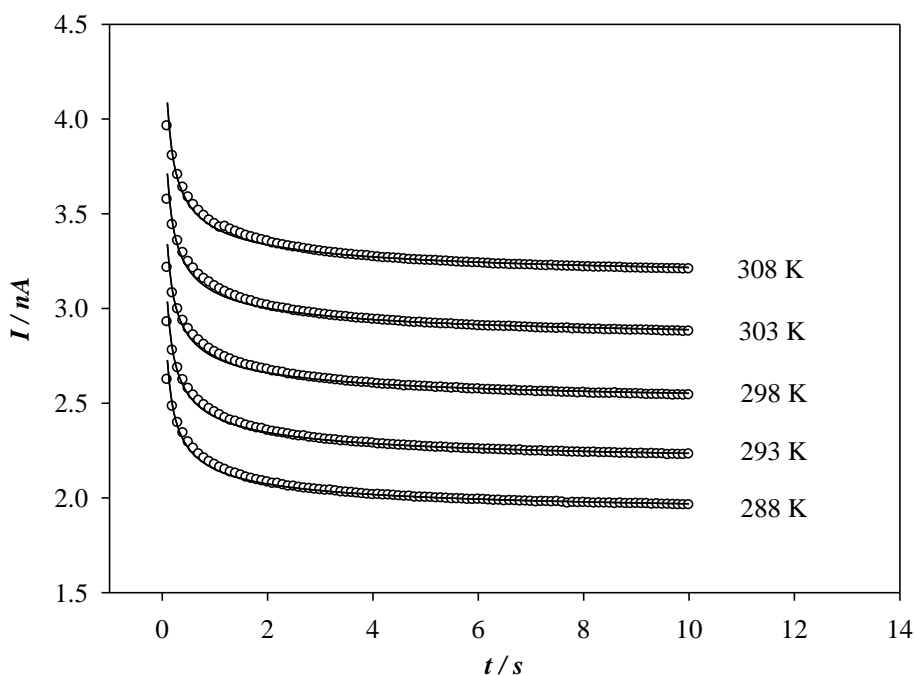


Figure 2.1 Potential step chronoamperometries for FcCOOH 1 mol L^{-1} in KCl 0.1 mol L^{-1} obtained at different temperatures using a platinum microelectrode in absence of PAP film. The empty dots represent the experimental points which are fitted to the Cottrell equation (solid line).

Table 2.1 Calculated diffusion coefficients and heterogeneous electron transfer constants for all the considered compounds 1 mol L⁻¹ solutions in KCl 0.1 mol L⁻¹ obtained at different temperatures using a platinum microelectrode.

Compound	<i>T</i> (K)	<i>D</i> (cm ² s ⁻¹)	<i>k_s</i> (m s ⁻¹)
ABTS	288	$(2.44 \pm 0.01) \times 10^{-6}$	$(3.80 \pm 0.02) \times 10^{-5}$
	293	$(2.86 \pm 0.01) \times 10^{-6}$	$(4.21 \pm 0.01) \times 10^{-5}$
	298	$(3.42 \pm 0.02) \times 10^{-6}$	$(5.47 \pm 0.03) \times 10^{-5}$
	303	$(3.92 \pm 0.01) \times 10^{-6}$	$(6.66 \pm 0.02) \times 10^{-5}$
	308	$(4.49 \pm 0.01) \times 10^{-6}$	$(7.97 \pm 0.02) \times 10^{-5}$
Catechol	288	$(1.01 \pm 0.01) \times 10^{-5}$	$(1.28 \pm 0.01) \times 10^{-4}$
	293	$(1.16 \pm 0.01) \times 10^{-5}$	$(1.48 \pm 0.01) \times 10^{-4}$
	298	$(1.33 \pm 0.01) \times 10^{-5}$	$(1.70 \pm 0.01) \times 10^{-4}$
	303	$(1.50 \pm 0.01) \times 10^{-5}$	$(1.95 \pm 0.01) \times 10^{-4}$
	308	$(1.69 \pm 0.01) \times 10^{-5}$	$(2.18 \pm 0.01) \times 10^{-4}$
Dopamine	288	$(5.33 \pm 0.01) \times 10^{-6}$	$(6.95 \pm 0.01) \times 10^{-5}$
	293	$(6.13 \pm 0.02) \times 10^{-6}$	$(7.85 \pm 0.03) \times 10^{-5}$
	298	$(6.97 \pm 0.01) \times 10^{-6}$	$(9.05 \pm 0.01) \times 10^{-5}$
	303	$(7.80 \pm 0.02) \times 10^{-6}$	$(1.01 \pm 0.03) \times 10^{-4}$
	308	$(8.74 \pm 0.01) \times 10^{-6}$	$(1.14 \pm 0.01) \times 10^{-4}$
FcCOOH	288	$(4.78 \pm 0.01) \times 10^{-6}$	$(6.93 \pm 0.01) \times 10^{-5}$
	293	$(5.44 \pm 0.01) \times 10^{-6}$	$(7.51 \pm 0.01) \times 10^{-5}$
	298	$(6.22 \pm 0.01) \times 10^{-6}$	$(8.40 \pm 0.01) \times 10^{-5}$
	303	$(7.11 \pm 0.02) \times 10^{-6}$	$(9.34 \pm 0.03) \times 10^{-5}$
	308	$(7.93 \pm 0.02) \times 10^{-6}$	$(1.06 \pm 0.03) \times 10^{-4}$
Fe(CN) ₆ ⁴⁻	288	$(4.08 \pm 0.01) \times 10^{-6}$	$(5.35 \pm 0.01) \times 10^{-5}$
	293	$(4.60 \pm 0.01) \times 10^{-6}$	$(6.08 \pm 0.01) \times 10^{-5}$
	298	$(5.21 \pm 0.01) \times 10^{-6}$	$(7.22 \pm 0.01) \times 10^{-5}$
	303	$(5.79 \pm 0.02) \times 10^{-6}$	$(8.37 \pm 0.03) \times 10^{-5}$
	308	$(6.59 \pm 0.04) \times 10^{-6}$	$(1.01 \pm 0.05) \times 10^{-4}$
Fe(CN) ₆ ³⁻	288	$(6.03 \pm 0.01) \times 10^{-6}$	$(7.88 \pm 0.01) \times 10^{-5}$
	293	$(6.73 \pm 0.01) \times 10^{-6}$	$(8.79 \pm 0.01) \times 10^{-5}$
	298	$(7.52 \pm 0.01) \times 10^{-6}$	$(9.81 \pm 0.01) \times 10^{-5}$
	303	$(8.30 \pm 0.01) \times 10^{-6}$	$(1.08 \pm 0.01) \times 10^{-4}$
	308	$(9.22 \pm 0.03) \times 10^{-6}$	$(1.20 \pm 0.04) \times 10^{-4}$
Os[(bpy) ₂ 4-AMP Cl] ⁺	288	$(1.11 \pm 0.01) \times 10^{-6}$	$(1.72 \pm 0.01) \times 10^{-5}$
	293	$(1.35 \pm 0.01) \times 10^{-6}$	$(2.10 \pm 0.01) \times 10^{-5}$
	298	$(1.79 \pm 0.01) \times 10^{-6}$	$(2.91 \pm 0.01) \times 10^{-5}$
	303	$(2.18 \pm 0.01) \times 10^{-6}$	$(3.41 \pm 0.01) \times 10^{-5}$
	308	$(2.66 \pm 0.01) \times 10^{-6}$	$(4.29 \pm 0.01) \times 10^{-5}$

As it is expected, an increase in the diffusion coefficients is observed when increasing the temperature, because of the decrease in the viscosity of the solvent media. The Stokes-Einstein equation,²⁰ shown below, predicts this inverse proportionality between diffusion coefficient and viscosity (η) of the solvent.

$$D = k_B T / 6\pi\eta a \quad (8)$$

where k_B is the Boltzmann constant ($1.38 \times 10^{-23} \text{ m}^2 \text{ kg s}^{-2} \text{ K}^{-1}$), T is the temperature and a is the hydrodynamic radius. The applicability of the Stokes-Einstein relationship has been evaluated and in Figure 2.2 are showed the plots of D vs. η^{-1} ; the viscosity of the measuring solution was calculated according to the literature.²¹

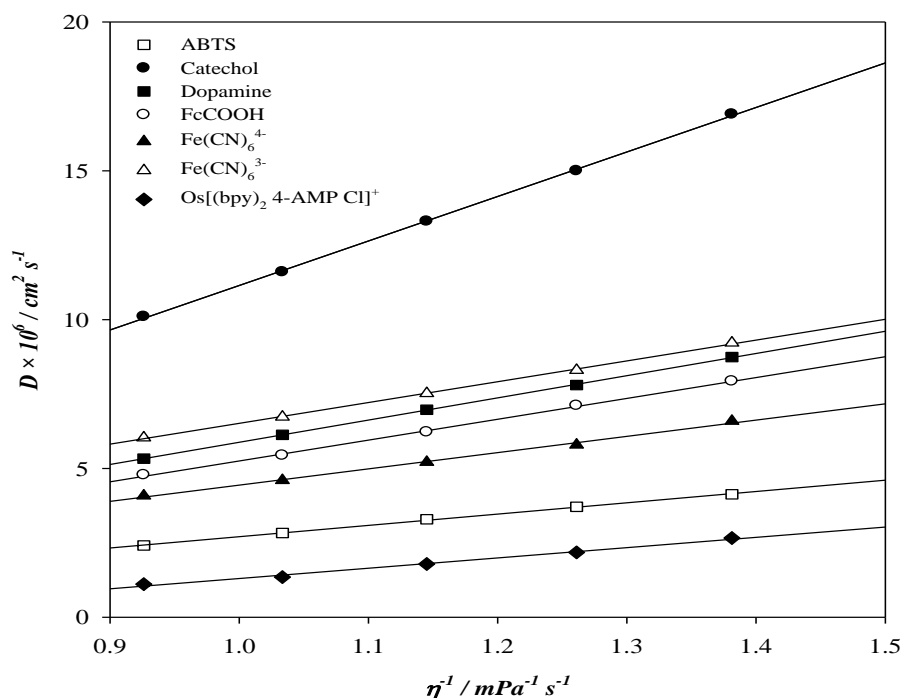


Figure 2.2 Calculated diffusion coefficient variation vs medium viscosity for all the considered compounds 1 mol L⁻¹ solutions in KCl 0.1 mol L⁻¹; all other experimental conditions are the same reported in the text. The dots represent the experimental points which are fitted to the Stokes-Einstein equation (solid lines).

²⁰ Compton R. G., Banks C. E. *Understanding Voltammetry*; World Scientific Publishing Co. Pte. Ltd.: Singapore, 2007.

²¹ Grimes C.E., Kestin J., Khalifa H.E. *J. Chem. Eng. Data* **1979**, 24, 121-126.

The hydrodynamic radii of the compounds have been determined and are listed in Table 2.2.

Table 2.2 Hydrodynamic radii for all the considered compounds 1 mol L⁻¹ solutions in KCl 0.1 mol L⁻¹ obtained at 298 K using a platinum microelectrode.

Compound	<i>a</i> (nm)
ABTS	0.674
Catechol	0.171
Dopamine	0.342
FcCOOH	0.364
Fe(CN) ₆ ⁴⁻	0.467
Fe(CN) ₆ ³⁻	0.365
Os[(bpy) ₂ 4-AMP Cl] ⁺	0.738

The heterogeneous rate constants k_s of the compounds, at different temperatures, were also determined using steady-state voltammetry and reported in Table 2.1. As an example, Figure 2.3 shows the steady-state voltammograms of the oxidation of FcCOOH in the range of temperature 288-308 K.

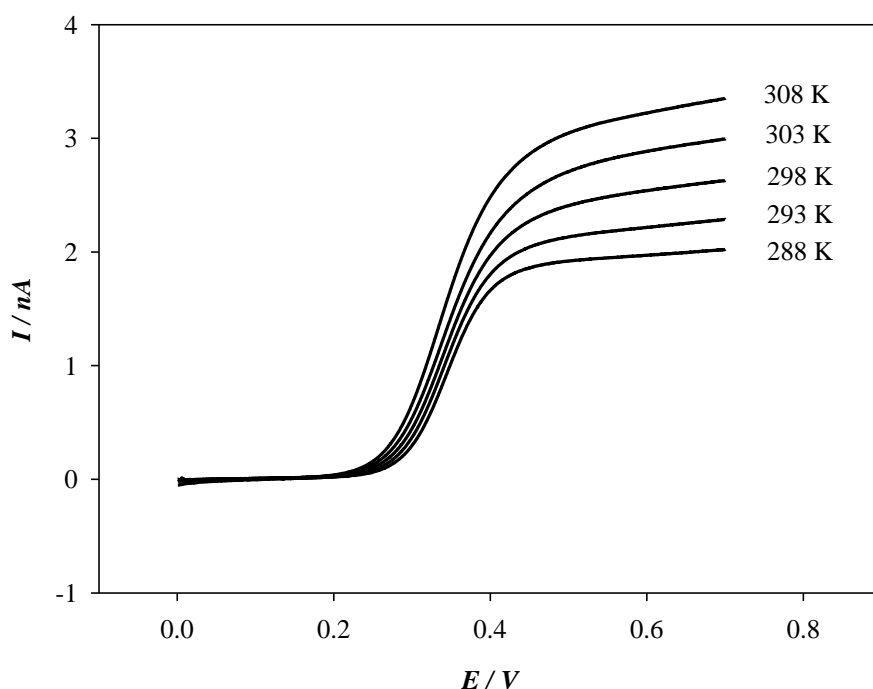


Figure 2.3 Steady-state voltammograms for FcCOOH 1 mol L⁻¹ in KCl 0.1 mol L⁻¹ obtained at different temperatures using a platinum microelectrode in absence of PAP film.

Before calculating the k_s from the experimental data, it is necessary to check whether steady-state assumptions are fulfilled under the experimental conditions. To do this, the parameter p presented by Aoki et al.²² was used:

$$p = (nFr^2v/RTD)^{1/2} \quad (9)$$

where v is the scan rate and the other symbols have their usual meanings. When p is large, linear diffusion predominates and the voltammogram is peak shaped. On the other hand, when p is small, radial diffusion predominates and a sigmoidal voltammogram is obtained. In contrast, when $p < 0.33$, the voltammogram current deviate from the steady-state current by less than 5%.²¹ In this case was used a scan rate of 5 mV s⁻¹ and a 10 μ m-radius electrode, so, according to Equation 9, p is smaller than 1.40 assuming that $D > 1.0 \times 10^{-7}$

²² Aoki K., Akimoto K., Tokuda K., Matsuda H., Osteryoung J. G. *J. Electroanal. Chem.* **1984**, 171, 219-230.

$\text{cm}^2 \text{s}^{-1}$. Under these conditions, the experimental voltammograms are acceptably close to a steady-state wave.

The data obtained from the steady-state voltammograms were fitted in accordance to the Equation 7, the heterogeneous rate constants were calculated and, as already mentioned, the obtained results for the compounds are listed in Table 2.1. Also in this case was observed an increase in the heterogeneous rate constants with increasing the temperature, because of the strict dependence of k_s on D . In fact, all the correlation plots of k_s vs. D give a straight line with $R^2 > 0.99$.

2.3.3 Determination at Different Temperatures of Diffusion Coefficient and Electron Exchange Constant Using PAP-Covered Microelectrode

The diffusion coefficients D of the same compounds were determined, at different temperatures, in the presence of PAP film. Figure 2.4 shows the potential-step chronoamperometry of FcCOOH in the range of temperature 288-308 K. Considering that in this case the unmodified Cottrell equation cannot be employed because the presence of the polymeric layer produces a variation in the concentration of the electroactive species near the electrodic surface, the data were fitted according to the Normalised Cottrell Equation (Equation 3) which allowed the calculation of the diffusion coefficient. In addition, from the current I_d according to Equation 2 the concentration of the compound inside the deposited matrix has been evaluated. The obtained results (diffusion coefficients and concentration) for all the substrates at different temperatures are listed in Table 2.3.

Table 2.3 Calculated diffusion coefficients, concentrations in the polymer film and heterogeneous electron transfer constants for all the considered compounds 1 mol L⁻¹ solutions in KCl 0.1 mol L⁻¹ obtained at different temperatures using a platinum microelectrode in presence of PAP film.

Compound	<i>T</i> (K)	<i>D</i> (cm ² s ⁻¹)	<i>C</i> (mmol L ⁻¹)	<i>k_s</i> (m s ⁻¹)
ABTS	288	$(1.63 \pm 0.07) \times 10^{-6}$	1.84	$(2.83 \pm 0.12) \times 10^{-5}$
	293	$(2.05 \pm 0.04) \times 10^{-6}$	1.99	$(3.54 \pm 0.07) \times 10^{-5}$
	298	$(2.44 \pm 0.04) \times 10^{-6}$	1.97	$(4.27 \pm 0.07) \times 10^{-5}$
	303	$(2.82 \pm 0.02) \times 10^{-6}$	2.02	$(4.92 \pm 0.03) \times 10^{-5}$
	308	$(3.31 \pm 0.07) \times 10^{-6}$	2.01	$(5.77 \pm 0.12) \times 10^{-5}$
Catechol	288	$(2.50 \pm 0.01) \times 10^{-6}$	4.12	$(1.02 \pm 0.01) \times 10^{-4}$
	293	$(2.69 \pm 0.11) \times 10^{-6}$	4.47	$(1.09 \pm 0.04) \times 10^{-4}$
	298	$(3.00 \pm 0.07) \times 10^{-6}$	4.58	$(1.24 \pm 0.03) \times 10^{-4}$
	303	$(3.20 \pm 0.10) \times 10^{-6}$	4.85	$(1.31 \pm 0.04) \times 10^{-4}$
	308	$(3.45 \pm 0.01) \times 10^{-6}$	5.06	$(1.44 \pm 0.01) \times 10^{-4}$
Dopamine	288	$(1.27 \pm 0.01) \times 10^{-6}$	4.54	$(4.71 \pm 0.04) \times 10^{-5}$
	293	$(1.39 \pm 0.02) \times 10^{-6}$	4.69	$(5.22 \pm 0.08) \times 10^{-5}$
	298	$(1.46 \pm 0.02) \times 10^{-6}$	5.04	$(5.60 \pm 0.08) \times 10^{-5}$
	303	$(1.64 \pm 0.05) \times 10^{-6}$	4.94	$(6.60 \pm 0.20) \times 10^{-5}$
	308	$(1.74 \pm 0.06) \times 10^{-6}$	5.02	$(6.93 \pm 0.24) \times 10^{-5}$
FcCOOH	288	$(1.76 \pm 0.02) \times 10^{-6}$	1.76	$(3.16 \pm 0.04) \times 10^{-5}$
	293	$(1.82 \pm 0.02) \times 10^{-6}$	1.84	$(3.26 \pm 0.04) \times 10^{-5}$
	298	$(1.92 \pm 0.03) \times 10^{-6}$	1.83	$(3.44 \pm 0.05) \times 10^{-5}$
	303	$(2.06 \pm 0.03) \times 10^{-6}$	1.84	$(3.69 \pm 0.05) \times 10^{-5}$
	308	$(2.16 \pm 0.03) \times 10^{-6}$	1.95	$(3.88 \pm 0.05) \times 10^{-5}$
Fe(CN) ₆ ⁴⁻	288	$(2.28 \pm 0.05) \times 10^{-7}$	34.43	$(4.33 \pm 0.09) \times 10^{-6}$
	293	$(3.63 \pm 0.23) \times 10^{-7}$	28.41	$(7.11 \pm 0.45) \times 10^{-6}$
	298	$(5.30 \pm 0.08) \times 10^{-7}$	25.13	$(1.09 \pm 0.02) \times 10^{-5}$
	303	$(7.47 \pm 0.27) \times 10^{-7}$	22.63	$(1.44 \pm 0.05) \times 10^{-5}$
	308	$(9.77 \pm 0.36) \times 10^{-7}$	19.46	$(1.92 \pm 0.07) \times 10^{-5}$
Fe(CN) ₆ ³⁻	288	$(4.00 \pm 0.03) \times 10^{-6}$	1.90	$(7.00 \pm 0.05) \times 10^{-5}$
	293	$(4.59 \pm 0.08) \times 10^{-6}$	2.00	$(8.00 \pm 0.14) \times 10^{-5}$
	298	$(5.26 \pm 0.09) \times 10^{-6}$	2.05	$(9.02 \pm 0.15) \times 10^{-5}$
	303	$(5.86 \pm 0.05) \times 10^{-6}$	2.05	$(1.02 \pm 0.01) \times 10^{-4}$
	308	$(6.47 \pm 0.23) \times 10^{-6}$	2.09	$(1.10 \pm 0.04) \times 10^{-4}$
Os[(bpy) ₂ 4-AMP Cl] ⁺	288	$(6.91 \pm 0.07) \times 10^{-7}$	1.84	$(1.83 \pm 0.02) \times 10^{-5}$
	293	$(8.44 \pm 0.22) \times 10^{-7}$	1.79	$(2.24 \pm 0.06) \times 10^{-5}$
	298	$(9.31 \pm 0.39) \times 10^{-7}$	1.96	$(2.89 \pm 0.12) \times 10^{-5}$
	303	$(1.02 \pm 0.01) \times 10^{-6}$	2.12	$(3.03 \pm 0.03) \times 10^{-5}$
	308	$(1.09 \pm 0.03) \times 10^{-6}$	2.51	$(3.13 \pm 0.09) \times 10^{-5}$

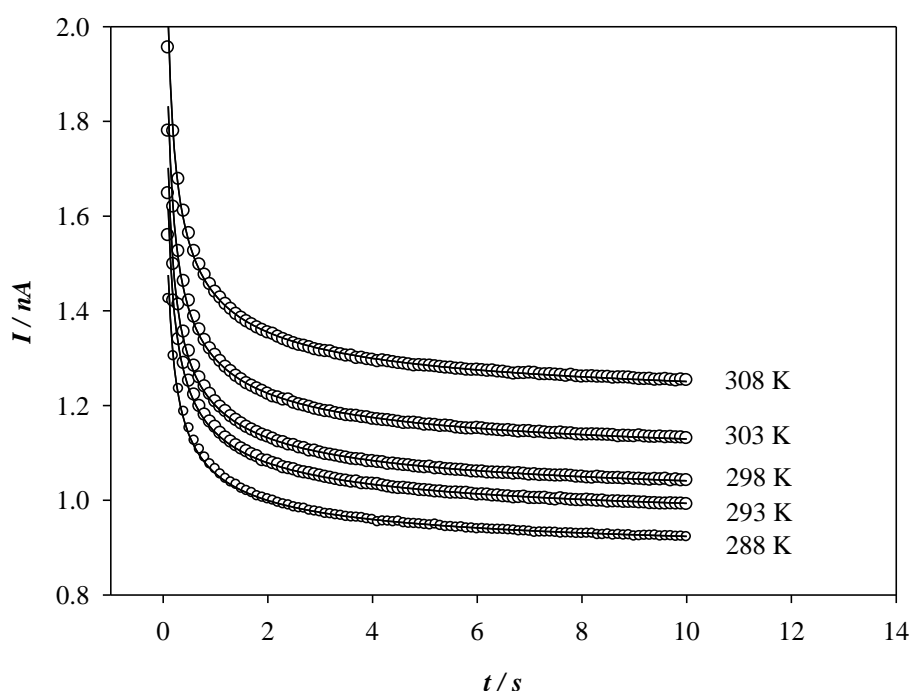


Figure 2.4 Potential step chronoamperometries for FcCOOH 1 mol L⁻¹ in KCl 0.1 mol L⁻¹ obtained at different temperatures using a platinum microelectrode in presence of PAP film. The empty dots represent the experimental points which are fitted to the Cottrell equation (solid line).

It is known that in the presence of a polymer film, the diffusion coefficient could be affected by electron-hopping process,²³ because of the charge propagation between redox sites anchored to the film. In this case the experimental diffusion coefficient is expressed by

$D = D_{phys} + D_{et}$,²⁴ where the first term is the contribution to physical diffusion and the second one is the contribution due to self-exchange electron transfer that is expressed by

$D_{et} = (k_{ex}\delta^2 C)/6$,²⁵ where k_{ex} is the electron self-exchange rate constant, δ is the distance between reaction pairs when electron exchange occurs and C is the redox sites concentration. Using: i) as δ values twice the value of the hydrodynamic radii reported in

²³ Kaufman F. B., Engler E. M. *J. Am. Chem. Soc.* **1979**, *101*, 547-549.

²⁴ (a) Dahms H. *J. Phys. Chem.* **1968**, *72*, 362-364; (b) Ruff I. *Electrochim. Acta* **1970**, *15*, 1059; (c) Ruff I.; Friedrich, V. J. *J. Phys. Chem.* **1971**, *75*, 3297-3302; (d) Ruff I., Friedrich V. J., Demeter K., Csillag K. *J. Phys. Chem.* **1971**, *75*, 3303-3309.

²⁵ Watanabe M., Wooster T. T., Murray R. W. *J. Phys. Chem.* **1991**, *95*, 4573-4579.

Table 2.2, ii) as C the concentration reported in Table 2.3 and iii) the values of k_{ex} reported in literature (ABTS,²⁶ catechol,²⁷ dopamine with good approximation was considered having the same k_{ex} of catechol, FcCOOH was approximated to the known value of k_{ex} of ferrocene,²⁸ taking into account that the ferrocenes derivatives should have similar values of λ_{ex} ,²⁹ $\text{Fe}(\text{CN})_6^{4-/3-}$,³⁰ $\text{Os}[(\text{bpy})_2 \text{ 4-AMP Cl}]^+$ ³¹) it is possible to estimate the contribution of the electron-hopping to the experimentally determined diffusion coefficients. Considering that, the determined values of D_{et} ($\text{cm}^2 \text{ s}^{-1}$) for the studied substrates result as follows: ABTS $\sim 10^{-10}$, catechol $\sim 10^{-14}$, dopamine $\sim 10^{-13}$, FcCOOH $\sim 10^{-11}$, $\text{Fe}(\text{CN})_6^{4-}$ $\sim 10^{-12}$, $\text{Fe}(\text{CN})_6^{3-}$ $\sim 10^{-13}$, $\text{Os}[(\text{bpy})_2 \text{ 4-AMP Cl}]^+$ $\sim 10^{-10}$; and comparing this values with those obtained experimentally and reported in Table 2.3 it can be assumed that the electron-hopping is negligible and the D values obtained involve only physical diffusion.

As already mentioned, also in the case of PAP-covered microelectrode, an increase of the diffusion coefficient values is observed with increasing the temperature, even if these calculated values are slightly lower with respect with those determined using the naked microelectrode, as expected. In order to shed light on this behaviour, two concurrent phenomena must be considered: i) the solvent viscosity decreases while increasing temperature thus leading to higher values of D as already observed, and ii) the presence of PAP film increases the overall viscosity of the whole system thus leading to lowers values of D . Nevertheless, even if this results in a decrease of D values in the presence of PAP film, compared to those measured in absence thereof, the excellent diffusion properties of this film are emphasised especially if they are compared with other similar polymer films

²⁶ Scott S. L., Chen W. J., Bakac A., Espenson J. H. *J. Phys. Chem.* **1993**, *97*, 6710-6714.

²⁷ Steenken S., Neta P. *J. Phys. Chem.* **1979**, *83*, 1134-1137.

²⁸ Nielson R. M., McManis G. E., Safford L. K., Weaver M. J. *J. Phys. Chem.* **1989**, *93*, 2152-2157.

²⁹ Baciocchi E., Bietti M., Di Fusco M., Lanzalunga O. *J. Org. Chem.* **2007**, *72*, 8748-8754.

³⁰ Khoshtariya D. E., Meusinger R., Billing R. *J. Phys. Chem.* **1995**, *99*, 3592-3597.

³¹ Zakeeruddin S. M., Fraser D. M., Nazeeruddin M. K., Gratzel M. *J. Electroanal. Chem.* **1992**, *337*, 253-283.

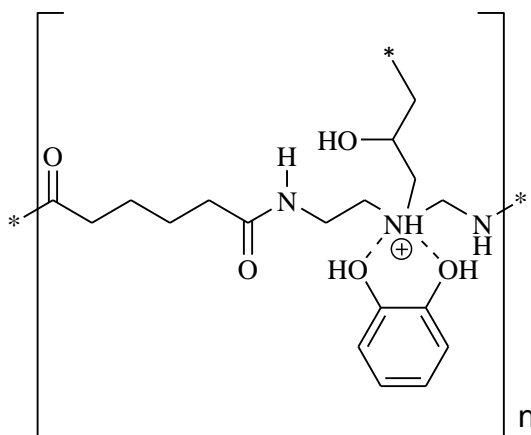
used for the same purpose.³² Really, for hydrogels overlapping an electrodic surface, it is quite common to reduce the diffusion coefficient of a significative extent (from a minimum of 10- up to 10³-fold reduction).^{32d,32e}

In particular, it can be observed that passing from the substrates free to diffuse from the solution to the substrates forced to cross a polymer film, the percent decrease of the diffusion coefficient values is different for the investigated compounds and in part correlated to their strength as electrolytes and their charge status. In fact, while ABTS and Fe(CN)₆³⁻ are only slightly hindered and the diffusion coefficients decrease by ~30%, the positive charged osmium complex is more affected and the diffusion coefficient decreases by ~50%; on the other hand, the weak electrolytes FcCOOH, catechol and dopamine are much more hindered and the diffusion coefficients are disrupted by ~70-80%. Finally is interesting to note that Fe(CN)₆⁴⁻ shows a completely different behaviour with respect to the other negative charged compounds since its *D* value is the most affected and it decreases by ~90%.

This clearly suggests that the polymeric structure of PAP is charged and this charge plays a crucial role in disrupting the diffusion of the selected compounds towards the electrodic surface. In fact, the deposited matrix structure is characterised by the presence of protonable moieties such as nitrogen atoms, and amide groups, that can cause a variable influence on the diffusion coefficients. For instance, the positive charged polymeric structure of PAP, probably cause a repulsion towards the osmium complex reducing of a significative extent the corresponding diffusion coefficient value. Similarly, also the substrates which are weak electrolytes could be hindered by electrostatic interactions

³² (a) Bodor S., Zook J. M., Lindner E., Toth K., Gyurcsanyi R. E. *Analyst (Cambridge, U. K.)* **2008**, *133*, 635-642; (b) Yin Y., Zhang H., Nishinari K. *J. Phys. Chem. B* **2007**, *111*, 1590-1596; (c) Yamauchi A., Mishima Y., EL Sayed A. M., Sugito Y. *J. Membr. Sci.* **2006**, *283*, 386-392; (d) Henry R. M., Ford C. A., Pyati R. *Solid State Ionics* **2002**, *146*, 151-156; (e) Crumbliss A.L., Perine S.C., Edwards A. K., Rillema D. P. *J. Phys. Chem. B* **1992**, *96*, 1388-1394.

between the protonated nitrogen atom of PAP and the –COOH and –OH groups present in their side chain. A possible interaction between catechol (and the same could also occur for dopamine) with PAP is showed in the Scheme 2.3.



Scheme 2.3 Possible interaction of catechol with PAP.

Besides this tentative approach based on electrostatic repulsion gives some explanation about the observed different behaviours, it is far from being exhaustive: in fact, $\text{Fe}(\text{CN})_6^{4-}$ shows a different behaviour with respect to the other negative charged compounds which seems to be unexplainable particularly in comparison to the behaviour of $\text{Fe}(\text{CN})_6^{3-}$. In addition, also the variation of the concentration value inside the PAP film for $\text{Fe}(\text{CN})_6^{4-}$ is puzzling: in fact, besides for all the considered compounds (including $\text{Fe}(\text{CN})_6^{3-}$) the concentration in the deposited matrix increases at increasing temperature, $\text{Fe}(\text{CN})_6^{4-}$ not only shows an opposite trend (i.e. it decreases at increasing temperature) but also the calculated values are noticeably higher with respect to all the other values. Moreover, when the polymer film is examined in a qualitative manner using a 10x magnification optical microscope, although it appears flat, transparent and hydrated after being used in presence of all the considered compounds, in the case of $\text{Fe}(\text{CN})_6^{4-}$ it becomes opaque and dry.

An explanation that well fits all these experimental evidences, could be the tendency of $\text{Fe}(\text{CN})_6^{4-}$ to form a stable ionic couple with quaternary ammonium ions while conversely, $\text{Fe}(\text{CN})_6^{3-}$ shows no effect at all under the same conditions.³³ In fact, with respect to $\text{Fe}(\text{CN})_6^{3-}$: i) the diffusion coefficient for $\text{Fe}(\text{CN})_6^{4-}$ is ten-fold lower, ii) the concentration in polymer film is about ten-fold higher and iii) the latter decreases for increasing temperature according to the thermolability of the ionic couple.

The heterogeneous electron transfer rate constants k_s of the compounds, at different temperatures, were also determined as described above. Figure 2.5 shows the steady-state voltammograms of the oxidation of FcCOOH in the range of temperature of 288-308 K.

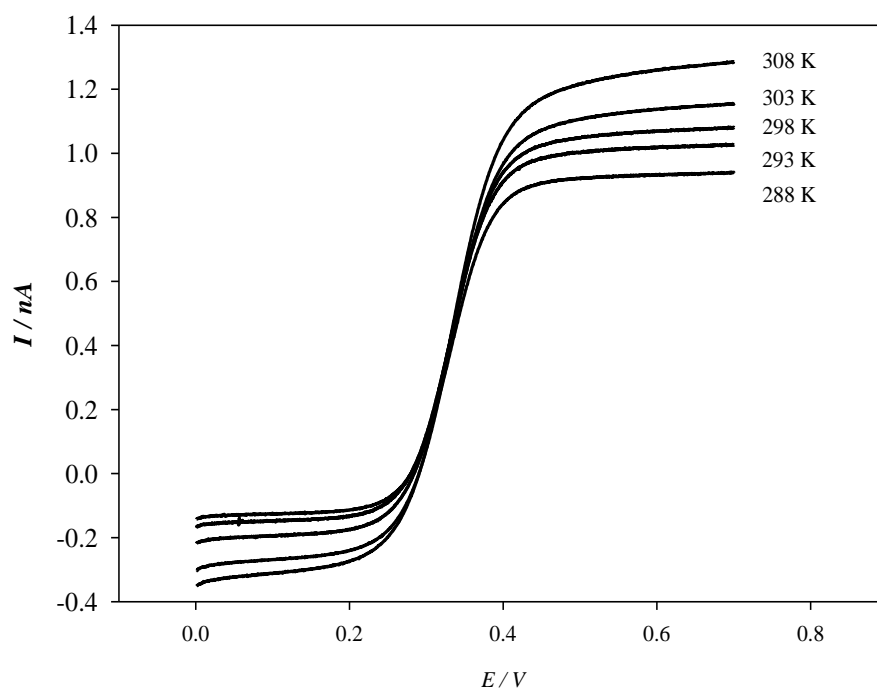


Figure 2.5 Steady-state voltammograms for FcCOOH 1 mol L⁻¹ in KCl 0.1 mol L⁻¹ obtained at different temperatures using a platinum microelectrode in presence of PAP film.

³³ Cohen S.R., Plane R.A. *J. Phys. Chem.* **1957**, *61*, 1096-1100.

The obtained results for all the substrates are listed in Table 2.3. Also in this case an increase in the heterogeneous rate constants with increasing the temperature was observed and the correlation with the diffusion coefficient values is very good (plots of k_s vs. D give a straight line with $R^2 > 0.99$). Hence, also in the case of the k_s values the same trend seen for the diffusion coefficients (i.e. correlated to electrostatic properties of the considered compounds already), is observed.

2.3.4 Calculation of Activation Energies for Diffusion and Heterogeneous Electron Exchange

The Arrhenius equations²⁰ below relate the diffusion coefficient D of electroactive species and the heterogeneous electron transfer rate constant k_s , to the temperature T :

$$D = D_{\infty} \exp(-E_{a,D}/RT) \quad (10)$$

$$k_s = A \exp(-E_{a,et}/RT) \quad (11)$$

where D_{∞} is a constant corresponding to the hypothetical diffusion coefficient at infinite temperature, E_a is the activation energy of the considered process and the other symbols have their usual meaning. Data obtained at different temperatures for both D and k_s using the microelectrode either in presence or in absence of PAP have been plotted in order to calculate the corresponding activation energy. For the sake of shortness only the plots obtained using the PAP-covered microelectrode are reported herein: in particular, Figure 2.6 shows the resulting plots of $\ln D$ vs T^{-1} and Figure 2.7 shows the resulting plots of $\ln k_s$ vs T^{-1} , respectively. The corresponding calculated values for the activation energies of diffusion and heterogeneous electron exchange, are summarised in Table 2.4.

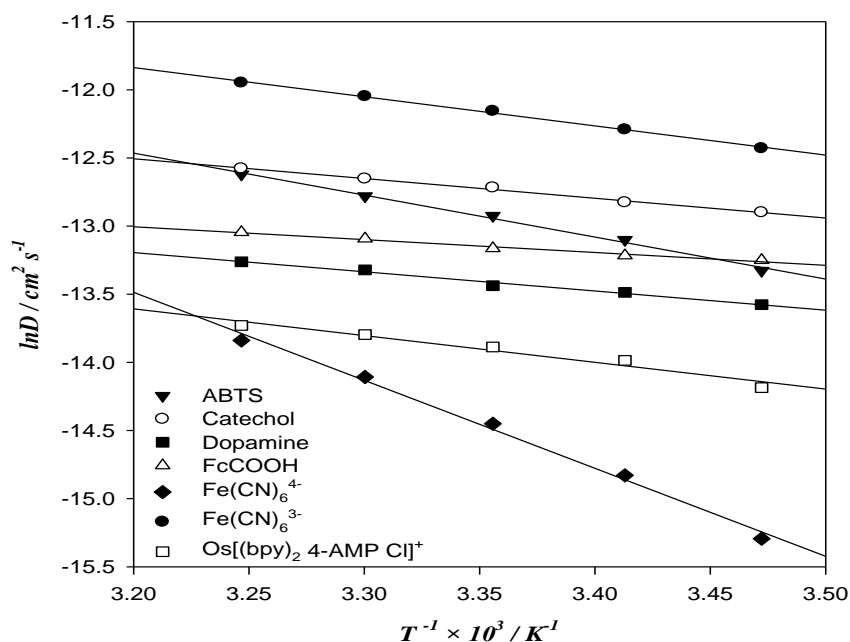


Figure 2.6 Calculated diffusion coefficient variation vs temperature for all the considered compounds 1 mol L⁻¹ solutions in KCl 0.1 mol L⁻¹; all other experimental conditions are the same reported in the text. The dots represent the experimental points which are fitted to the Arrhenius equation (solid lines).

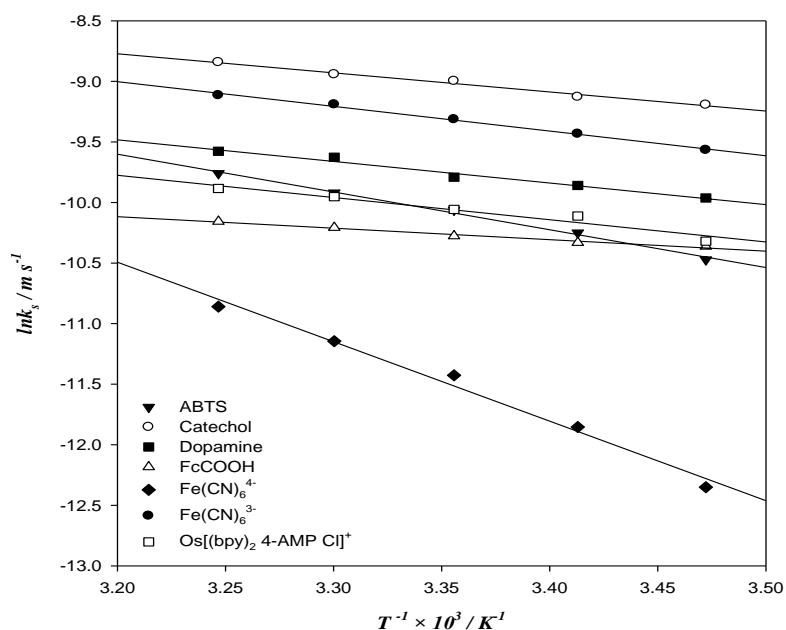


Figure 2.7 Calculated heterogeneous electron transfer constant variation vs temperature for all the considered compounds 1 mol L⁻¹ solutions in KCl 0.1 mol L⁻¹; all other experimental conditions are the same reported in the text. The dots represent the experimental points which are fitted to the Arrhenius equation (solid lines).

Table 2.4 Calculated activation energies for diffusion and for heterogeneous electron transfer for all the considered compounds 1 mol L⁻¹ solutions in KCl 0.1 mol L⁻¹ using a platinum microelectrode either in absence and in presence of PAP film.

Compound	$E_{a,D}$ (kJ mol ⁻¹) in solution	$E_{a,D}$ (kJ mol ⁻¹) in PAP	$E_{a,et}$ (kJ mol ⁻¹) in solution	$E_{a,et}$ (kJ mol ⁻¹) in PAP
ABTS	19.9	21.2	23.3	25.9
Catechol	19.0	12.1	19.8	13.1
Dopamine	18.2	11.7	18.3	14.8
FcCOOH	18.9	7.9	15.7	7.9
Fe(CN) ₆ ⁴⁻	17.5	53.5	23.4	54.4
Fe(CN) ₆ ³⁻	15.6	18.2	15.4	16.9
Os[(bpy) ₂ 4-AMP Cl] ⁺	32.9	16.3	34.1	20.4

As it can be noticed, passing from the situation in which the substrates are free to diffuse from the solution to that one where the substrates are hindered by the presence of PAP film, a negligible increase of the activation energies is observed for the both ABTS and Fe(CN)₆³⁻ while a halfway decrease is detected for the other ones except for Fe(CN)₆⁴⁻. Again, the unexpected behaviour of Fe(CN)₆⁴⁻ could be explained taking into account the previously discussed hypothesis of the formation of an ionic couple between the complex and the deposited matrix, resulting in a reduction of the mobility of the compound also confirmed by the three-fold increase in activation energies.

Nevertheless, the calculated values of activation energies for diffusion and heterogeneous electron transfer, measure the effect of temperature variation on the values of D and k_s , respectively. It can be concluded that the presence of PAP disrupts the influence of temperature as follows: it is i) practically the same for ABTS and Fe(CN)₆³⁻, ii) about halfway decreased for catechol, dopamine, FcCOOH and Osmium complex and iii) three-fold greater for Fe(CN)₆⁴⁻.

2.4 Conclusions

The properties of PAP film toward the diffusion and electron exchange of a series of seven simple redox molecules has been studied by steady-state voltammetry and potential-step chronoamperometry. Diffusion coefficients, concentration of the compounds in the deposited matrix and heterogeneous rate constants have been reported as a function of temperature. Also the influence of temperature on the parameters above, have been evaluated calculating the activation energies from the relative Arrhenius equations. Even if D and k_s values in the presence of PAP are smaller than in solution, this reduction is enough small to indicate that the PAP film shows excellent diffusion and electron exchange properties, with respect to other polymer films frequently used and reported in literature. The results indicate a very good permeability of the PAP layer to classical electrochemical mediators, except for $\text{Fe}(\text{CN})_6^{4-}$ whose performances are probably disrupted by the formation of a quite stable ionic couple with the polymeric structure of the hydrogel. This is of great importance in view of the use of PAP as immobilising agent in second-generation biosensors development.

Chapter 3

Electrokinetic Characterisation of Different Laccases

3.1 Introduction

3.1.1 Laccases

Laccases (*p*-diphenol: oxygen oxidoreductase, E.C: 1.10.3.2) are copper containing oxidoreductases detected in many plants and secreted by numerous fungi, as well as bacteria and insects.¹ They are able to oxidise many different substrates, i.e. *ortho*- and *para*-diphenols, aminophenols, aryl diamines, polyphenols, polyamines, and lignin, as well as some inorganic ions, with the contemporary reduction of molecular dioxygen to water,² according to the reaction depicted in Figure 3.1.

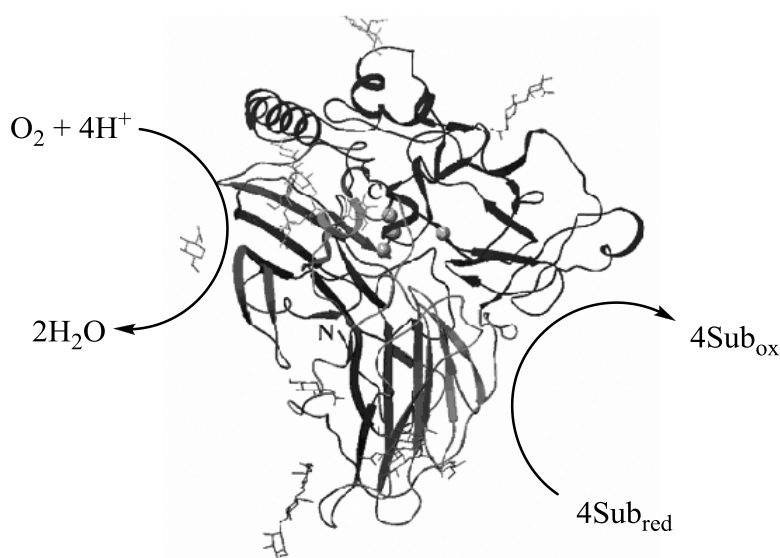


Figure 3.1 Representation of the catalytic cycle of Laccase.

¹ (a) Gramss G., Voigt K.-D., Firsche B. *Chemosphere* **1999**, *38*, 1481-1494; (b) Luterek J., Gianfreda L., Wojtas-Wasilewska M., Rogalski J., Jaszek M., Malarczyk E., Dawidowicz A., Ginalska G., Leonowicz A. *Acta Biochim. Pol. Acta* **1997**, *46*, 297-311; (c) Ten Have R., Teunissen P. J. M. *Chem. Rev.* **2001**, *101*, 3397-3413; (d) Martins L. O., Soares C. M., Pereira M. M., Teixeira M., Costa T., Jones G. H., Henriques A. O. *J. Biol. Chem.* **2002**, *277*, 18849-18859.

² (a) Xu F. *Biochemistry* **1996**, *35*, 7608-7614; (b) Yaropolov A. I., Skorobogatko O. V., Vartanov S. S., Varfolomeyev S. D. *Appl. Biochem. Biotechnol.* **1994**, *49*, 257-280.

where Sub_{ox} and Sub_{red} are the oxidised and the reduced forms of the substrate, respectively.

The first Laccase was extracted in 1883 from the tree of Japanese lacquer, *Rhus vernicifera*.³ Subsequently, the Laccases have been discovered in many other plants such as poplar,⁴ tobacco⁵ and peach.⁶ In the plants, the Laccases have the function of oxidise the phenolic units of hydroxycinnamic acids to phenoxyl radicals, that are the first step of lignification.⁷ Moreover, these enzymes are involved in the first-stage repair of laceration of the leaves.⁵

The purification of Laccases is often difficult, because the plant extract contains a great number of enzymes. The major part of Laccases, that have been characterised, are from fungi of different species, as *Agaricus bisporus*,⁸ *Botrytis cinerea*,⁹ *Chaetomium thermophilum*,¹⁰ *Coprinus cinereus*,¹¹ *Pycnoporus cinnabarinus*,¹² *Phlebia radiata*,¹³ *Melanocarpus albomyces*,¹⁴ *Trametes versicolor*¹⁵ and *Trametes hirsuta*.¹⁶

The physiologic roles of Laccases are different, for example those from fungi of the family of *white-rot*, as *Trametes versicolor* and *Pycnoporus cinnabarinus*, oxidise the phenolic

³ Levine W.G. *The Biochemistry of Copper*, Academic Press Inc., New York **1965**, 371-385.

⁴ Ranocha P., McDougall G., Hawkins S., Stejiades R., Borderies G., Stewart D., Cabanes-Macheteau M., Boudet A. M., Goffner D. *Eur. J. Biochem.* **1999**, *259*, 485-495.

⁵ De Marco A., Roubelakis-Angelakis K. A. *Phytochemistry* **1997**, *46*, 412-425.

⁶ Lehman E., Harel E., Mayer A. M. *Phytochemistry* **1974**, *13*, 1713-1717.

⁷ (a) Mayer A. M., Staples R. C. *Phytochemistry* **2002**, *60*, 551-565; (b) Gavnholt B., Larsen K. *Physiol. Plant.* **2002**, *116*, 273-280.

⁸ Wood D. A. *J. Gen. Microbiol.* **1980**, *117*, 327-338.

⁹ Marbach I., Harel E., Mayer A. M. *Phytochemistry* **1984**, *23*, 2713-2717.

¹⁰ Chefetz B., Chen Y., Hadar Y. *Appl. Environ. Microbiol.* **1998**, *64*, 3175-3179.

¹¹ Schneider P., Caspersen M. B., Mondorf K., Halkier T., Skov L. K., Østergaard P. R., Brown K. M., Xu F. *Enz. Microb. Technol.* **1999**, *25*, 502-508.

¹² Eggert C., Temp U., Erikson K. E. L. *Appl. Environ. Microbiol.* **1996**, *62*, 1151-1158.

¹³ Niku-Paavola M. L., Karhunen E., Salola P., Raunio V. *Biochem J.* **1998**, *254*, 877-884.

¹⁴ Kiiskinen L. L., Viikari L., Kruus K. *Appl. Environ. Microbiol.* **2002**, *59*, 198-204.

¹⁵ Rogalski J., Lundell T., Leonowics A., Hatakka A. *Acta Microbiol. Polon.* **1991**, *40*, 221-234.

¹⁶ Koroljova-Skorobogatko O. V., Stepanova E. V., Gavrilova V. P., Morozova O. V., Lubimova N. V., Dzchafarova A. N., Jaropolov A. I., Makower A. *Biotechnol. Appl. Biochem.* **1998**, *28*, 47-54.

subunits, participating to the biodegradation of lignin,¹⁷ while the Laccase from *Aspergillus nidulans* regulates the production of pigments.¹⁸

During the past decades, oxidoreductases enzymes have received a great attention in the environmental and biotechnological fields because of their great potential to catalyse a great variety of redox processes with no hazardous side effects.¹⁹ Therefore, Laccase has been applied to many industrial processes including decolourisation of dyes,²⁰ pulp delignification,²¹ oxidation of organic pollutants,¹⁹ microbial transformation of natural products²² and the development of biosensors²³ or biofuel cells.²⁴

3.1.2 Laccase Structure and Catalytic Mechanism

The crystal structure of Laccases was determined only for a small number of them. The fungal Laccases, as well as the cupredoxin, are characterised by the presence of three domains (A, B and C) of comparable size.²⁵ All three domains are important for the catalytic activity, in fact, the binding site of the substrate is placed in a cavity between the domains B and C, a mononuclear copper centre is located in domain C and a trinuclear copper site is located at the interface between domains B and C. The mononuclear centre is constituted by a type-1 copper atom (T1), trigonally coordinated with two histidine and one

¹⁷ Hatakka A. *Biopolymers. Lignin, Humic Substances and Coal*, Vol. 1 (Hofrichter M. and Steinbüchel A., Eds.), Wiley-VCH, Weinheim, Germany **2001**, 129-180.

¹⁸ Adams T. H., Wieser J. K., Yu J. H. *Microbial. Mol. Biol. Rev.* **1998**, *62*, 35-54.

¹⁹ Lante A., Crapisi A., Krastanov A., Spettoli P. *Process Biochem.* **2000**, *36*, 51-58.

²⁰ Abadulla E., Tzanov T., Costa S., Robra K.-H., Cavaco-Paulo A., Gubitz G. M. *Appl. Environ. Microbiol.* **2000**, *66*, 3357-3362.

²¹ Crestini C., Argyropoulos D. S. *Bioorg. Med. Chem.* **1998**, *6*, 2161-2169.

²² Hosny M., Rosazza J. P. N. *J. Agric. Food Chem.* **2002**, *50*, 5539-5545.

²³ (a) Gomes S. A. S. S., Nogueira J. M. F., Rebelo M. J. F. *Biosens. Bioelectron.* **2004**, *20*, 1211-1216; (b) Freire R. S., Duran N., Kubota L. T. *Anal. Chim. Acta* **2002**, *463*, 229-238; (c) Freire R. S., Duran N., Kubota L. T. *Talanta* **2001**, *54*, 681-686; (d) Jaroz-Wilkolazka A., Ruzgas T., Gorton L. *Talanta* **2005**, *66*, 1219-1224; (e) Vianello F., Cambria A., Ragusa S., Cambria M. T., Zennaro L., Rigo A. *Biosens. Bioelectron.* **2004**, *20*, 315-321; (f) Jaroz-Wilkolazka A., Ruzgas T., Gorton L. *Enzyme Microb. Technol.* **2004**, *35*, 238-241; (g) Gomes S. A. S. S., Rebelo M. J. F. *Sensors* **2003**, *3*, 166-175.

²⁴ Tayhas G., Palmore R., Kim H.-H. *J. Electronanal. Chem.* **1999**, *464*, 110-117.

²⁵ (a) Pinotek K., Antorini M., Choinowski T. *J. Biol. Chem.* **2002**, *277*, 37663-37669; (b) Antorini M., Herpoel-Gimbert I., Choinowski T., Sigoillot J. G., Asther M., Winterhalter K., Pinotek K. *Biochim. Biophys. Acta* **2002**, *1594*, 109-114.

cysteine residues (the covalent bond between T1 and the sulphur cysteine atom gives to Laccase the typical blue coloration).²⁶ Instead, the trinuclear cluster is constituted by one type-2 copper atom (T2) and two type-3 copper atoms (T3). The atoms T1 and T2 are paramagnetic and they can be detected with the electronic paramagnetic resonance spectroscopy (EPR), while the couple T3 is inactive at the EPR because of the antiferromagnetic coupling between the two ions and the presence of a bridging oxydrilic ligand.²⁶

As said, Laccases oxidise diphenols with the consumption of molecular oxygen as electron acceptor. Unlike other enzymes, that are very specific with respect to a substrate or a class of them, Laccases catalyse the oxidation of many compounds. The substrate of the Laccase, when oxidised, loose one electron to form a free radical²⁷ which could incurs in subsequent oxidations catalysed by the Laccase or non enzymatic processes, as hydration, polymerisation and disproportion. Among the substrates of the Laccases, some of the most important are 2,2'-azinobis(3-ethylbenzothiazoline-6-sulfonate) (ABTS), syringaldazine, *p*-diphenol, 1-naphtol, 1-hydroxy-4-methylbenzene (*p*-cresol), 2-methoxyphenol (guaiacol), 1-hydroxybenzotriazole (HBT) and *N*-hydroxyphthalimide (HPI). In Figure 3.2 is showed the catalytic oxidation of ABTS (a non-phenolic substrate) and *p*-diphenol (a phenolic substrate).

It is assumed that the Laccase catalysis firstly involves T1 site reduction by the substrate, followed by internal electron transfer from T1 to T2 and T3 sites and, finally, dioxygen reduction at T2 and T3 sites. A catalytic cycle involves the overall transfer of four electrons from T1 to T2/T3 cluster, probably through the bonds of the tripeptide His-Cys-His or through-space.²⁸

²⁶ Solomon E. I., Sundaram U. M., Machonkin T. E. *Chem. Rev.* **1996**, *96*, 2563-2606.

²⁷ Thurston C. *Microbiology* **1994**, *140*, 19-26.

²⁸ Bertrand T., Jolivald C., Briozzo P., Caminade E., Joly N., Madzak C., Mougin C. *Biochemistry* **2002**, *41*, 7325-7333.

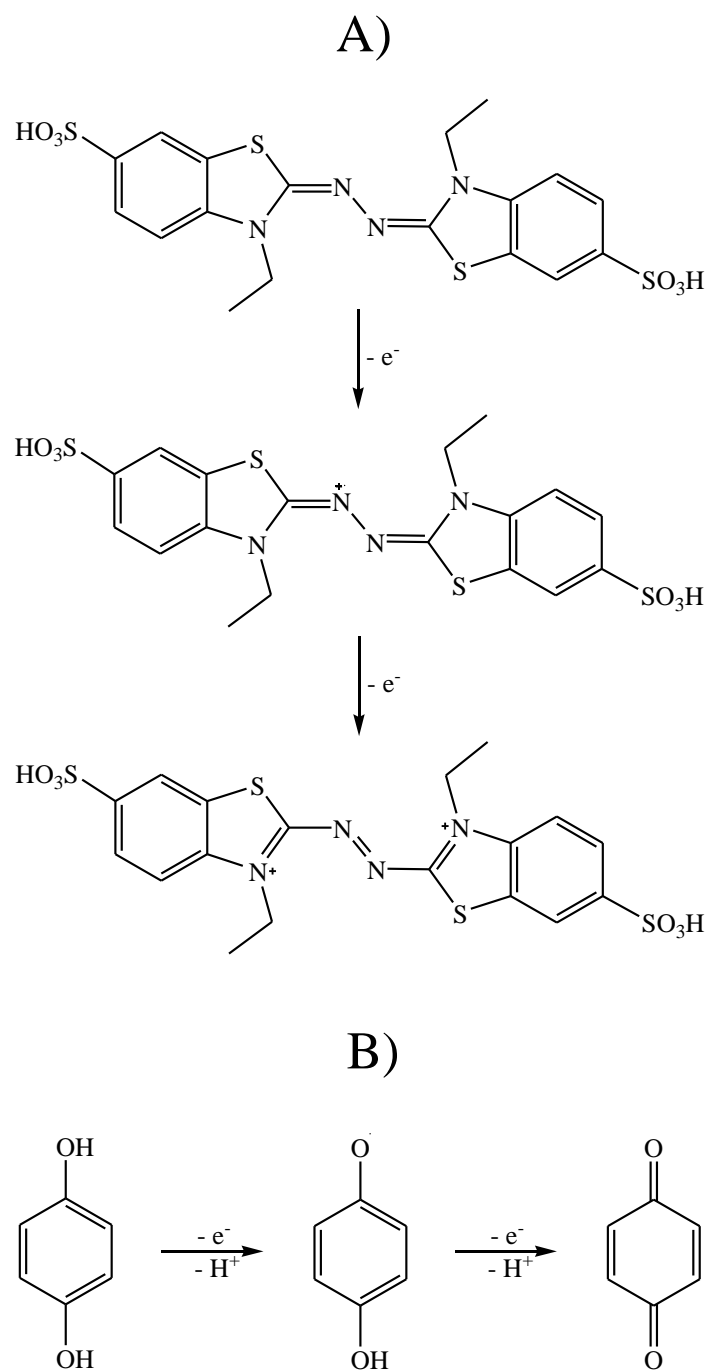


Figure 3.2 Schematic illustration of the Laccase catalyzed oxidation of ABTS (A) and *p*-diphenol (B).

The reaction mechanism of the Laccases has been studied, following the coordination states of the copper atoms during the reaction cycle, with the use of spectroscopic methods (EPR), magnetic circular dichroism (MCD) and X-ray absorption spectroscopy (XAS),

however, the reduction mechanism of molecular oxygen in the trinuclear centre is still unclear.^{26,29}

A chemical compound must have two peculiar features to be a good substrate of Laccase: i) it must be able to interact with the copper site T1 (this is related to the nature and position of the substituents on its phenoxylic ring)^{2a,28} and ii) it must have a redox potential low enough, because the reaction rate depends on the difference of potential between enzyme and substrate.³⁰

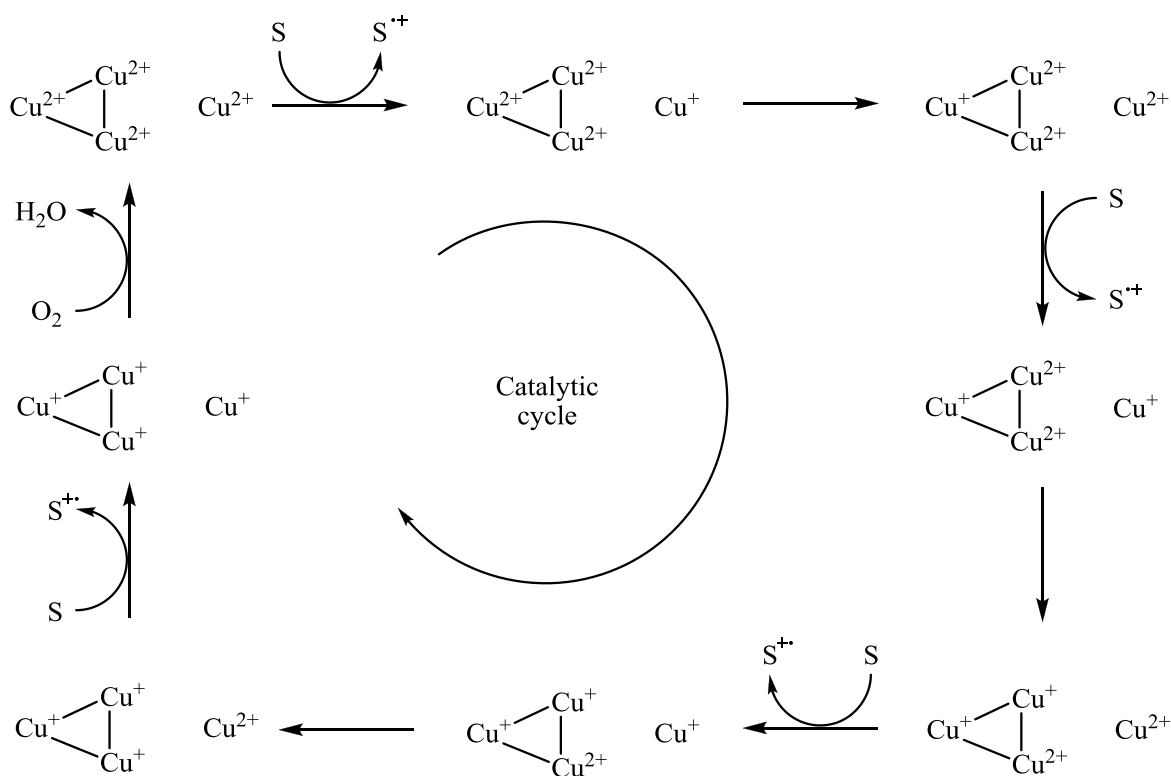
An important feature of the Laccase enzyme is the standard redox potential of the T1, T2 and T3 sites. The redox potential of the copper T1 has been determined through spectrophotometric titration, with the use of different redox mediators, and it has been found that it ranges between 430 and 780 mV vs NHE.³¹

The fact that the catalytic efficiency of a Laccase depends on the redox potential of the T1 site (i.e., higher is the redox potential and higher is the efficiency), suggests that the limiting step of the enzymatic reaction is the electron transfer from the substrate to the protein, in particular to the T1 site.^{30a} As already said, the catalytic cycle starts with the transfer of one electron from the substrate to the T1 site of the Laccase, that transfer it to the T2/T3 cluster. This first step is repeated four times, until a completely reduced Laccase was formed. In this situation the initially double charged copper atoms (i.e. Cu(II)) have been reduced to Cu(I). Subsequently, a single molecule of oxygen oxidise the reduced Laccase, probably through a peroxydic intermediate, with the formation of water (Scheme 3.1).

²⁹ Lee S. K., George S. D., Antholine W. E., Hedman B., Hodgson K. O., Solomon E. I. *J. Am. Chem. Soc.* **2002**, *124*, 6180-6193.

³⁰ (a) Xu F., Kulys J. J., Duke K., Li K., Krikstopaitis K., Deussen H. J., Abbate E., Galinyte V., Schneider P. *Appl. Environ. Microbiol.* **2000**, *66*, 2052-2056; (b) Xu F., Deussen H. J., Lopez B., Lam L., Li K. *Eur. J. Biochem.* **2001**, *268*, 4169-4176.

³¹ (a) Reinhammar B. R. M. *Biochim. Biophys. Acta* **1972**, *275*, 245-259; (b) Schneider P., Caspersen M. B., Mondorf K., Halkier T., Skov L. K., Østergaard P. R., Brown K. M., Brown S. H., Xu F. *Enzyme Microb. Tech.* **1999**, *25*, 502-508.



Scheme 3.1 Catalytic cycle of Laccase active site

From an electrochemical point of view, Laccases can be divided into three main groups, depending on T1 site redox potential: i) low potential Laccases, that include those from plants, as for example the Laccase from *Rhus vernicifera*, that have a redox potential of about 430 mV vs NHE;^{31a} ii) medium potential Laccases include those from fungi, as that from *Myceliophthora thermophila*, having a redox potential ranging from 470 to 710 mV vs NHE;^{2a} iii) high potential Laccases (*Trametes versicolor*, *Trametes hirsuta*) that have a redox potential around 780 mV vs NHE.³² The Laccase potential is influenced by the coordination sphere in active site and it has been hypothesised that the axial ligand has a crucial role in determining it. In fact, Laccases that have a phenylalanine residue as axial

³² Koroleva O. V., Yavmetdiov I. S., Shleev S. V., Stepanova E. V., Gavrilova V. P. *Biochemistry* (Moscow) **2001**, 66, 618-622.

ligand possess an high redox potential, while those with a leucine have a low redox potential.³³

3.1.3 Laccases Applications

Oxidation reactions are widely used in industrial processes, for example in textile and wood processing fields, and in chemical industries. Many methods used are not suitable both economically and environmentally, because they produce unwanted reactions and the chemicals used are often hazardous. The enzymatic oxidation is a potential alternative to chemical methods, because enzymes are very specific, efficient and environmentally sustainable. The Laccases, because of their ability to oxidise a wide range of substrates, are considered to be particularly interesting in the industrial field. In fact, they are widely used in paper production, where, coupled with low molecular weight redox mediators, ensure high yields of bleaching with a low environmental impact.³⁴ In these processes, Laccase oxidises the mediator, which in turn promotes the oxidation of subunits of lignin that would otherwise not be oxidised by Laccase due to problems arising from the redox potential and steric hindrance (Figure 3.3).

³³ Eggerd C., LaFayette P. R., Temp U., Eriksson K. E. L., Dean J. F. D. *Appl. Environ. Microbiol.* **1998**, *64*, 1766-1772.

³⁴ (a) Soares G. M. B., Pessoa de Amorim M. T., Costa-Ferreira M. *J. Biotechnol.* **2001**, *89*, 123-129; (b) Barreca A. M., Fabbrini M., Galli C., Gentili P., Ljunggren S. *J. Mol. Cat. B: Enzym.* **2003**, *26*, 105-110; (c) Barreca A. M., Sjögren B., Fabbrini M., Galli C., Gentili P. *Biocatal. Biotransform.* **2004**, *22*, 105-112.

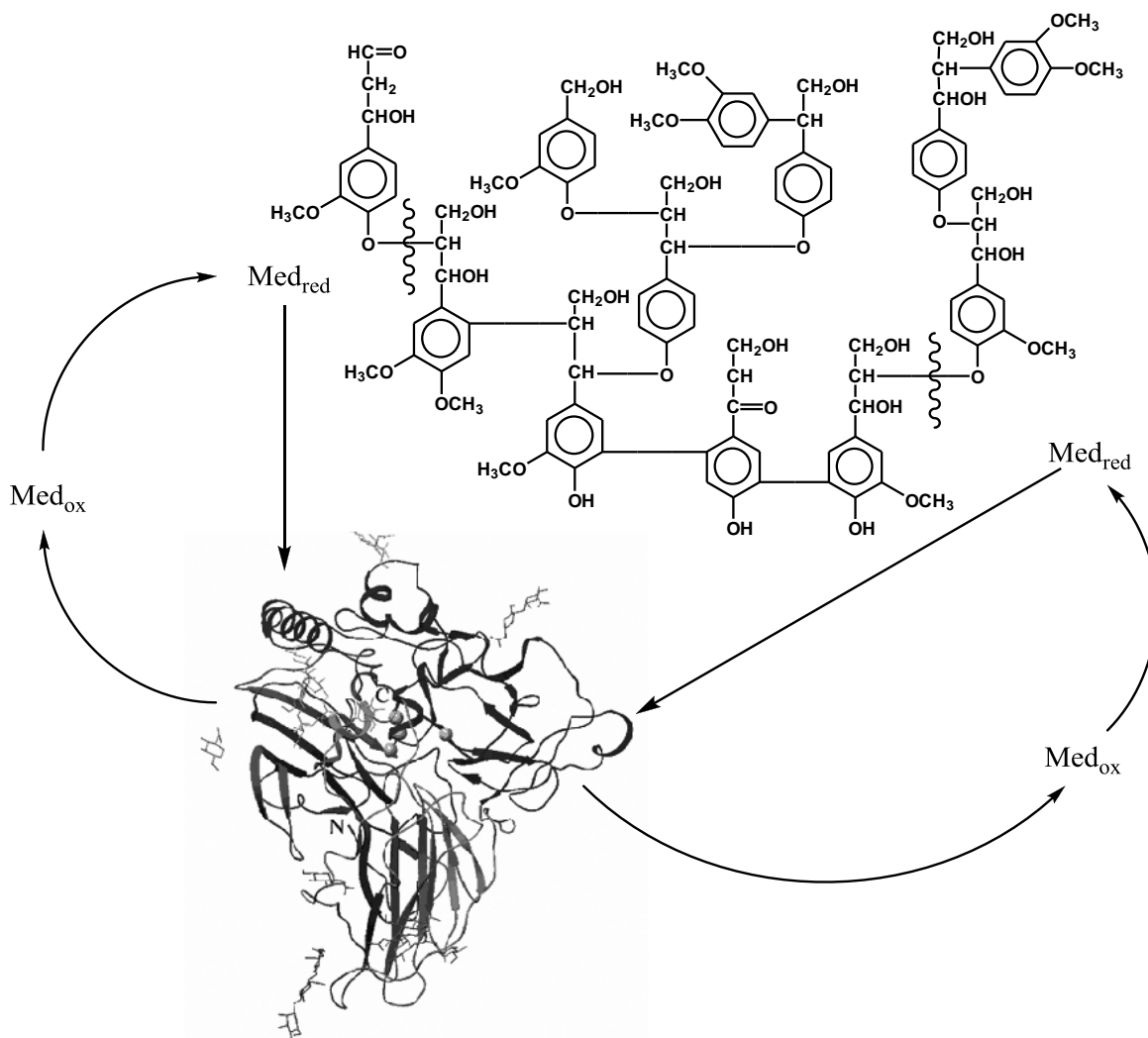


Figure 3.3 Lignin degradation mediated by Laccase

In addition to the ability of Laccases to catalyse electron transfer reactions with an enzyme-mediator mechanism, they are able to directly transfer electrons to an electrodic surface. Thanks to these features, in addition to the large variety of substrate that Laccases are able to oxidise, they are widely use in the development of second and third-generation biosensors for the detection of catecholamines³⁵ and polyphenols.³⁶ Moreover, thanks to the their high redox potential and to the use of molecular oxygen as final acceptor of electrons, Laccases can be utilised in the construction of the biofuel cells cathodic

³⁵ Ferry I., Leech D. *Electroanalysis* **2005**, *17*, 113-119.

³⁶ (a) Jarosz-Wilkolazka A., Ruzgas T., Gorton L. *Talanta* **2005**, *66*, 1219-1224; (b) Gamella M., Campuzano S., Reviejo J., Pingarrón J. M. *J. Agric. Food Chem.* **2006**, *54*, 7960-7967.

compartments.³⁷ The biofuel cells are defined as fuel cells that convert, with high efficiency, chemical energy in electric energy, exploiting a biocatalytic process.³⁸ With respect to a traditional fuel cell, the introduction of an enzyme allows to not separate the compartments (i.e. anodic and cathodic) to use milder experimental conditions and to utilise as fuel a great variety of renewable chemicals. A functional biofuel cell should have enzymes with high chemical efficiency, stability and economicity. Moreover, the redox potential of the anodic compartment must be as low as possible (viceversa for the cathodic compartment) to ensure the maximum possible difference of potential. Finally, the bioelectrocatalysis process requires the development of mediators and enzymatic immobilisation methodologies that ensure a continuous and efficient electron transfer between enzymes and electrodes.^{38c} In Figure 3.4 an example of biofuel cell that uses glucose as fuel and molecular oxygen as oxidant, is showed.³⁹ It is composed as follows: i) in the anodic compartment the electron transfer is constituted by the complex PQQ-FAD-GOx, that oxidises glucose to gluconic acid; ii) in the cathodic compartment the oxygen reduction relies on Laccase. The use of molecular oxygen as final acceptor of electrons allows to the system to work in air and this is a crucial advantage of the biofuel cells, that do not require a continuous flow of inert gas.

A final goal of the development of biofuel cells is their *in vivo* application but the major problems arising are the reduced lifetime of the used enzymes and the deterioration of the electrodic material utilised.⁴⁰

³⁷ (a) Soukharev V., Mano N., Heller A. *J. Am. Chem. Soc.* **2004**, *126*, 8368-8369; (b) Barrière F., Ferry Y., Rochefort D., Leech D. *Electrochem. Commun.* **2004**, *6*, 237-241; (c) Kamitaka Y., Tsujimura S., Setoyama N., Kajino T., Kano K. *Phys. Chem. Chem. Phys.* **2007**, *9*, 1793-1801.

³⁸ (a) Service R. F. *Science* **2002**, *296*, 1222-1224; (b) Kendall K. *Nature Mat.* **2002**, *1*, 211-212; (c) Calabrese Barton S., Gallaway G., Atanassov P. *Chem. Rev.* **2004**, *104*, 4867-4886.

³⁹ (a) Willner I. *Science* **2002**, *298*, 2407-2408; (b) Brunel L., Denel J., Servat K., Kokoh K. B., Jolivald C., Innocent C., Cretin M., Rolland M., Tingry S. *Electrochem. Commun.* **2007**, *9*, 331-336.

⁴⁰ Bullen R. A., Arnot T. C., Lakeman J. B., Walch F. C. *Biosens. Bioelectron.* **2006**, *21*, 2015-2045.

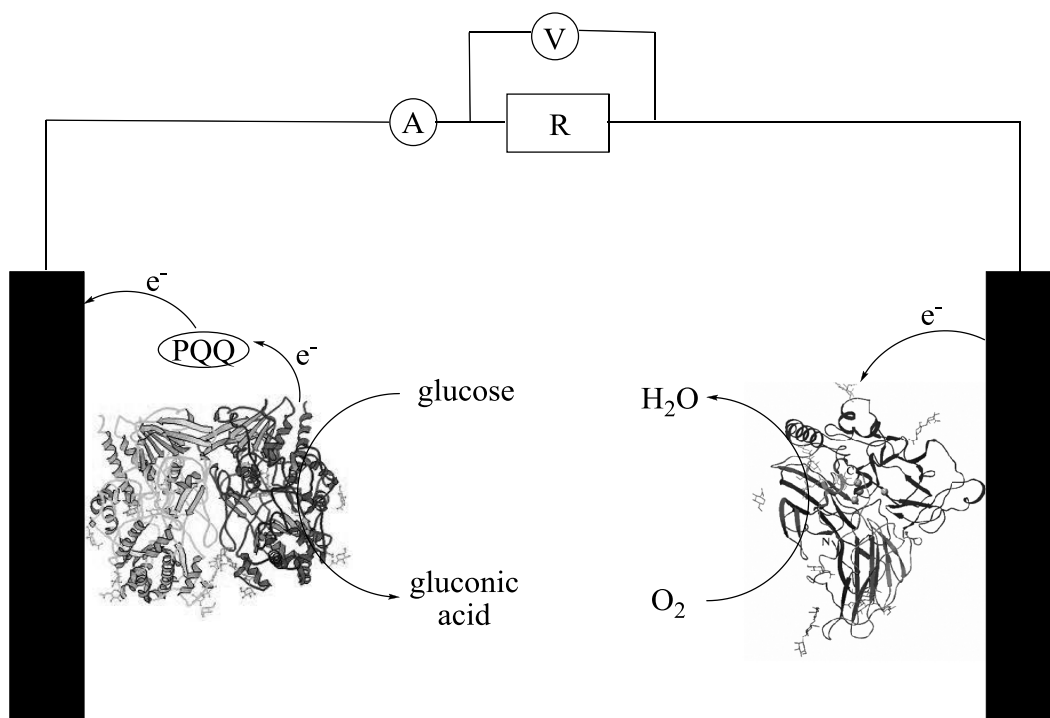


Figure 3.4 Schematic representation of a biofuel cell that uses glucose as fuel and molecular oxygen as oxidant.

3.2 Experimental Section

In this research a series of Laccases from different sources has been taken into account, in particular Laccase from *Lentinus edodes* (LeL), *Panus tigrinus* (PtL), *Trametes versicolor* (TvL) and *Trametes hirsuta* (ThL), and they have been studied from a kinetic point of view with different mediators by means of different electrochemical methods. LeL and PtL were adsorbed onto the electrode surface and the kinetic parameters were obtained for means of cyclic voltammetry (CV), while TvL and ThL, whose characterisation by means of CV has already been performed,⁴¹ were immobilised with PAP membrane onto the electrode and the kinetic parameters were obtained using chronoamperometry (CA).

3.2.1 Materials

4-hydroxy-3,5-dimethoxybenzaldehyde azine (syringaldazine), 2,2'-azino-bis(3-ethylbenzothiazoline-6-sulfonic acid) diammonium salt (ABTS), 1,2-dihydroxybenzene (catechol), 3,4,5-trihydroxybenzoic acid (gallic acid), 3-(3,4-Dihydroxyphenyl)-2-propenoic acid (caffeic acid), 3,4-dihydroxyphenethylamine (dopamine), 3,4-dihydroxy-L-phenylalanine (L-dopa), S-(-)- α -hydrazino-3,4-dihydroxy-2-methylbenzenepropanoic acid (carbidopa), 3-(3,4-dihydroxyphenyl)-2-methyl-L-alanine (methyl-dopa), ferrocene carboxylic acid (FcCOOH) and potassium hexacyanoferrate (II) ($K_4[Fe(CN)_6]^{3-}$) were used as received. Laccase from *Trametes versicolor* was supplied by Fluka (EC 1.10.3.2, activity: 30.6 U mg⁻¹, according to Sigma-Aldrich supplier, the enzyme content of this Laccase is approximately 10%), Laccases from *Lentinus Edodes* and *Panus Tigrinus* were gently donated by the Department of Agrobiological and Agrochemistry of the University of Tuscia (Viterbo, Italy), Laccase from *Trametes hirsuta* (3.9 mg ml⁻¹ in citrate buffer pH 5; activity: 421 U ml⁻¹) was gently donated by VTT Technical Research Centre of Finland.

⁴¹ Frascioni M., Favero G., Boer H., Koivula A., Mazzei F. *Biochim. Biophys. Acta* **2010**, 1804, 899-908.

The polymeric film used was poly-1-(aminomethyl)-1-{2-[(6-oxysesane)amino]ethyl}-3-hydroxyazetidinium chloride (polyazetidine prepolymer, PAP®), donated by Hercules Inc. Wilmington DE (USA). Other chemicals were all of analytical grade. High purity deionised water (Resistance: $18.2 \text{ M}\Omega \times \text{cm}$ at $25 \text{ }^\circ\text{C}$; $\text{TOC} < 10 \text{ }\mu\text{g L}^{-1}$) obtained from Millipore (France) has been used to prepare all the solutions.

3.2.2 Apparatus

Electrochemical experiments were performed by using a μ -Autolab type III potentiostat (Eco Chemie, Netherlands) controlled by means of the GPES Manager program. The measurements were performed in a thermostated 10 ml glass cell with a conventional three-electrode configuration: $\text{Ag}/\text{AgCl}/\text{Cl}^{-1}$ (Metrohm, Switzerland, 198 mV vs NHE) was used as reference electrode, a graphite rod as counter and different electrodic materials as working electrodes (see below).

All measurements were carried out in aerobic conditions in Britton-Robinson buffer 0.1 mol L^{-1} , pH 5.

3.2.3 Electrochemical Measurements with Laccase from *Lentinus edodes* and *Panus tigrinus*

Cyclic voltammetry (CV) measurements were performed with a typical three-electrodes system using Glassy Carbon (GC) as working electrode (diameter 3 mm). The GC electrode was first polished on alumina powder and then ultrasonically cleaned in water for about 5 minutes. The electrode was not used until reversible cyclic voltammetrical curves were observed in an aqueous solution containing 0.1 mol L^{-1} KCl and 1.0 mmol L^{-1} $\text{Fe}(\text{CN})_6^{3-}$.

In the voltammetric measurements, for all mediator concentrations was recorded a CV at a scan rate of 5 mV s^{-1} and then $5 \mu\text{l}$ of an enzyme solution 0.5 U ml^{-1} were deposited on the electrode surface and left dry for about 30 minutes. Then, was recorded another CV at same mediator concentration. The I_{lim} values were taken as the differences between the cathodic currents.

3.2.4 Electrochemical Measurements with Laccase from *Trametes versicolor* and *Trametes hirsuta*

Chronoamperometric (CA) batch experiments were performed with a conventional three-electrode configuration using MWCNT-SPE as working electrode. MWCNT-SPEs were preliminary treated by depositing on the working electrode $10 \mu\text{l}$ of 0.5 mol L^{-1} nitric acid solution as reported in literature⁴² in order to obtain the carboxyl functionalisation on their surface. The biosensors were prepared by depositing $3 \mu\text{l}$ of a solution of PAP, containing TvL or ThL, to have a final concentration of 0.8 U of enzyme onto the electrode surface. Then, the electrode were left to dry overnight at room temperature.

In the CA experiments, for all mediator concentrations the relative current response was recorded at a fixed potential where they are completely reduced and the I_{lim} values were took as the differences between the baseline and the amperometric signal obtained after every addition of mediator.

⁴² Kim S.N., Rusling J.F., Papadimitrakopoulos F. *Adv. Mat.* **2007**, *19*, 3214-3228.

3.3 Results and Discussion

3.3.1 Laccases from *Lentinus edodes* and *Panus tigrinus*

The determination of the kinetic parameters of the two Laccases was carried out using ABTS, syringaldazine, $\text{Fe}(\text{CN})_6^{4-}$, dopamine, catechol and FcCOOH as mediators. As said, the kinetic characterisation was performed using the enzymes adsorbed onto the electrode surface, in aerobic conditions and cyclic voltammetry as electrochemical method. Even if this kind of physical immobilisation is quite weak, however it is sufficient to carry out a single reproducible experiment. Moreover, in a previous work it was demonstrated that the kinetic parameters measured in the homogenous reaction system correlated well with those measured with the adsorbed enzymes. In addition, they are in good agreement with those reported with reference techniques, suggesting that the electrochemical methods employed (i.e. cyclic voltammetry with adsorbed Laccase modified GC electrode) can be applied well in place of the traditional techniques commonly used for the kinetic characterisation of Laccases.

In Figure 3.5 are reported the CVs, recorded at slow scan rate with a GC electrode, of the mediators in absence and in presence of Laccase from *Lentinus edodes*. As it can be seen, at slow scan rate a decrease of the oxidation peaks and an increase of the cathodic current of the mediator in presence of the enzyme, is observed. This variations means that the nature of the observed process changes from diffusive control (i.e. in absence of enzyme) to catalytic control (i.e. in presence of enzyme), marked by the characteristic sigmoidal curve.

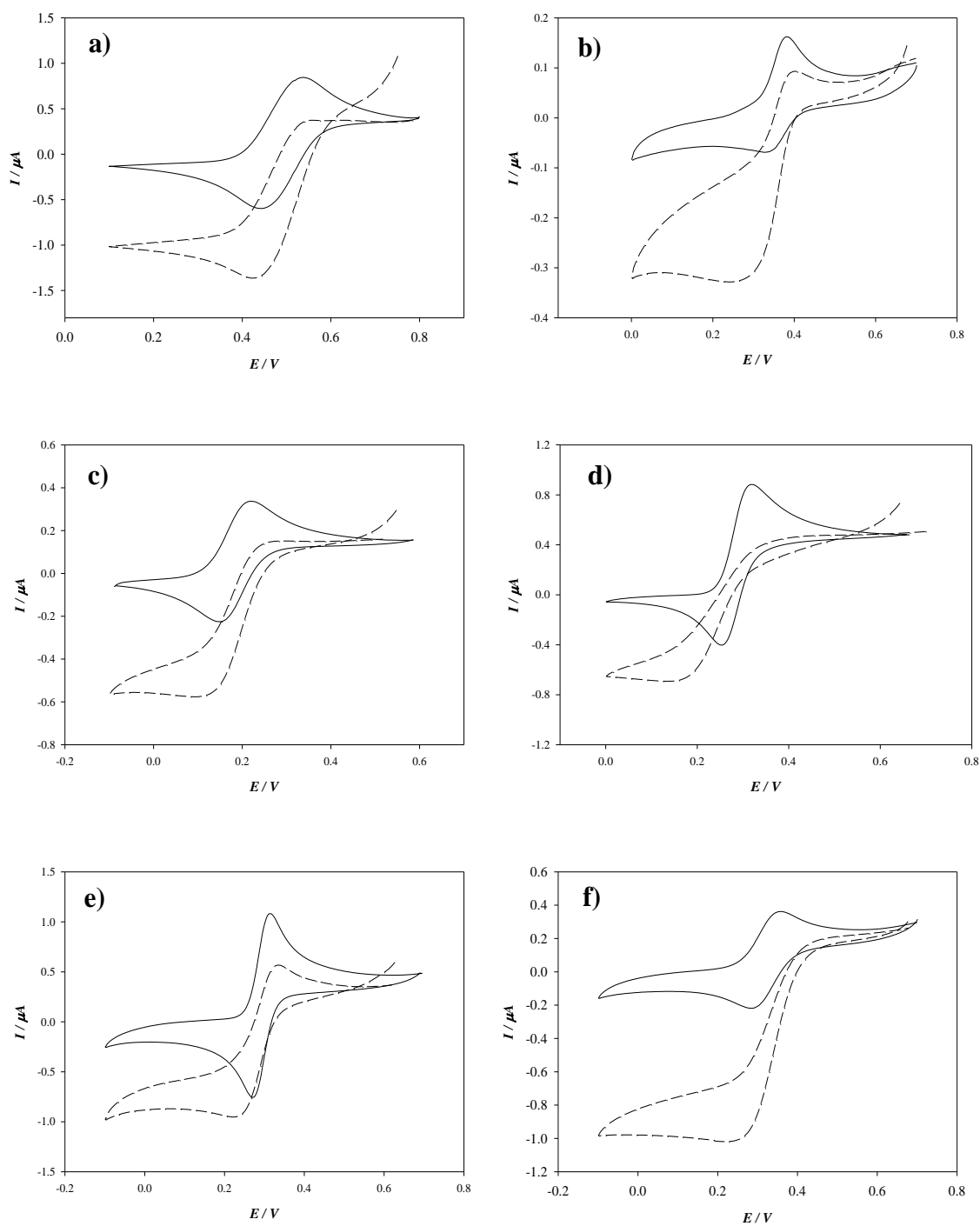
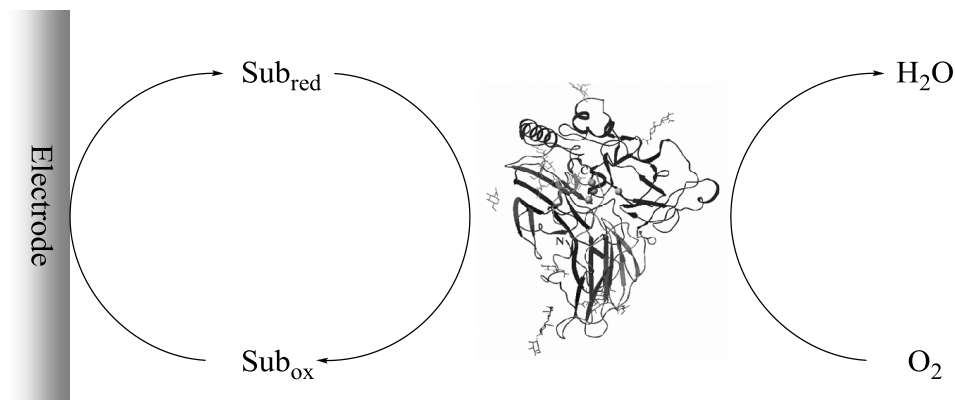


Figure 3.5 CVs recorded at a scan rate of 5 mV s⁻¹ in absence (solid line) and in presence (dashed line) of Laccase from *Lentinus edodes* adsorbed on the surface of GC electrode: a) ABTS 0.5 mmol L⁻¹; b) syringaldazine 0.02 mmol L⁻¹; c) Fe(CN)₆⁴⁻ 0.1 mmol L⁻¹; d) dopamine 0.1 mmol L⁻¹; e) catechol 0.1 mmol L⁻¹; f) FcCOOH 0.1 mmol L⁻¹.

At slow scan rate and in cathodic polarisation conditions, the mediators undergo an electronic shuttling between the enzyme and the electrode surface and are continuously

reduced by the electrode itself, with the concomitant reduction of the molecular oxygen borne by the enzyme, generating cathodic currents (catalytic currents) higher than those of the mediators alone, according with the reaction Scheme 3.2.



Scheme 3.2 Catalytic mediated reduction of the mediator

By the cyclic voltammograms, obtained as described, it is possible to get the diffusional current (i_d), recorded with the mediator in absence of enzyme, and the cathodic current (i_c), recorded with the mediator in presence of enzyme. The difference between these two current provides the limit current (I_{lim}), that is a measure of the catalytic current.

Because of the high Laccase affinity with the oxygen (the affinity constant K_{O_2} of the complex Laccase- O_2 ranges between 0.01 and 0.02 mmol L⁻¹)⁴³ and considering that in the experimental conditions the oxygen concentration in solution was about 260 μ mol L⁻¹, all the enzymatic active sites can be considered filled^{43a} by oxygen and the dependence of I_{lim} from the mediator concentration can be expressed by Equation 3.1.

$$I_{lim} = \frac{I_{max} [S_{ox}]}{[S_{ox}] + K_M^{app}} \quad (3.1)$$

⁴³ (a) Kuznetsov B. A., Shumakovich G. P., Koroleva O. V., Yaropolov A. I. *Biosens. Bioelectron.* **2001**, *16*, 73-84; (b) Rodakiewicz-Nowak J., Kasture S. M., Dudek B., Haber J. *J. Mol. Cat. B: Enzym.* **2000**, *11*, 1-11.

where $[S_{ox}]$ is the concentration of the oxidised mediator, I_{lim} is the catalytic current, K_M^{app} is the apparent Michaelis-Menten constant for the enzymatic reaction and I_{max} is the current at the steady-state, when all the active sites of the enzyme are substrate saturated. The kinetic parameters were obtained using the linearisation of Lineweaver-Burk expressed by Equation 3.2.

$$\frac{1}{I_{lim}} = \frac{1}{I_{max}} + \frac{K_M}{I_{max}} \frac{1}{[S_{ox}]} \quad (3.2)$$

Because the immobilised enzymes may incur in phenomena that could deviate the kinetic from the Michaelis-Menten behaviour, the applicability of the Michaelis-Menten approach for the immobilised Laccases was evaluated, employing the Hill's equation.⁴⁴ This equation is often used in enzyme kinetics to describe the dependence of the steady-state rate of an enzymatic reaction on the mediator concentration (Equation 3.3):

$$v = \frac{v_{max} \left(\frac{[S]}{[S]_{0.5}} \right)^h}{1 + \left(\frac{[S]}{[S]_{0.5}} \right)^h} \quad (3.3)$$

At $h = 1$, Hill's equation is the classic Michaelis-Menten equation ($[S]_{0.5}$ corresponds to the Michaelis constant K_M). The Hill coefficient (h) was experimentally obtained by fitting the $\log[I_{lim}/(I_{max}-I_{lim})]$ vs $\log[S_{ox}]$ and h values were obtained ranging from 0.97 to 1.05.

⁴⁴ Borisov I.A., Lobanov A.V., Reshetilov A.N., Kurganov B.I. *Appl. Biochem. Microb.* **2000**, 36, 215-220.

From these results, it can be assessed that Laccases adsorbed onto the electrode surface follow the Michaelis-Menten kinetic model.

In Figure 3.6 the catalytic current dependence from the ABTS concentration using Laccase from *Lentinus edodes* and the relative linear plot obtained using Equation 3.2 are showed, respectively. In Table 3.1 the results related to the kinetic parameters obtained with Laccase from *Lentinus edodes* adsorbed on the surface of a GC electrode are summarised.

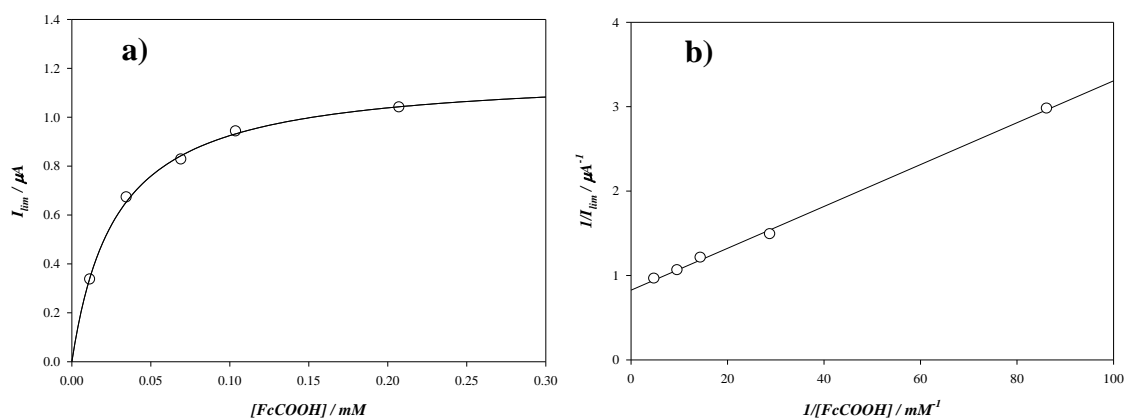


Figure 3.6 (a) Catalytic current dependence from the mediator concentration using Laccase from *Lentinus edodes* adsorbed on the surface of a GC electrode and (b) linear plot obtained using Equation 3.2.

Table 3.1 Kinetic parameters of Laccase from *Lentinus edodes*.

Mediator	I_{max} (μA)	K_M^{app} (mM)	I_{max}/K_M^{app} ($\mu\text{A mM}^{-1}$)
ABTS	0.71	5.23×10^{-2}	13.6
Syringaldazine	0.53	1.57×10^{-2}	33.8
Catechol	0.28	9.56×10^{-3}	29.1
Dopamine	0.58	6.53×10^{-2}	8.9
FcCOOH	1.21	3.00×10^{-2}	40.3
$\text{Fe}(\text{CN})_6^{4-}$	2.67	4.60×10^{-1}	5.8

In Figure 3.7 are reported the CVs of the mediators in absence and in presence of Laccase from *Panus tigrinus*. Also in this case the same trend obtained with the other Laccase can

be seen, i.e. an increase of the cathodic peak, as well as a decrease of the anodic one with respect to the CVs recorded in absence of adsorbed Laccase.

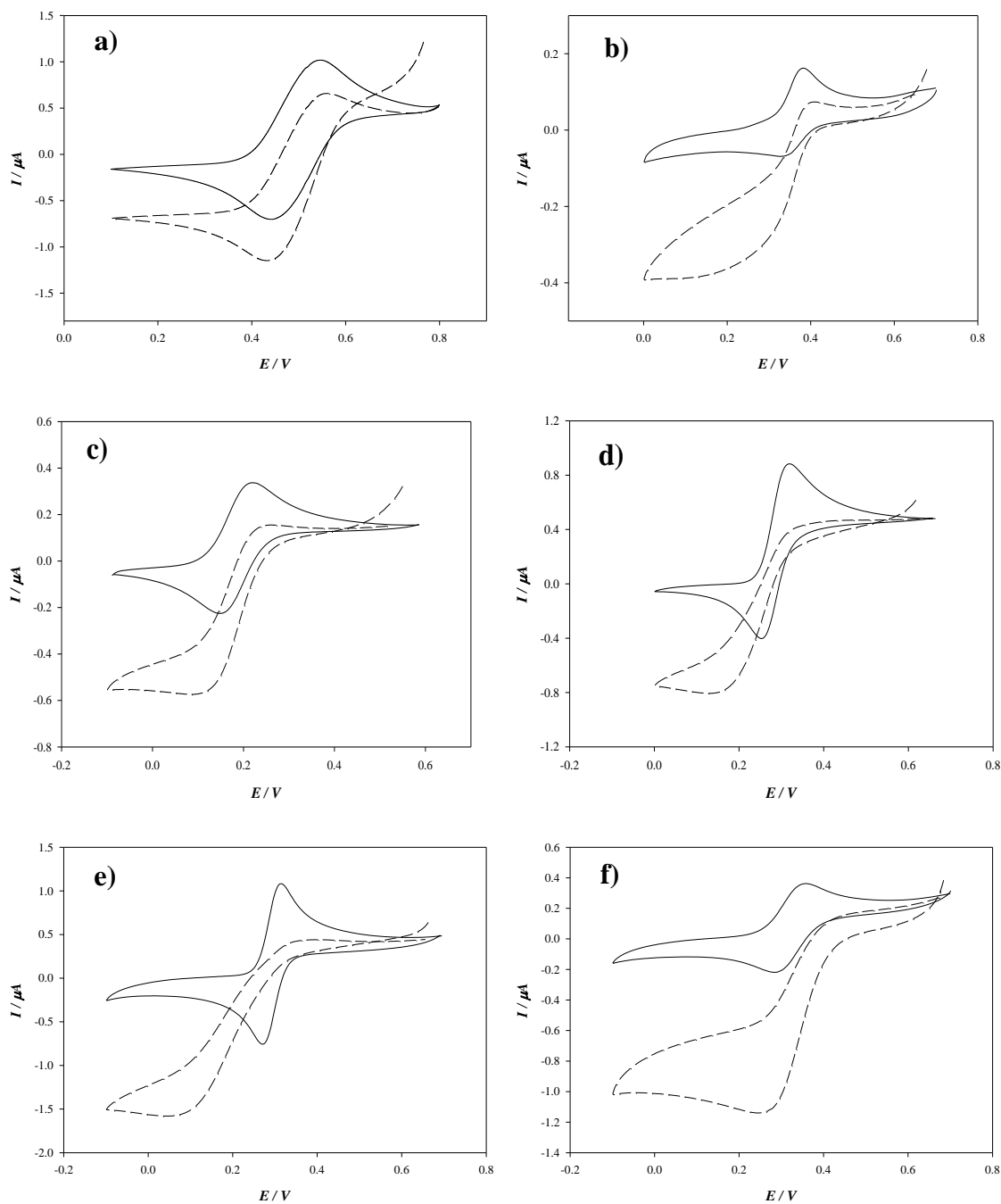


Figure 3.7 CVs recorded at a scan rate of 5 mV s⁻¹ in absence (solid line) and in presence (dashed line) of Laccase from *Panus tigrinus* adsorbed on the surface of GC electrode: a) ABTS 0.5 mmol L⁻¹; b) syringaldazine 0.02 mmol L⁻¹; c) Fe(CN)₆⁴⁻ 0.1 mmol L⁻¹; d) dopamine 0.1 mmol L⁻¹; e) catechol 0.1 mmol L⁻¹; f) FcCOOH 0.1 mmol L⁻¹.

In Figure 3.8 is showed the catalytic current dependence from the FcCOOH concentration using Laccase from *Panus tigrinus* and the relative linear plot obtained using Equation 3.2.

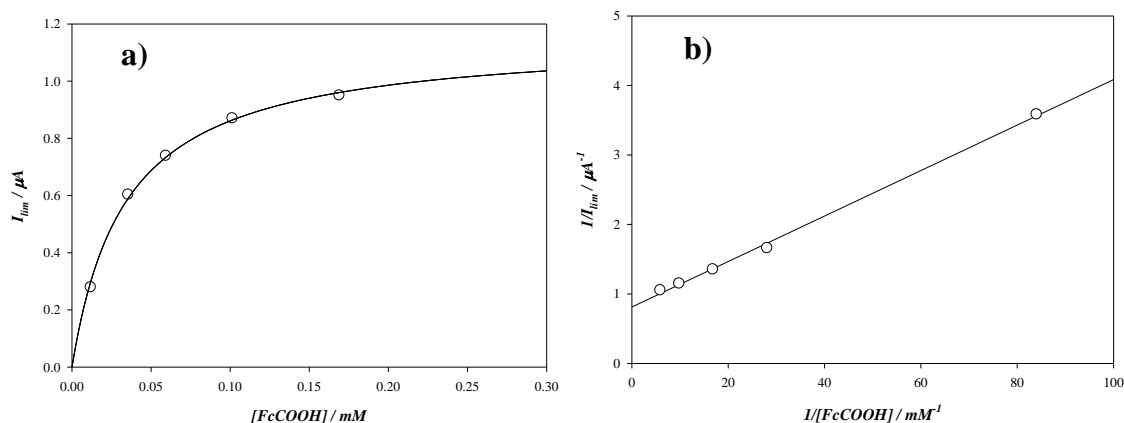


Figure 3.8 (a) Catalytic current dependence from the mediator concentration using Laccase from *Panus tigrinus* adsorbed on the surface of a GC electrode and (b) linear plot obtained using Equation 3.2.

In Table 3.2 are presented the results related to the kinetic parameters obtained with Laccase from *Panus tigrinus* adsorbed on the surface of a GC electrode.

Table 3.2 Kinetic parameters of Laccase from *Panus tigrinus*.

Mediator	I_{max} (μA)	K_M^{app} (mM)	I_{max} / K_M^{app} ($\mu A \text{ mM}^{-1}$)
ABTS	1.59	2.15	0.7
Syringaldazine	0.45	5.29×10^{-3}	85.1
Catechol	1.02	3.51×10^{-2}	29.1
Dopamine	0.71	5.21×10^{-2}	13.6
FcCOOH	1.23	2.79×10^{-2}	44.1
$Fe(CN)_6^{4-}$	3.98	8.20×10^{-1}	4.9

The I_{max} / K_M^{app} ratio gives an estimation of the affinity of the mediator to the enzyme. A great value of this ratio points out a better ability of the Laccase-mediator system to reduce oxygen to water. The data reported in Table 3.1 show that Laccase from *Lentinus edodes* have a good affinity with all the mediators, in particular with ferrocenecarboxylic acid, catechol and syringaldazine. The Laccase from *Panus tigrinus*, as LeL, have a good

affinity with ferrocenecarboxylic acid, catechol and syringaldazine, but have a very low affinity for ABTS.

In the previous work cited above,⁴¹ Laccases from *Melanocarpus albomyces* (r-MaL), *Rhus vernicifera* (RvL), *Trametes versicolor* (TvL) and *Trametes hirsuta* (ThL) were employed to obtain their kinetic parameters using the same electrochemical method and mediators of the present work. RvL presented a major affinity for ABTS ($I_{max}/K_M^{app} = 6.9$), r-MaL for syringaldazine ($I_{max}/K_M^{app} = 1010$) and both had a certain affinity with potassium ferrocyanide ($I_{max}/K_M^{app} = 0.11$ and 0.53 , respectively). Instead, TvL and ThL presented a major affinity for ABTS ($I_{max}/K_M^{app} = 15.4$ and 31.4 , respectively) and syringaldazine ($I_{max}/K_M^{app} = 15.5$ and 35.7 , respectively).

In general, the results obtained with Laccases from *Lentinus edodes* and *Panus tigrinus* are in line with those reported for other Laccases, even if with no particular increase in the overall performances. Conversely, from the comparison of all the six considered laccases (RvL, r-MaL, PtL, LeL, TvL and ThL) it can be concluded that TvL and ThL are the most promising in view of their possible use as biological components in biosensing, hence only these two Laccases were employed to this end.

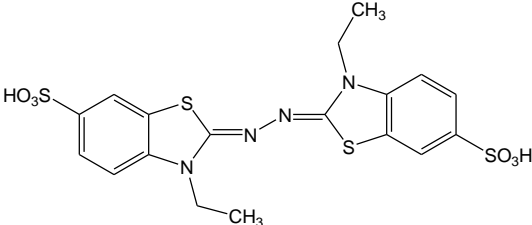
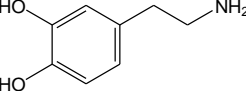
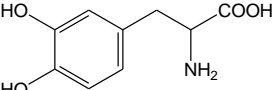
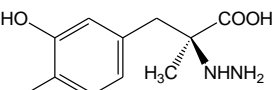
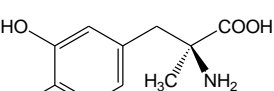
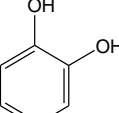
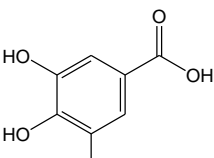
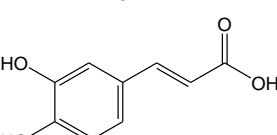
3.3.2 Laccases from *Trametes versicolor* and *Trametes hirsuta*

It has been demonstrated that TvL and ThL are very functional in the oxidation of phenolic compounds,⁴² for this reason the determination of the kinetic parameters of the two Laccases was carried out using dopamine, L-dopa, carbidopa, methyldopa, catechol, gallic acid and caffeic acid as mediators. As said, in the present study either TvL and ThL were immobilised by means of polyazetidine prepolymer (PAP) on MWCNT-SPEs and the kinetic characterisation was performed in aerobic conditions using chronoamperometry (CA) as electrochemical method.

All the redox compounds tested have been previously checked to be effective electron donors in the Laccase catalysed reduction of molecular dioxygen to water. The feasibility of the voltammetric detection of their interaction with Laccase implies the following assessments: (i) each mediator undergoes redox reactions at the working electrode which gives rise to either reversible or quasi-reversible electrodic processes within a suitable potential window; (ii) both oxidised and reduced species of the corresponding redox pair should be stable chemically and should not inhibit the enzymatic reaction.

To this aim, the compounds taken into account were characterised in their main electrochemical parameters; the results obtained are reported in Table 3.3. Each compound shows a quasi reversible (sometimes fully reversible) cyclic voltammogram on the MWCNTs electrode. The corresponding average formal potential (E^0) of each considered mediator was obtained as midpoint between the anodic and cathodic peak potential. The redox mediators displayed E^0 values between 271 and 421 mV (vs Ag/AgCl/Cl⁻), with a peak potential separation values (ΔE_p) between 56 and 195 mV except for catecholamines, whose ΔE_p is higher than 200 mV.

Table 3.3 Electrochemical parameters for the redox mediators, obtained in 0.1 mol L⁻¹ Britton-Robinson buffer, pH = 5.5, at 25 °C.

Mediator	Structure	E^0 (mV vs Ag/AgCl)	ΔE_p (mV)
ABTS		421	56
Dopamine		271	63
L-Dopa		332	217
Carbidopa		342	257
Methyldopa		370	309
Catechol		304	123
Gallic acid		279	195
Caffeic acid		310	111

The electrochemical detection of mediated Laccase interaction was performed by recording the redox processes that the mediators undergo onto the electrode surface, as seen above (Scheme 3.2). The recycling process of the mediator causes an amplification cycle that increases the mediators discharge, if compared with their discharge by direct electrochemical oxidation.

In the past years, it was demonstrated that the response time of tyrosinase-modified carbon electrode was limited by the electrochemical reduction of the quinone back to the diphenolic compound.⁴⁵ In fact, the presence of a polymer layer on the surface of the working electrode reduces the diffusion coefficient of both the mediator and the reaction product through the membrane, which consequently increases the response time of the biosensor.

To better understand the parameters involved in the Laccase-mediators interaction, a kinetic study was carried out on the series of diphenolic compounds trying to correlate the electrochemical response to the structure of the mediators.

The bioelectrochemical behaviour of Laccase modified electrode in presence of the different redox compounds was characterised by cyclic voltammetry (CV). Slow-scan voltammograms were recorded in 0.25 mmol L⁻¹ mediator solutions, pH 5.5, with both PAP-MWCNTs and Laccase-PAP-MWCNTs electrodes. A significant change in the shape of the corresponding signal was observed for all the considered compounds; in particular, the obtained results for dopamine is reported as examples in Figure 3.9.

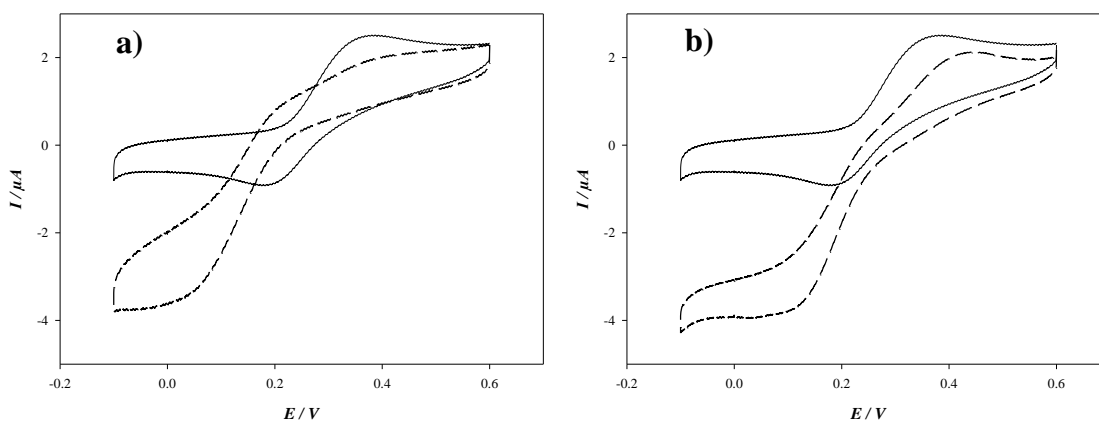


Figure 3.9 Cyclic voltammograms of dopamine 0.50 mmol L⁻¹, obtained in absence (solid line) and in presence (dashed line) of either TvL (a) or ThL (b), immobilised onto the electrode surface; measurements carried out in 0.1 mol L⁻¹ Britton-Robinson buffer, pH 5.5 at a scan rate of 5 mV s⁻¹.

⁴⁵ Burestedt E., Narvaez A., Ruzgas T., Gorton L., Emneus J., Dominguez E., Marko-Varga G. *Anal. Chem.* **1996**, *68*, 1605-1611.

The CV shape changes according to a catalytic process, as already seen in the precedent section and basing on this findings, the kinetic parameters for each mediator were determined by monitoring the variation of catalytic steady state current at increasing mediator concentration.

Even in this case, in order to evaluate the applicability of the Michaelis-Menten approach to describe the kinetic behaviour of immobilised Laccases, the Hill's equation (Equation 3.3) has been employed and h values ranging from 0.96 to 1.05 were obtained. In light of these results, the current-concentration dependence of the analysed compounds were modelled using a Michaelis-Menten non linear fitting (Equation 3.1) thus allowing the calculation of the kinetic parameters; results are shown in Table 3.4 for both TvL and ThL.

Table 3.4 Calculated kinetic parameters of Laccase-PAP-MWCNT integrated system for each mediator.

	Mediator	I_{max} (μA)	K_M^{app} (mM)	I_{max} / K_M^{app} ($\mu\text{A mM}^{-1}$)
TvL	Dopamine	2.7	0.142	19
	L-Dopa	1.4	0.272	5
	Carbidopa	2.0	0.091	22
	Methyldopa	2.0	0.061	33
	Catechol	5.5	0.076	72
	Gallic acid	3.3	0.156	21
	Caffeic acid	1.9	0.007	276
ThL	Dopamine	28.5	0.185	154
	L-Dopa	5.6	0.019	295
	Carbidopa	24.4	0.891	2700
	Methyldopa	5.6	0.0005	11000
	Catechol	14.5	0.016	906
	Gallic acid	7.6	0.115	66
	Caffeic acid	11.7	0.005	2200

By comparing the calculated I_{max}/K_M^{app} ratio for the different compounds, an estimation of the affinity of the Laccase for each mediator, is allowed: the higher values would indicate a better effectiveness of the TvL-mediated reduction of O₂ to H₂O. Among the studied phenolic compounds, caffeic acid appears to be the best mediator for TvL, on the other hand, dopamine shows the poorest interaction with this enzyme.

The different oxidation rate could be ascribed to the electron density of the oxidising group. In fact, since the catalysed reaction consists in withdrawing one electron from the mediator, it is conceivable that the electron density at the level of the oxidising group plays an important role in determining the rates of oxidation of the mediators. In a comparison of a series of ortho- and para-substituted phenols presented by Xu,^{2a} it was indicated that the presence of electron-withdrawing substituents decreased the activity of phenol towards recombinant Laccase from *Polyporus pinsitus*. These substituents reduce the electron density at the phenoxylic group, thus making it more difficult to be oxidised, less reactive in surrendering an electron to the T1 copper of Laccase and less basic.

Finally, the K_M^{app} values obtained for the TvL immobilised electrode were in the same order of magnitude with respect to those measured in an homogeneous enzyme reaction system, indicating a good retention of the structural properties of TvL in the immobilising matrix.

3.4 Conclusions

This study investigated the bioelectrochemical properties of Laccases from *Lentinus edodes*, *Panus tigrinus*, *Trametes versicolor* and *Trametes hirsuta*, absorbed on GC electrode or immobilised, by means of polyazetidine prepolymer, on multi-walled carbon nanotubes screen printed electrodes. The immobilisation procedures does not lead to deactivation of the enzyme, as demonstrated by kinetic parameters obtained by comparatively testing several different compounds.

The results obtained with Laccases from *Lentinus edodes* and *Panus tigrinus* are in line with those previously reported for other Laccases, bioelectrochemically characterised using the same immobilisation procedure and mediators. Instead, *Trametes versicolor* and *Trametes hirsuta* Laccases are the most efficient among the considered Laccases and in addition they are readily available; for this reason they are more suitable for the development of electrochemical biosensors.

TvL and ThL were bioelectrochemically characterised using a series of different diphenols and the obtained results show that these enzymes are very promising to be used in the development of efficient biosensors for the determination of phenols.

Chapter 4

Electrokinetic Characterisation of Amine Oxidase from *Lathyrus sativus* (LSAO)

4.1 Introduction

4.1.1 Amine Oxidases

The Amine Oxidases (oxygen oxidoreductase deaminating) (AOs) are a class of enzymes specifically acting on the CH-NH₂ group of a series of amino compounds, as spermine, spermidine, cadaverine, putrescine, histamine, tyramine and tryptamine, with the concomitant reduction of dioxygen to hydrogen peroxide and the formation of the corresponding aldehyde and ammonia, as illustrated in Figure 4.1.

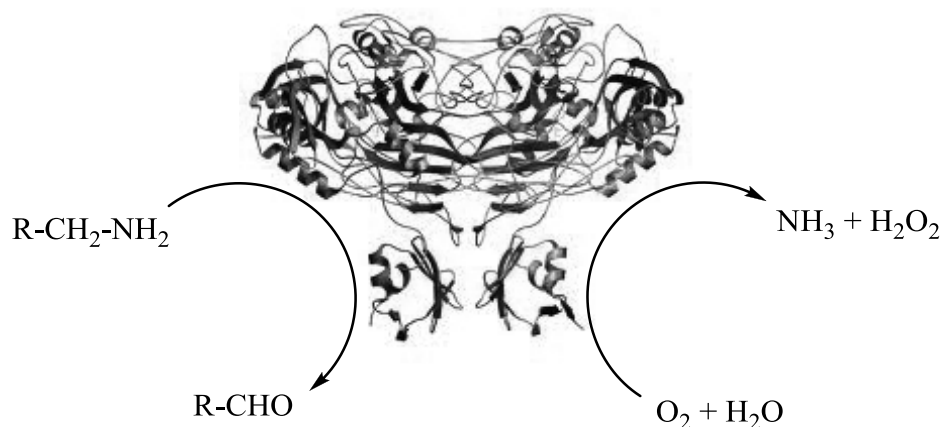


Figure 4.1 Representation of the catalytic cycle of Amine Oxidase.

The family of Amino Oxidases can be divided into two main groups, found both in lower and higher organism: quinone copper-containing AOs (CuAOs), as for example Bovine

Serum Amine Oxidase (BSAO) and Diamine Oxidase (DAO), or flavin-dependent AOs, as Polyamine Oxidase (PAO) and Monoamine Oxidase (MAO). They act on polyamines, which are ubiquitous compounds essential for cell growth and proliferation. Far from being only a means of degrading cellular polyamines and, thus, contributing to polyamine homeostasis, AOs participate in important physiological processes through their reaction products.

CuAOs were found in bacteria, where have a role in the utilisation of primary amines as a source of nitrogen or carbon,¹ in higher organisms, where they are important in a variety of functions including cell adhesion and signalling,² and in plants, where the production of hydrogen peroxide deriving from polyamine oxidation has been correlated with cell wall maturation and lignification during development, as well as with wound-healing, cell wall reinforcement, during pathogen invasion and, as a signal molecule, with cell death, the hypersensitive response and the expression of defence genes.³

In humans three CuAOs have been identified: AOC1, also known as amiloride binding protein, AOC2, a retinal form, and AOC3, or vascular adhesion protein (VAP-1).⁴ CuAOs production of formaldehyde has been implicated in the alteration of protein structure, which may subsequently cause protein deposition associated with chronic vascular and neurobiological disorders, such as diabetic complications, atherosclerosis, and

¹ (a) Parrott S., Jones S., Cooper R. A. *J. Gen. Microbiol.* **1987**, *133*, 347-351; (b) Hacisalihoglu A., Jongejan J. A., Duine, J. A. *Microbiology* **1997**, *143*, 505-512.

² (a) Knowles P. F., Dooley D. M. Metalloenzymes involving amino acid-residue and related radicals, in *Metal Ions in Biological Systems* (Sigel H., and Sigel, A., Eds.) **1994**, 361-403, Marcel Dekker, New York; (b) Moller S., McPherson M. J. *Plant J.* **1998**, *13*, 781-791; (c) Salmi M., Hellman J., Jalkanen S. *J. Immunol.* **1998**, *160*, 5629-5636; (d) Elmore B. O., Bollinger J. A., Dooley D. M. *J. Biol. Inorg. Chem.* **2002**, *7*, 565-579; (e) Yu P. H., Wright S., Fan E. H., Lun Z. R., Gubisne-Harberle D. *Biochim. Biophys. Acta* **2003**, *1647*, 193-199; (f) Wang S. X., Mure M., Medzihradzky K., Burlingame A., Brown D. E., Dooley D. M., Smith A., Kagan H. M., Klinman, J. P. *Science* **1996**, *273*, 1078-1084.

³ Cona A., Rea G., Angelini R., Federico F., Tavladoraki P. *Trends in Plant Science* **2006**, *11*, 80-88.

⁴ Schwelberger H. G. *J. Neural. Transm.* **2007**, *114*, 757-762.

neurodegenerative disease.^{2e,5} These enzymes are also implicated in adipose tissue regulation.⁶

In humans also flavin-dependent AOs involved in a myriad of biological activities are present, for example was found that PAO might contribute to the protection of the fetoplacental unit from possible maternal immune rejection⁷ and that MAO could be involved in age-related neurological disorders such as Parkinson's Disease.⁸

AOs are involved also in cancer growth inhibition because of the higher content in tumour cells of biogenic amines, with respect to healthy cells.⁹ The cancer inhibition effect of AOs could be explained by taking into consideration the full pattern of the enzyme content of the cell. The balance of Amine Oxidases and antioxidant enzymes appear to be a crucial point for cancer inhibition or progression. A long lasting imbalance of these enzymes appears to be carcinogenic, while, for a short time, Amine Oxidases are cytotoxic for cancer cells.

The ubiquity and functional diversity of this family of enzymes underlie its importance and have prompted many structural and biochemical studies.

4.1.2 Amine Oxidases Structure and Catalytic Mechanism

As said, AOs can be divided into two main groups based on the cofactors they utilise: quinone and copper-containing Amine Oxidases (CuAOs) and flavin-dependent Amine Oxidases (AOs). AOs are located exclusively in the outer mitochondrial membrane of almost all cell types and can oxidise primary, secondary, and tertiary amines either by a concerted covalent catalysis or by a single electron-transfer mechanism, both requiring

⁵ Gubisne-Haberle D., Hill W., Kazachkov M., Richardson J. S., Yu P. H. *J. Pharmacol. Exp. Ther.* **2004**, *310*, 1125-1132.

⁶ Moldes M., Feve B., Pairault J. *J. Biol. Chem.* **1999**, *274*, 9515-9523.

⁷ Morgan D. M. L., Illei G. *Br. Med. J.* **1980**, *280*, 1295-1297.

⁸ Fowler J. S., Volkow N. D., Logan J., Schlyer D. J., MacGregor R. R., Wang G-J., Wolf A. P., Pappas N., Alexoff D., Shea C., Gatley S. J., Dorflinger E., Yoo K., Morawsky L., Fazzini E. *Neurology* **1993**, *43*, 1984-1993.

⁹ Toninello A., Pietrangeli P., De Marchi U., Salvi M., Mondovì B. *Biochim. Biophys. Acta* **2006**, *1765*, 1-13.

FAD as a cofactor. The flavin-dependent Amine Oxidases form two structurally related groups: i) D-Amino Acid Oxidase,¹⁰ Sarcosine Oxidase,¹¹ Glycine Oxidase¹² and related enzymes have a common fold, differing in the details of substrate orientation and the specific bond which is oxidised; ii) Monoamine Oxidase,¹³ L-Amino Acid Oxidase,¹⁴ Polyamine Oxidase,¹⁵ Spermine Oxidase¹⁶ and related enzymes can be grouped into a second much larger family with a wider range of substrates. The substrate specificities of the two families overlap, in that enzymes that oxidise amino acids, primary amines, and secondary amines are found in both.

Among the AOs, *Zea mays* Polyamine Oxidase (ZmPAO) was the first PAO for which both the primary and tertiary structures were determined. The crystal structure of ZmPAO has been determined by X-ray diffraction in the oxidised and reduced state as well as in complex with PAO-specific inhibitors (Figure 4.2).^{13,15}

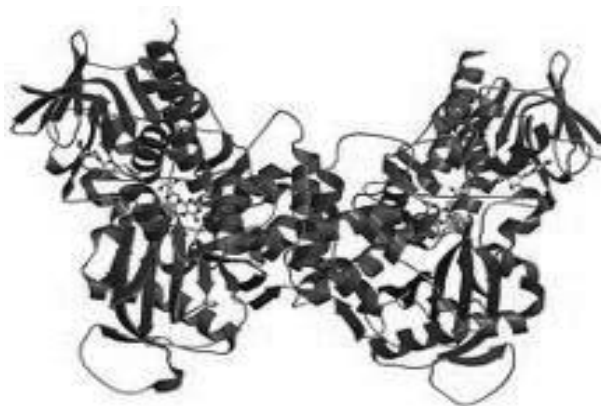


Figure 4.2 Structure of ZmPAO.

¹⁰ Mattevi A., Vanoni M. A., Todone F., Rizzi M., Teplyakov A., Coda A., Bolognesi M., Curti B. *Proc. Natl. Acad. Sci. USA* **1996**, *93*, 7496-7501.

¹¹ Trickey P., Wagner M. A., Jorns M. S., Mathews F. S. *Structure* **1999**, *7*, 331-345.

¹² Settembre E. C., Dorrestein P. C., Park J., Augustine A. M., Begley T. P., Ealick S. E. *Biochemistry* **2003**, *42*, 2971-2981.

¹³ Binda C., Newton-Vinson P., Hubalek F., Edmondson D. E., Mattevi A. *Nat. Struct. Biol.* **2002**, *9*, 22-26.

¹⁴ Pawelek P. D., Cheah J., Coulombe R., Macheroux P., Ghisla S., Vrielink A. *EMBO J.* **2000**, *19*, 4204-4215.

¹⁵ Binda C., Coda A., Angelini R., Federico R., Ascenzi P., Mattevi A. *Structure* **1999**, *7*, 265-276.

¹⁶ Huang Q., Liu Q., Hao Q. *J. Mol. Biol.* **2005**, *348*, 951-959.

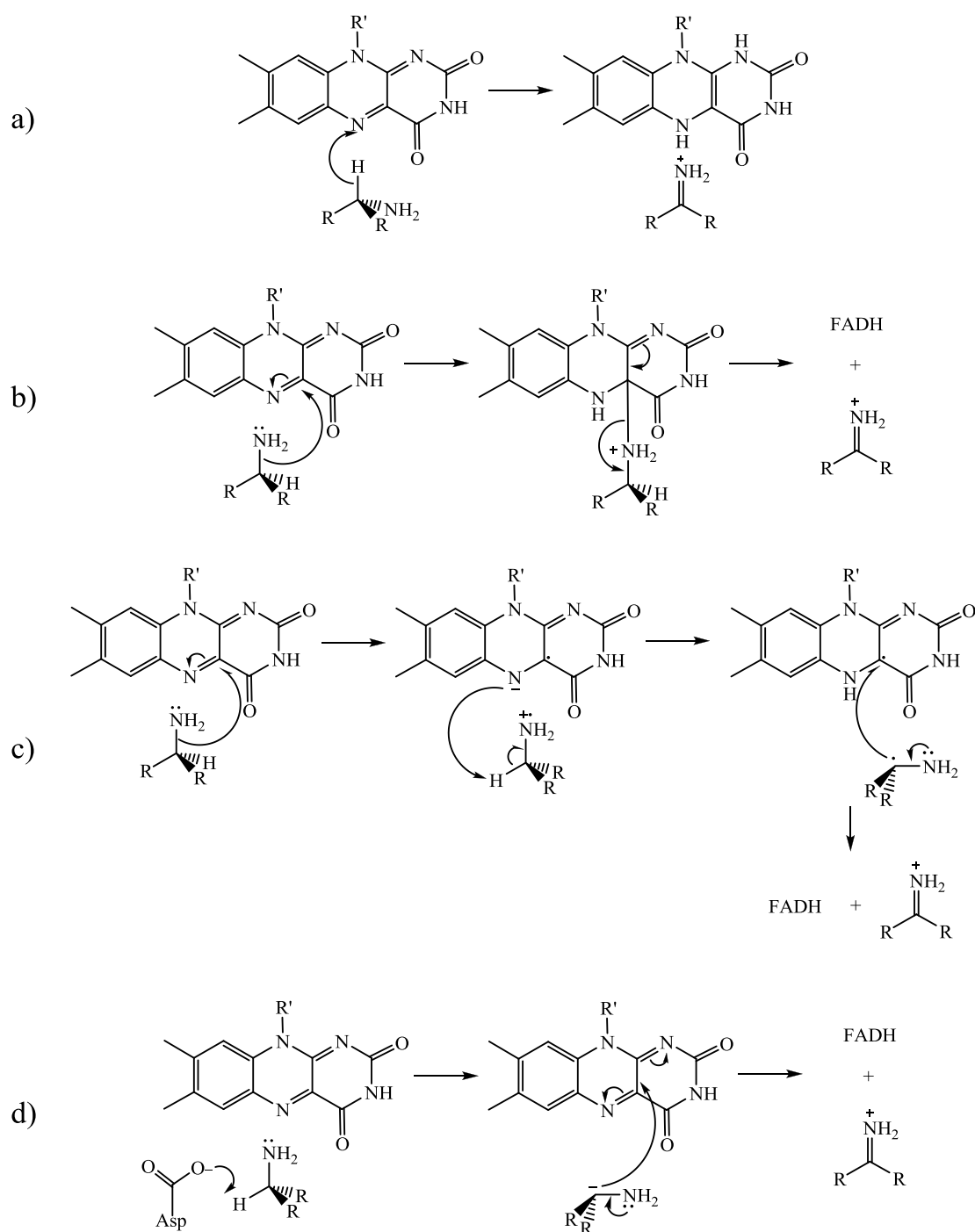
The oxidation mechanism includes four different patterns that have been proposed for flavoproteins. These include direct hydride transfer from the neutral amine to the flavin (Scheme 4.1a),¹⁷ nucleophilic addition of the amine to the flavin (Scheme 4.1b),¹⁸ single electron transfer reactions (Scheme 4.1c)¹⁹ and formation of a carbanionic substrate by loss of a proton (Scheme 4.1d).²⁰ These oxidation patterns all yield the reduced flavin and the imino acid product (with most but not all substrates this step is effectively irreversible). The reduced enzyme then reacts with O₂ to yield the oxidised flavin and H₂O₂. Finally, the product dissociates from the oxidised enzyme and is subsequently hydrolysed non-enzymatically to the respective aldehyde (or keto acid, when the substrate is an amino acid) and ammonia. This mechanism is common for all the flavin-dependent Oxidases, with slight differences in whether the oxidised substrate dissociates before or after flavin oxidation.

¹⁷ Kurtz K. A., Rishavy M. A., Cleland W. W., Fitzpatrick P. F. *J. Am. Chem. Soc.* **2000**, *122*, 12896-12897.

¹⁸ Miller J. R., Edmondson D. E. *Biochemistry* **1999**, *38*, 13670-13683.

¹⁹ Silverman R. B. *Acc. Chem. Res.* **1995**, *28*, 335-342.

²⁰ Fitzpatrick P. F. *Bioorg. Chem.* **2004**, *32*, 125-139.



Scheme 4.1 Different patterns proposed for AOs oxidation mechanism

Quinone copper-containing Amine Oxidases generally oxidise primary amines and can be subdivided into two subclasses depending on the modified tyrosine residue present in the active site: 2,4,5-trihydroxyphenylalanine quinone (TPQ; E.C. 1.4.3.6) or lysine

tyrosylquinone (LTQ; E.C. 1.4.3.13). TPQ is formed by the post-translational six-electron oxidation of a conserved tyrosine residue, while LTQ is formed by means of the oxidation and crosslinking of a tyrosine and a lysine residue. Formation of both cofactors is a self-processing event requiring only copper and molecular oxygen.²¹

Five CuAO structures have been experimentally determined: *Escherichia coli* Amine Oxidase (ECAO),²² *Pisum sativum* Amine Oxidase (PSAO),²³ *Pichia pastoris* Lysyl Oxidase (PPLO),²⁴ *Hansenula polymorpha* Amine Oxidase (HPAO),²⁵ recently reclassified as *Pichia angusta* (PAAO), and *Arthrobacter globiformis* Amine Oxidase (AGAO).²⁶ Crystal structures of the ECAO have provided a basis for detailed structure-function studies. This enzyme is a homodimer of ~160 kDa (Figure 4.3) and contains a single active site per monomer composed of a mononuclear Type II copper ion and the TPQ cofactor.²⁷ All the structurally characterised CuAOs display the same overall architecture and topology as ECAO, with the exception of the N-terminal domain which only exists in Gram-negative bacterial enzymes.

²¹ (a) Ruggiero C. E., Dooley D. M. *Biochemistry* **1999**, *38*, 2892-2898; (b) Ruggiero C. E., Smith J. A., Tanizawa K., Dooley D. M. *Biochemistry* **1997**, *36*, 1953-1959; (c) Bollinger J. A., Brown D. E., Dooley D. M. *Biochemistry* **2005**, *44*, 11708-11714; (d) DuBois J. L., Klinman J. P. *Arch. Biochem. Biophys.* **2005**, *433*, 255-265.

²² Parsons M. R., Convery M. A., Wilmot C. M., Yadav K. D. S., Blakeley V., Corner A. S., Phillips S. E. V., McPherson M. J., Knowles P. F. *Structure* **1995**, *3*, 1171-1184.

²³ Kumar V., Dooley D. M., Freeman H. C., Guss J. M., Harvey I., McGuirl M. A., Wilce M. C. J., Zubak V. M. *Structure* **1996**, *4*, 943-955.

²⁴ Duff A. P., Cohen A. E., Ellis P. J., Kuchar J. A., Langley D. B., Shepard E. M., Dooley D. M., Freeman H. C., Guss J. M. *Biochemistry* **2003**, *42*, 15148-15157.

²⁵ (a) Li R. B., Klinman J. P., Mathews F. S. *Structure* **1998**, *6*, 293-307; (b) Chen Z. W., Schwartz B., Williams N. K., Li R. B., Klinman J. P., Mathews F. S. *Biochemistry* **2000**, *39*, 9709-9717.

²⁶ Wilce M. C. J., Dooley D. M., Freeman H. C., Guss J. M., Matsunami H., McIntire W. S., Ruggiero C. E., Tanizawa K., Yamaguchi H. *Biochemistry* **1997**, *36*, 16116-16133.

²⁷ (a) Dove J. E., Klinman J. P. *Adv. Protein Chem.* **2001**, *58*, 141-174; (b) Dawkes H. C., Phillips S. E. V. *Curr. Opin. Struct. Biol.* **2001**, *11*, 666-673.

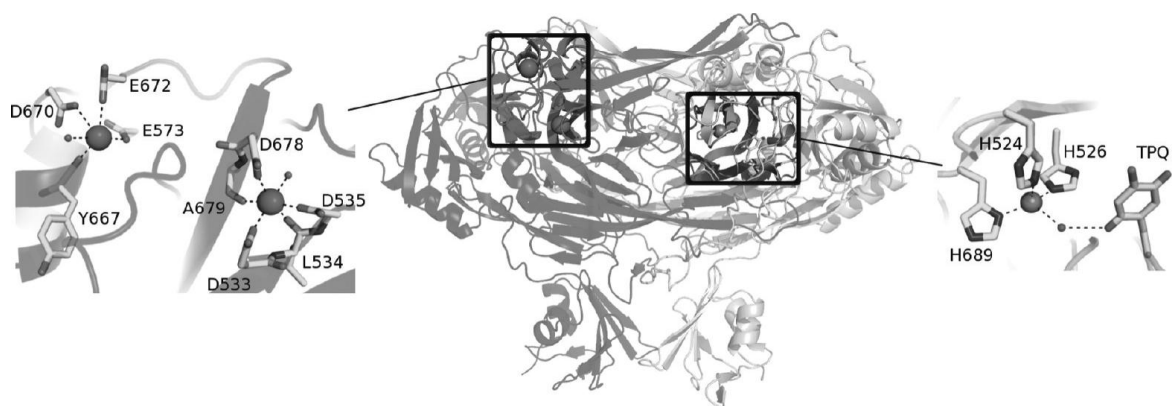
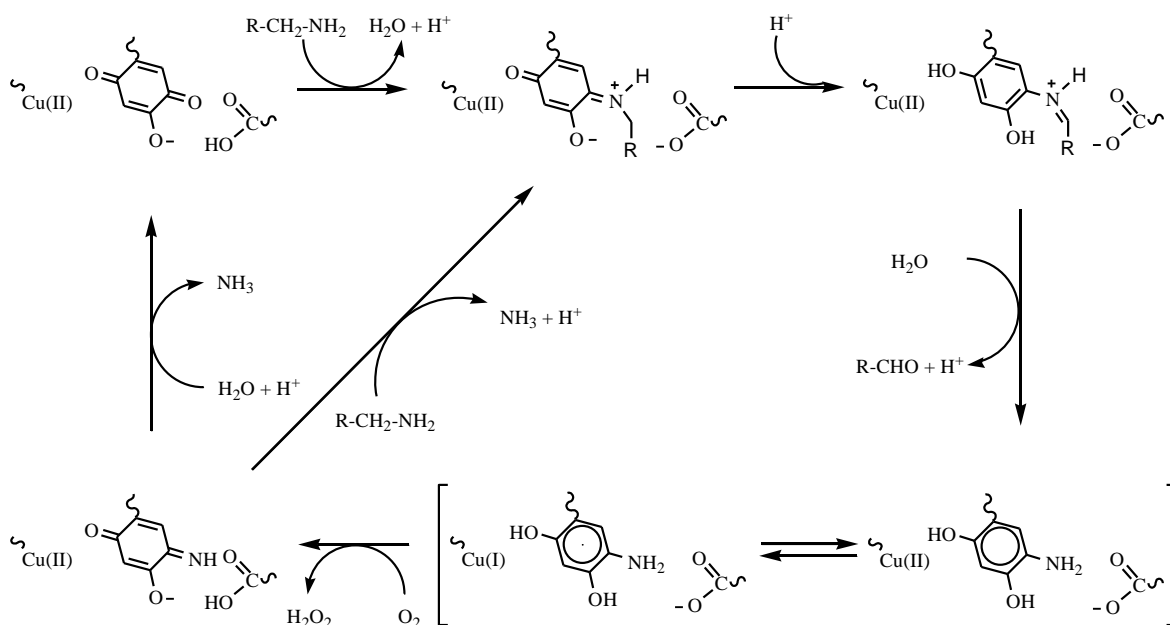


Figure 4.3 Structural overview of ECAO. In the centre the ECAO dimer, to the left a more detailed view of the peripheral metal binding sites and to the right a detailed view of the active site, are shown.

CuAOs oxidise primary amines through a ping-pong mechanism (Scheme 4.2). The critical step in this reaction is the abstraction of a proton from the α carbon of the amine substrate carried out by a conserved aspartate acting as general base. In this step, the enzyme converts the initial “substrate Schiff base”, a quinoneimine, to the “product Schiff base”, a quinolaldimine. Subsequently the aldehyde product is released through hydrolysis, yielding Cu(II)-aminoresorcinol (Cu(II)-TPQ_{AMQ}) in equilibrium with Cu(I)-semiquinone (Cu(I)-TPQ_{SQ}) with the magnitude of K_{eq} being highly dependent upon temperature and the enzyme source.²⁸ In the presence of O₂, oxidation to an iminoquinone species occurs, producing H₂O₂. This species is then hydrolysed, liberating NH₃ and the resting cofactor.²⁶ In addition, NH₃ may be released by a transimination reaction between the iminoquinone and substrate, thereby forming the “substrate Schiff base”.

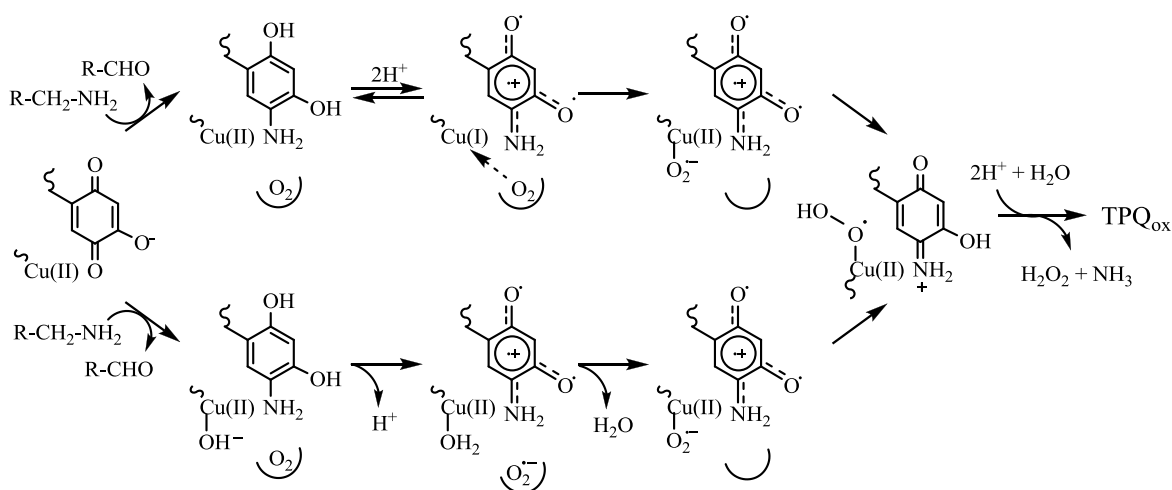
²⁸ Dooley D. M., McGuirl M. A., Brown D. E., Turowski P. N., McIntire W. S., Knowles P. F. *Nature* **1991**, 349, 262-264.



Scheme 4.2 CuAOs oxidation of amines through the ping-pong mechanism

Significant questions remain with regard to which species initially reduces O_2 , and whether or not the reoxidation mechanism differs for CuAOs purified from various sources. The two most plausible reoxidation mechanisms are detailed in Scheme 4.3 and they can be summarised as follow: i) copper plays an essential role in inner-sphere electron transfer from TPQ_{AMQ} to O_2 by providing a binding site for reduced oxygen species, suggesting a potential redox-active role for copper;²⁸ ii) electron transfer occurs by an outer-sphere mechanism whereby TPQ_{AMQ} directly reduces dioxygen which is bound and activated in a hydrophobic pocket adjacent to the metal site, with no requirement for a change in the copper oxidation state.²⁹

²⁹ Mills S. A., Goto Y., Su Q. J., Plastino J., Klinman J. P. *Biochemistry* **2002**, *41*, 10577-10584.



Scheme 4.3 Most plausible re-oxidation mechanisms of CuAOs

In the first proposal, the initial reduction of O_2 occurs by an inner-sphere reaction with Cu(I) (upside of Scheme 4.3), resulting in a Cu(II) bound superoxide species.³⁰ This proposal circumvents the spin conversion problem associated with two-electron reduction reactions of oxygen,³¹ and is substantiated by the ample precedence for the reactivity of three-coordinate Cu(I) sites with O_2 in copper-containing metalloproteins.³² Furthermore, detailed kinetics studies of the CuAO from lentil seedlings strongly supported the participation of the $[Cu(I)-TPQ_{SQ}]$ intermediate in the reduction of O_2 .³³ Additional support for an inner-sphere mechanism for re-oxidation comes from metal-substitution experiments in *Arthrobacter globiformis* Amine Oxidase.³⁴

³⁰ (a) Dooley D. M., McGuirl M. A., Brown D. E., Turowski P. N., McIntire W. S., Knowles P. F. *Nature* **1991**, 349, 262-264; (b) Turowski P. N., McGuirl M. A., Dooley D. M. *J. Biol. Chem.* **1993**, 268, 17680-17682; (c) Dooley D. M., Brown D. E. *J. Biol. Inorg. Chem.* **1996**, 1, 205-209.

³¹ Ho R. Y. N., Liebman J. F., Valentine J. S. *Active Oxygen in Chemistry* (Foote C. S., Valentine J. S., Greenberg A., Liebman J. F. editors, Blackie Academic and Professional; New York) **1995**, 1-23.

³² (a) Murthy N. N., Karlin K. D. *Mechanistic Bioinorganic Chemistry* (Thorp H. H., Pecoraro V. L. editors, American Chemical Society; Washington D.C.) **1995**, 165-193; (b) Karlin K. D., Tyekl'ar Z. *Bioinorganic Chemistry of Copper* (Chapman and Hall; New York) **1993**; (c) Whittaker J. W. *Essays Biochem.* **1999**, 34, 155-172.

³³ (a) Medda R., Padiglia A., Bellelli A., Sarti P., Santanche S., Agro A. F., Floris G. *Biochem. J.* **1998**, 332, 431-437; (b) Padiglia A., Medda R., Bellelli A., Agostinelli E., Morpurgo L., Mondovi B., Finazzi-Agrò A., Floris G. *Eur. J. Inorg. Chem.* **2001**, 1, 35-42.

³⁴ Kishishita S., Okajima T., Kim M., Yamaguchi H., Hirota S., Suzuki S., Kuroda S., Tanizawa K., Mure M. *J. Am. Chem. Soc.* **2003**, 125, 1041-1055.

In contrast, results obtained using the Amine Oxidases from *Hansenula polymorpha* and bovine plasma were consistent with an outer-sphere mechanism (downside of Scheme 4.3).³⁵ These studies suggest that O₂ binds in a hydrophobic pocket near the quinone cofactor and the first electron transfer reaction occurs via a classical outer-sphere step between TPQ_{AMQ} and O₂, with the Cu(I)-TPQ_{sq} intermediate existing off-pathway, in equilibrium with species (the semiquinone is not depicted in pathway for the sake of clarity). Then, the superoxide anion that is generated in the hydrophobic pocket migrates to the Cu(II) centre.³⁶

³⁵ (a) Mills S. A., Klinman J. P. *J. Am. Chem. Soc.* **2000**, *122*, 9897-9904; (b) Schwartz B., Olgin A. K., Klinman J. P. *Biochemistry* **2001**, *40*, 2954-2963; (c) Su Q. J., Klinman J. P. *Biochemistry* **1998**, *37*, 12513-12525.

³⁶ Mure M., Mills S. A., Klinman J. P. *Biochemistry* **2002**, *41*, 9269-9278.

4.2 Experimental Section

In this research the quinone copper-containing Amine Oxidase from *Lathyrus sativus* (LSAO) has been taken into account. It has been studied from a kinetic point of view with different substrates, using chronoamperometry (CA) as electrochemical method. LSAO kinetic parameters were obtained monitoring the H₂O₂ discharge both with immobilised enzyme and free in solution.

4.2.1 Materials

N,N'-bis(3-aminopropyl)butane-1,4-diamine (spermine), *N*-(3-aminopropyl)butane-1,4-diamine (spermidine), 2-(1*H*-imidazol-4-yl)ethanamine (histamine), 1,5-diaminopentane (cadaverine), 1,4-diaminobutane (putrescine), 2-(4-hydroxyphenyl)ethylamine (tyramine) and 2-phenylethylamine were purchased from Sigma-Aldrich and used as received. Amine Oxidase from *Lathyrus sativus* (EC 1.4.3.22, activity 131 U ml⁻¹, concentration 2 mg ml⁻¹, M_r = 148 kDa),³⁷ were gently donated by the research groups of Alberto Boffi (Department of Biochemical Sciences “A. Rossi Fanelli”, Sapienza University of Rome) and Rodolfo Federico (Department of Biology, 3rd University of Rome). The polymeric film used was poly-1-(aminomethyl)-1-{2-[(6-oxysesane)amino]ethyl}-3-hydroxyazetidinium chloride (polyazetidine prepolymer, PAP®), donated by Hercules Inc. Wilmington DE (USA). Other chemicals were all of analytical grade. High purity deionised water (Resistance: 18.2 MΩ × cm at 25 °C; TOC < 10 µg L⁻¹), obtained from Millipore (France), has been used to prepare all the solutions.

³⁷ Suresch M. R., Adiga P. R. *J. Biosci.* **1979**, *1*, 109-124.

4.2.2 Apparatus

Electrochemical experiments were performed by using a μ -Autolab type III potentiostat (Eco Chemie, Netherlands) controlled by means of the GPES Manager program. The measurements were performed in a thermostated 10 ml glass cell with a conventional three-electrode configuration: Ag/AgCl/Cl⁻ (Metrohm, Switzerland, 198 mV vs NHE) was used as reference electrode, a graphite rod as counter and different electrodic materials as working electrodes (see below).

All measurements were carried out in aerobic conditions in phosphate buffer with a pH value differing from enzyme to enzyme.

4.2.3 Electrochemical Measurements with Amine Oxidase from *Lathyrus sativus* (LSAO)

Chronoamperometric (CA) measurements were performed with a typical three-electrodes system using as working electrodes a Platinum Screen Printed Electrodes (Pt-SPE, diameter of 1 mm) (BVT Technologies Brno, CZ) for the kinetic measurements with immobilised LSAO and a platinum disk (Pt, diameter of 3 mm) for the measurements with LSAO free in solution.

LSAO Pt-SPE biosensors were prepared by spreading 3 μ l of a solution, containing 2 μ l of enzyme and 1 μ l of PAP, onto the platinum working electrode surface to have a final amount of enzyme 0.26 U. All the electrodes were left to dry overnight at room temperature and when not in use were stored at 4°C. In the measurements with LSAO free in solution 2 μ l of enzymatic solution were added to 2.5 ml of buffer solution in order to have a final amount of enzyme 0.26 U. Chronoamperometric experiments were carried out at a fixed potential of 700 mV vs Ag/AgCl/Cl⁻, under a constant magnetic stirring in a 10 ml thermostated glass cell, at 25°C in phosphate buffer solution 0.1 mol L⁻¹, pH = 7.4.

4.3 Results and Discussion

The determination of the kinetic parameters of immobilised LSAO was carried out using histamine, cadaverine, putrescine, spermine, spermidine, tyramine and phenylethylamine as substrates. In order to evaluate the applicability of the Michaelis-Menten approach to describe the kinetic behaviour of immobilised LSAO, the Hill's equation (see Equation 3.3 in Chapter 3) has been employed and h values ranging from 0.99 to 1.04 were obtained (Table 4.1). From these results, it can be assessed that LSAO immobilised onto the electrode surface follow the Michaelis-Menten kinetic model.

The kinetic parameters were calculated according to a simplified approach which entails the application of Equation 3.1 and its Lineweaver-Burk-type linearisation, as expressed in Equation 3.2 (see Equations 3.1 and 3.2 in Chapter 3).

In Table 4.1 the data obtained with LSAO modified electrode towards several substrates, are summarised; as an example, in Figure 4.4 is also reported the Lineweaver-Burk linearisation plot obtained for cadaverine.

As it can be observed, the affinity of the enzyme (correlated to K_M^{app}) towards the selected substrates is practically the same with the exception of cadaverine; on the other hand the efficiency (that can be roughly evaluated by I_{max}/K_M^{app}) is maximum for putrescine, suggesting that the latter could be considered as standard to be used for expressing the total content of BA using a LSAO-based biosensor in the food quality monitoring.

Table 4.1 kinetic characteristics obtained with LSAO modified electrodes in phosphate buffer solution 0.1 mol L⁻¹, pH 7.4.

Substrate	I_{max} (nA)	K_M^{app} (mM)	I_{max} / K_M^{app} (nA mM ⁻¹)	h
Histamine	386.7 ± 17.8	1.05 ± 0.05	368.3	1.02 ± 0.03
Cadaverine	748.4 ± 24.9	2.84 ± 0.12	263.5	0.99 ± 0.01
Putrescine	633.4 ± 16.7	1.58 ± 0.03	400.9	1.01 ± 0.01
Spermine	295.8 ± 7.7	1.14 ± 0.08	259.5	1.04 ± 0.01
Spermidine	590.4 ± 23.6	1.77 ± 0.19	333.6	1.02 ± 0.02
Tyramine	117.7 ± 0.6	0.53 ± 0.03	222.1	1.03 ± 0.04
Phenylethylamine	126.1 ± 2.2	0.84 ± 0.02	150.1	1.01 ± 0.03

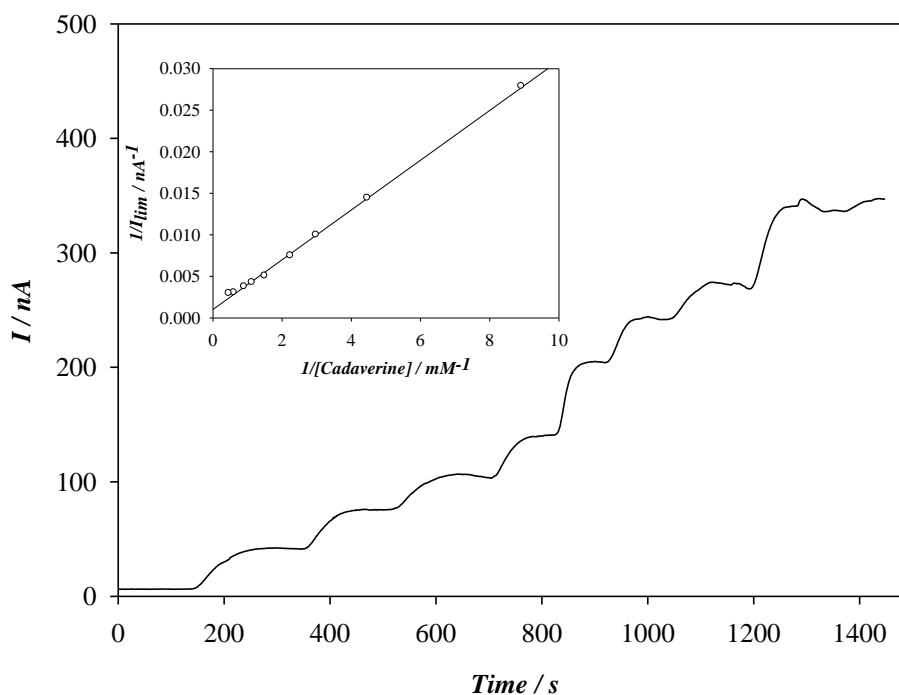


Figure 4.4 Amperometric response, using LSAO-modified Pt-SPE electrode, for different additions of cadaverine. Inset: linearisation according to Lineweaver-Burk.

Also the enzyme free in solution was bioelectrochemical characterised in the presence of the same substrates used in the case of immobilised LSAO. The kinetic parameters were obtained by Lineweaver-Burk linearisation (Equation 4.2) of the classical Michaelis-Menten kinetics (Equation 4.1).

$$v_0 = \frac{v_{\max} [S_{ox}]}{[S_{ox}] + K_M} \quad (4.1)$$

$$\frac{1}{v_0} = \frac{1}{v_{\max}} + \frac{K_M}{v_{\max} [S_{ox}]} \quad (4.2)$$

where $[S_{ox}]$ is the concentration of the oxidised substrate, v_0 is the initial rate of the enzymatic reaction, K_M is the Michaelis-Menten constant for the enzymatic reaction and v_{\max} is the maximum rate. From the obtained v_{\max} values, knowing the enzyme concentration, it is possible to estimate the catalytic constant k_{cat} , that results to be equal to $v_{\max}/[Enz]$, with $[Enz] = 1.08 \times 10^{-5} \text{ mmol L}^{-1}$.

In these experiments, the variation of H_2O_2 produced by the enzymatic reaction was monitored by detecting the corresponding oxidation current at a fixed potential of +700 mV vs Ag/AgCl/Cl⁻. Before every measurements, it was necessary to construct a calibration plot for hydrogen peroxide under the same conditions: this allowed to modify the current vs time responses, obtained from the experiments, in $[\text{H}_2\text{O}_2]$ vs time curves and consequently, to determine the initial rate of the enzymatic reaction (v_0).

In Table 4.2 the main kinetic parameters obtained with a series of substrates and LSAO free in solution, are summarised. In Figure 4.5 and 4.6 the amperometric responses obtained for different concentration of cadaverine and the slopes determined from them for v_0 calculation, are reported respectively.

Table 4.2 kinetic characteristics obtained with LSAO free in solution, in phosphate buffer solution 0.1 mol L^{-1} , pH 7.4.

Substrate	$k_{cat} \text{ (s}^{-1}\text{)}$	$K_M \text{ (mM)}$	$k_{cat}/K_M \text{ (mM}^{-1} \text{s}^{-1}\text{)}$
Histamine	23.4 ± 0.2	$(1.1 \pm 0.1) \times 10^{-1}$	208.9
Cadaverine	316.7 ± 22.2	$(1.7 \pm 0.2) \times 10^{-1}$	1841.3
Putrescine	227.8 ± 17.6	$(2.2 \pm 0.2) \times 10^{-1}$	1040.2
Spermine	12.8 ± 1.1	$(5.9 \pm 0.3) \times 10^{-2}$	218.1
Spermidine	70.4 ± 3.0	$(1.0 \pm 0.1) \times 10^{-1}$	704.0

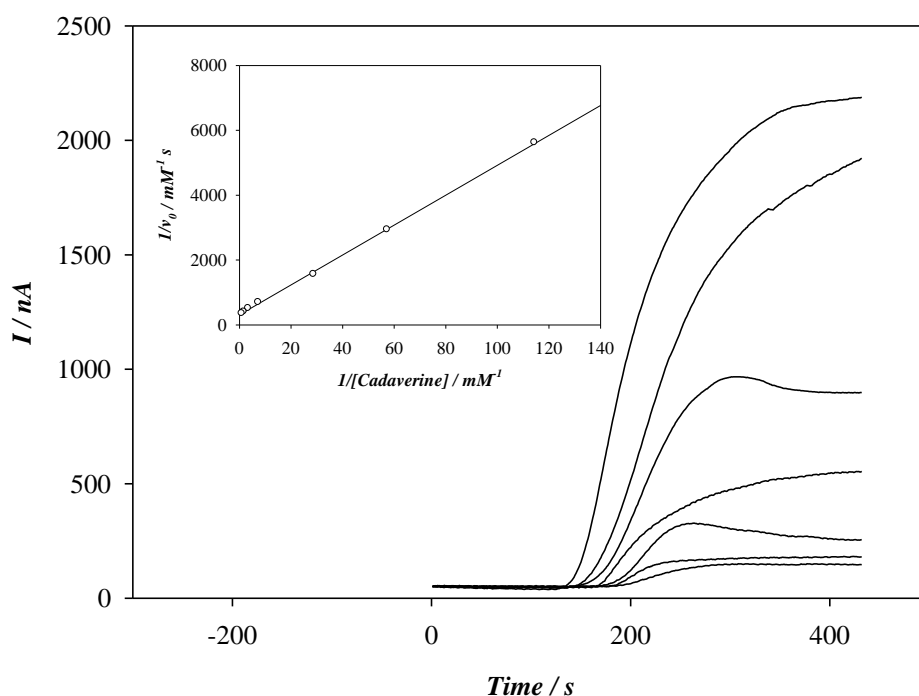


Figure 4.5 Amperometric response, using 0.26 U of LSAO free in solution, for different additions of cadaverine. Inset: linearisation of Lineweaver-Burk.

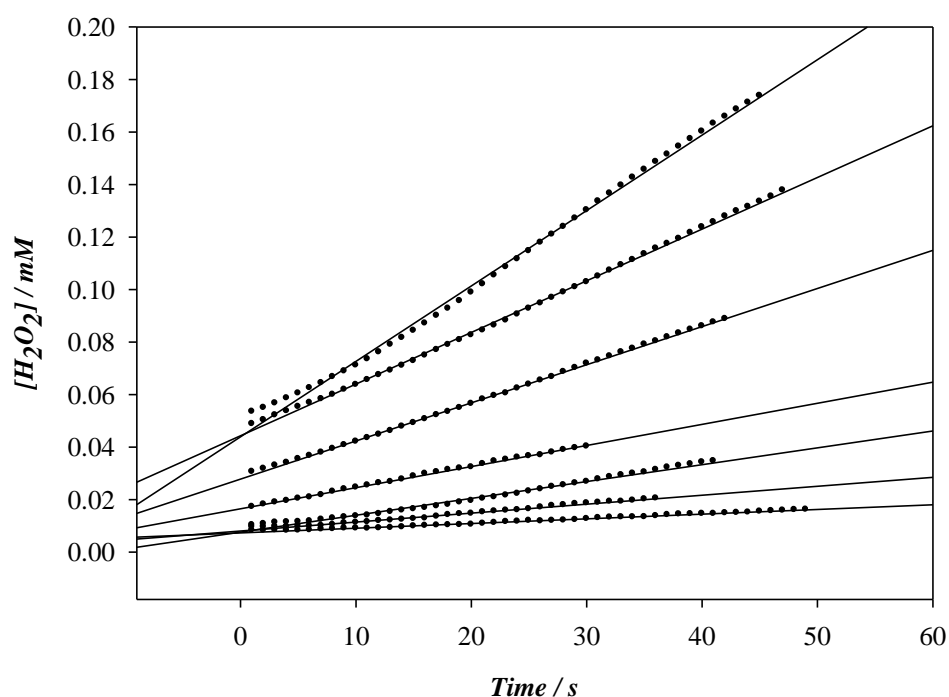


Figure 4.6 Initial rates extrapolated from the amperometric responses of LSAO free in solution with different additions of cadaverine.

Comparing the data reported in Table 4.2, obtained with the use of Amine Oxidase from *Lathyrus sativus* (LSAO), with those reported in literature for Amine Oxidase from *Lathyrus cicera* (LCAO),³⁸ that is an enzyme belonging to the same family, it can be observed that their behaviours differ only a few. In fact the reported K_M values for LCAO relatively to putrescine and cadaverine are 2.7×10^{-1} and 1.0×10^{-1} mM, respectively; these values are almost the same of those reported in table 4.2 for LSAO indicating that both enzymes display the same affinity towards these substrates. Conversely, LSAO has a greater affinity toward histamine, spermine and spermidine with respect to LCAO, being in this case the reported values of K_M for histamine, spermine and spermidine 7.9×10^{-1} , 6.3×10^{-1} and 2.1 mM, respectively. On the other hand, as far as the enzymatic efficiency is concerned, the k_{cat}/K_M values show the same trend for the two considered enzymes; taking into account the data in Table 4.2, the higher efficiency is towards cadaverine, followed by

³⁸ Pietrangeli P., Federico R., Mondovì B., Morpurgo L. *J. Inorg. Biochem.* **2007**, *101*, 997-1004.

putrescine, spermidine, spermine and finally histamine. This order is respected by LCAO in fact the reported values of k_{cat}/K_M for cadaverine, putrescine, spermidine, spermine and histamine are 1600, 970, 48, 45 and 13 $\text{mM}^{-1} \text{s}^{-1}$, respectively.

4.4 Conclusions

This study investigated the bioelectrochemical properties of Amine Oxidase from *Lathyrus sativus* (LSAO) either immobilised with PAP on Pt-SPE and free in solution. The kinetic parameters obtained with LSAO free in solution, i.e. K_M values, are quite similar to those of the analogue enzyme LCAO reported in literature with the exception that LSAO has a higher affinity toward histamine, spermine and spermidine with respect to LCAO. Instead, with regard to the turnover it can be assessed that there is the same trend for the two considered enzymes.

On the other hand, the kinetic parameters obtained with immobilised LSAO demonstrate that the enzyme displays the same the affinity towards all the selected substrates with the exception of cadaverine (highest affinity). On the other hand, the efficiency is maximum for putrescine, suggesting that the latter could be considered as standard to be used for expressing the total content of BA using a LSAO-based biosensor in the food quality monitoring.

In conclusion, LSAO was bioelectrochemically characterised using a series of different biogenic amines and the obtained results show that this enzyme is very promising to be used in the development of an efficient biosensor for the determination of biogenic amines in real samples.

Chapter 5

Development of Laccase-Based Biosensors for Real Samples Analysis

5.1 Introduction

Nowadays, quantitative analysis of wine samples is becoming of great importance in food chemistry area because to the general effort to achieve an adequate quality. Wine is a complex food mixture of several hundred compounds, present simultaneously at different concentrations. The dominants ones are water, ethanol, glycerol, sugars, organic acids and various ions. Except ethanol and glycerol, other aliphatic and aromatic alcohols, amino acids, and phenolic compounds are present at much lower concentration.¹ Polyphenols are well known for their antioxidants properties,² which have been associated with reduced risk of cancer,³ stroke,⁴ heart disease,⁵ and diabetes.⁶ They also play an important role in food quality.⁷

Many analytical procedures, developed for determination of polyphenols are often expensive and require several operations.⁸ Besides, it is not easy to monitor these compounds in real matrices for different reasons such as their chemical complexity, difficult extraction procedure and the presence of interferences. Wine contains a variety of

¹ Tarantilis P.A., Troianou V.E., Pappas C.S., Kotseridis Y.S., Polissiou M.G. *Food Chem.* **2008**, *111*, 192-196.

² (a) Fogliano V., Verde V., Randazzo G., Ritieni A. *J. Agric. Food Chem.* **1999**, *47*, 1035-1040; (b) Mannino S., Brenna O., Buratti S., Cosio M.S. *Electroanalysis* **1998**, *10*, 908-912; (c) Simonetti P., Pietta P., Testolin G. *J. Agric. Food Chem.* **1997**, *45*, 1152-1155; (d) Ghiselli A., Nardini M., Baldi A., Scaccini C. *J. Agric. Food Chem.* **1998**, *46*, 361-367.

³ He S., Sun C., Pan Y. *Int. J. Mol. Sci.* **2008**, *9*, 842-853.

⁴ Ghosh D., Scheepens A. *Mol. Nutr. Food Res.* **2009**, *53*, 322-331.

⁵ Aruoma O. I., Murcia A., Butler J., Halliwell B. *J. Agric. Food Chem.* **1993**, *41*, 1880-1885.

⁶ Sabu M. C., Smitha K., Kuttan R. *J. of Ethnopharmacology* **2002**, *83*, 109-116.

⁷ Manach C., Scalbert A., Morand C., Rémésy C., Jiménez L. *American J. Of Clinical Nutrition* **2004**, *79*, 727-747.

⁸ (a) Hayes P. J., Smyth M. R., McMurrrough I. *Analyst.* **1987**, *112*, 1205-1207; (b) Goldberg D. M., Tsang E., Karumanchiri A., Diamandis E. P., Soleas G. *Anal. Chem.* **1996**, *68*, 1688-1694.

phenolic compounds, commonly called tannins; in Figure 5.1 the chemical structure of some of them is showed below.

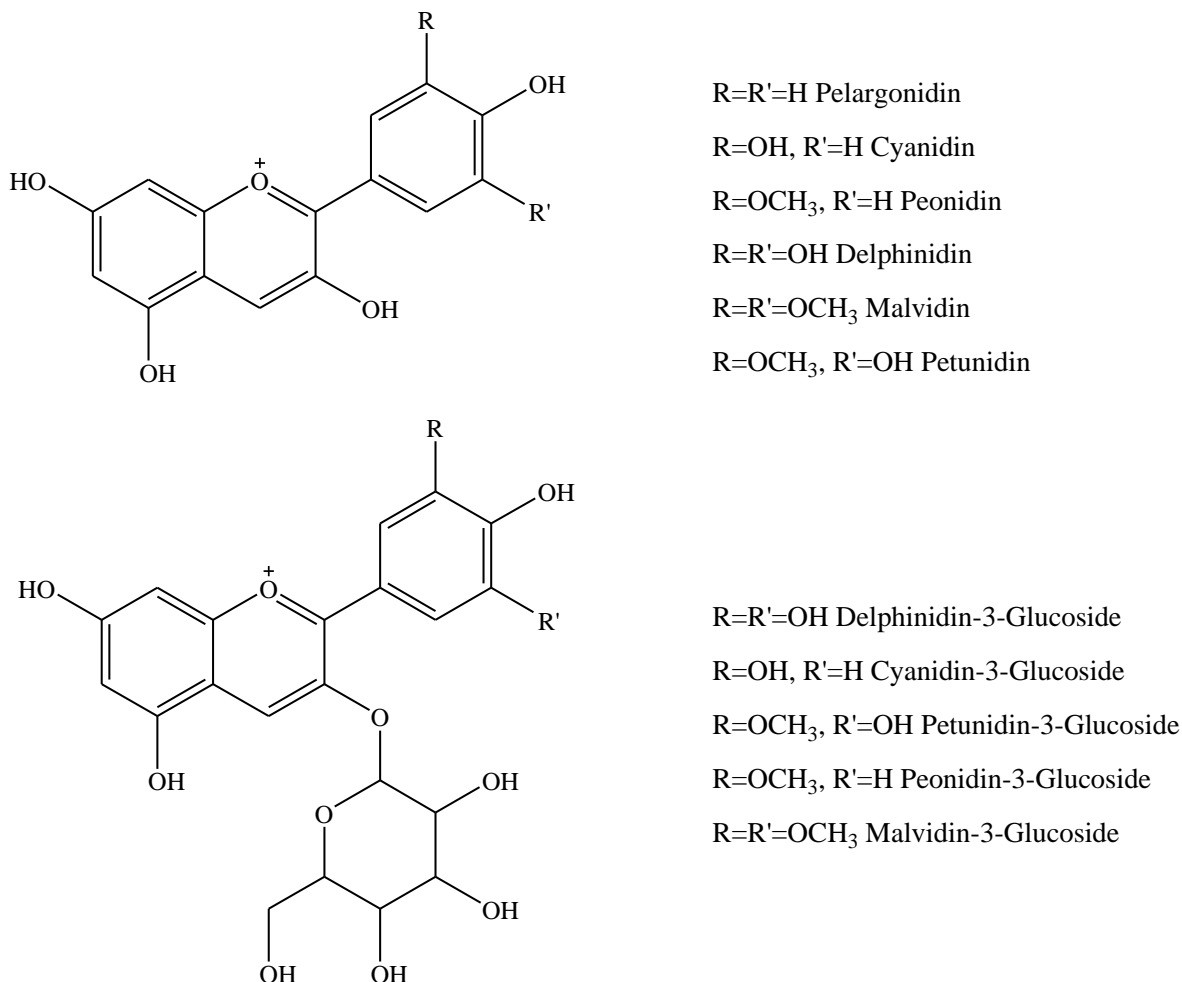


Figure 5.1 Chemical structures of some polyphenols

These compounds cannot be determined singly, so they are measured collectively as so called total polyphenol index.⁹ The reference method commonly used involves monitoring colorimetric chemical reduction and can be time-consuming and also produces chemical waste. Moreover, often is reported that colorimetric procedure leads to an overestimation of total polyphenol index because of the interference of sulphur dioxide, reducing sugars

⁹ Blasco A. J., Rogerio M. C., Gonzalez M. C., Escarpa A. *Anal. Chim. Acta* **2005**, 539, 237-244.

and ascorbic acid in real samples.¹⁰ In addition, it is reported that the co-concurrence of sulphur dioxide and reducing sugars can result in synergistic effects.⁹

Other most important phenols are catecholamines. They are sympathomimetic "fight-or-flight" hormones released by the adrenal glands in response to stress.¹¹ They are part of the sympathetic nervous system and are called catecholamines because they contain a catechol or 3,4-dihydroxyphenyl group and an ethylamine moiety, and are derived from the amino acid tyrosine.¹² They have the distinct structure of a benzene ring with two hydroxyl groups, an intermediate ethyl chain, and a terminal amine group (Figure 5.2). Phenylethanamines such as norepinephrine have a hydroxyl group on the ethyl chain.

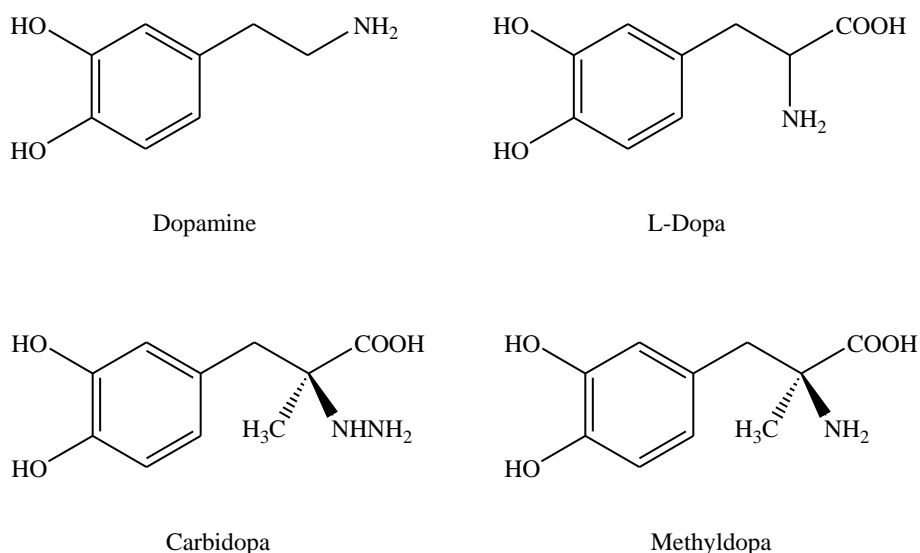


Figure 5.2 Chemical structures of some catecholamines.

In the human body, the most abundant catecholamines are epinephrine (adrenaline), norepinephrine (noradrenaline) and dopamine; the latter has been widely accepted to be one of the most important neurotransmitters involved in physiological process mammalian

¹⁰ Celeste M., Tomás C., Cladera A., Estela J. M., Cerdà V. *Anal. Chim. Acta* **1992**, 269, 21-28.

¹¹ Dimsdale J. E., Moss J. *Psychosom. Med.* **1980**, 42, 493-497.

¹² Dale P., Augustine G. J., Fitzpatrick D., Hall W. C., LaMantia A.-S., McNamara J. O., White L. E. *Neuroscience* **2008** (4th ed. Sinauer Associates), 137-138.

central nervous system and as a prognostic biomarker for several kind of diseases, as Parkinson's disease.¹³

Because of catecholamines have a half-life of a few minutes when circulating in the blood, their detection is much difficult. Biosensor technology appears to be suitable for this purpose because they are portable and in addition they exhibit advantages as easy sample preparation, selectivity, sensitivity, reproducibility and low costs.¹⁴

Electrochemical biosensors, in particular amperometric ones, are an attractive alternative to current used analytical methods, as chromatographic techniques, to measure polyphenols in wine samples and catecholamines in blood. Commonly used amperometric biosensors for phenols are based on Tyrosinase,¹⁵ Peroxidase,¹⁶ pyrroloquinoline quinine dependent Glucose Dehydrogenase (GDH)¹⁷ or Cellobiose Dehydrogenase (CDH).¹⁸

In the previous Chapter 3, TvL and ThL have been bioelectrochemically characterised using a series of different diphenols and the obtained results showed that they are very promising to be used in the development of efficient biosensors for the determination of diphenols (e.g. polyphenols and catecholamines). For this reason, aim of this part of work is the development of Laccase biosensors for the determination of catecholamines in pharmaceutical preparations and polyphenol index in wines, and the comparison of the data obtained by the spectrophotometric Folin-Ciocalteu method, commonly used for real

¹³ (a) Adams R. N. *Anal. Chem.* **1976**, *48*, 1126-; (b) Boulton A. A., Baker G. B., Bateson A. N. (Eds.) *In vivo Neuromethods* **1998** (Human Press Inc., Totowa, New Jersey); (c) Gessa G. L., Serra G. (Eds.) *Dopamine and Mental Depression* **1989** (Pergamon Press., Oxford, New York).

¹⁴ (a) Freire R. S., Ferreira M. M. C., Duràn N., Kubota L. T. *Anal.Chim.Acta* **2003**, *485*, 263-269; (b) Gomes S. A. S. S., Nogueira J. M. F., Rebelo M. J. F. *Biosens. Bioelectron.* **2004**, *20*, 1211-1216.

¹⁵ (a) Wang J., Lu F., Kane S. A., Choi Y. K., Smyth M. R., Rogers K. *Electroanalysis* **1997**, *9*, 1102-1106; (b) Carralero V., Mena M. L., González-Cortés A., Yáñez-Sedeño P., Pingarrón J. M. *Anal. Chim. Acta* **2005**, *528*, 1-8.

¹⁶ Munteanu F. D., Lindgren A., Emneus J., Gorton L., Rutzgas T., Csoregi E., Ciucu A., van Huystee R. B., Gazaryan I. G., Lagrimini L. M. *Anal. Chem.* **1998**, *70*, 2596-2600.

¹⁷ Szeponik J., Moller B., Pfeiffer D., Lisdat F., Wollenberger U., Makower A., Scheller F. W. *Biosens. Bioelectron.* **1997**, *12*, 947-952.

¹⁸ Lindgren A., Rutzgas T., Stoica L., Munteanu F. D., Gorton L. *Chemical and Biological Sensors for Environmental Monitoring* (Mulchandani A., Sadki O. A. Editors), ACS Symposium Series, Washington DC **2000**, *762*, 113-124.

matrices,¹⁹ to those obtained by the proposed electrochemical biosensors operating in Flow Injection Analysis (FIA) conditions.

The biosensors proposed in this section are realised by employing the two different Laccases, *Trametes versicolor* (TvL) and *Trametes hirsuta* (ThL) and using polyazetidine prepolymer (PAP) as immobilising agent. TvL was just used, in the past years, to detect the polyphenol index in wines,²⁰ such as catecholamines,²¹ but immobilised with other techniques; conversely, ThL, before this work, was never used for the same purpose. Its use has been limited so far to the development of biofuel cells²² and to detect the phenolic compounds without an applicative use on real matrices.²³

In the development of Laccase-based biosensors for the determination of polyphenol index in wine, generally, the index is referred to gallic acid (total concentration thereof); the corresponding reaction is described in Figure 5.3.

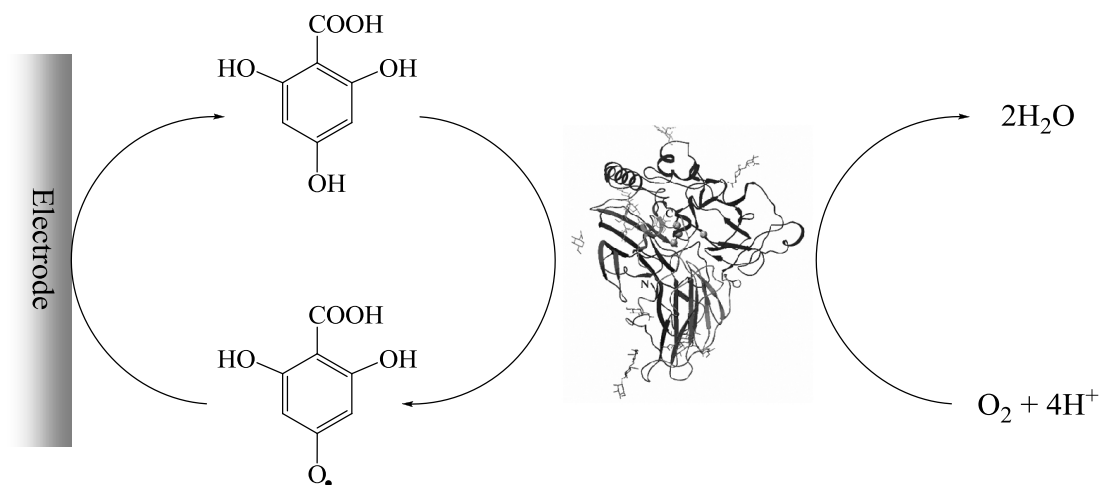


Figure 5.3 Electron transfer mechanism of gallic acid oxidation on a Laccase biosensor.

¹⁹ (a) Escarpa A., González M. C. *Anal. Chim. Acta* **2001**, 427, 119-127; (b) Gamella M., Campuzano S., Reviejo A. J., Pingarrón J. M. *J. Agric. Food Chem.* **2006**, 54, 7960-7967.

²⁰ (a) Freire R. S., Duran N., Kubota L. T. *Talanta* **2001**, 54, 681-686; (b) Vianello F., Cambria A., Ragusa S., Cambria M. T., Zennaro L., Rigo A. *Biosens. Bioelectron.* **2004**, 20, 315-321; (c) Leite O. D., Lupetti K. O., Fatibello-Filho O., Vieira I. C., de M. Barbosa A. *Talanta* **2003**, 59, 889-896; (d) Freire R. S., Durán N., Kubota L. T. *Anal. Chim. Acta* **2002**, 463, 229-238; (e) Freire R. S., Durán N., Wang J., Kubota L. T. *Anal. Lett.* **2002**, 35, 29-38.

²¹ (a) Ferry Y., Leech D. *Electroanalysis* **2005**, 17, 113-119; (b) Xiang L., Lin Y., Yu P., Su L., Mao L. *Electroch. Acta* **2007**, 52, 4144-4152.

²² Vaz-Dominguez C., Campuzano S., Rüdiger O., Pita M., Gorbacheva M., Shleev S., Fernandez V. M., De Lacey A. L. *Biosens. Bioelectron.* **2008**, 24, 531-537.

²³ Haghghi B., Ramati-Panah A., Shleev S., Gorton L. *Electroanalysis* **2007**, 19, 907-917.

Also in the case of catecholamines, the reaction occurring on electrode surface is the same of that one described in Figure 5.3, with the enzymatic formation of a phenoxyl radical.

Finally, in order to increase the stability of the biosensors, the PAP entrapping properties have been integrated with the conductivity, high surface area matrix, flexibility and reactivity of either Multi-Walled Carbon Nanotubes (MWCNTs) or Single-Walled Carbon Nanotubes (SWCNTs) chosen as electrodic materials.²⁴

²⁴ Katz C. E., Willner I. *ChemPhysChem* **2004**, 5, 1084-1104.

5.2 Experimental Section

5.2.1 Materials

Fungal Laccase from *Trametes versicolor* was supplied by Fluka (EC 1.10.3.2, activity: 30.6 U mg⁻¹, according to Sigma-Aldrich supplier, the enzyme content of this Laccase is approximately 10%) and stored at -18 °C. *Trametes hirsuta* Laccase was gently donated by VTT Technical Research Centre of Finland (3.9 mg ml⁻¹ in citrate buffer pH 5; activity: 421 U ml⁻¹). Bovine Serum Albumin (BSA, EC 232-936-2), 3,4-dihydroxyphenethylamine (dopamine), 3,4,5-trihydroxybenzoic acid (gallic acid), sodium metabisulphite, ascorbic acid, glucose and fructose were purchased from Sigma and used as received. Kit for measurement of total polyphenols concentration in wines was purchased from Biogamma (Rome, Italy). The kit contains Folin-Ciocalteu reagent (composed by a mixture of H₃PW₁₂O₄₀ and H₃PMo₁₂O₄₀), carbonate buffer and a standard solution of gallic acid 3.0 g L⁻¹. Stock solutions of gallic acid were prepared in 0.1 mol L⁻¹ Britton-Robinson buffer, pH 5, daily. More diluted standard solutions were prepared by suitable dilutions with the same buffer. The polymeric film employed for protein entrapping was poly-1-(aminomethyl)-1-{2-[(6-oxyesane)amino]ethyl}-3-hydroxyazetidinium chloride (polyazetidine prepolymer, PAP®), donated by Hercules Inc. Wilmington DE (USA). Other chemicals were all of analytical grade. High purity deionised water (Resistance: 18.2 MΩ × cm at 25 °C; TOC<10 µg/L) obtained from Millipore (France) has been used to prepare all the solutions.

Different wine samples were acquired from a local market in Rome (Italy). The only sample treatment required consisted of an appropriate dilution with a buffer solution before analysis.

5.2.2 Apparatus

Amperometric experiments were performed by using a μ -Autolab type III potentiostat (Eco Chemie) controlled by means of the GPES Manager program (Eco Chemie). Screen Printed Electrodes (SPEs) (DropSens Oviedo, Spain), constituted by a MWCNTs or SWCNTs working electrode with a surface diameter of 4 mm, carbon as counter electrode and silver as pseudoreference one, were used. Flow experiments were carried out using a microliter cell (DropSens Oviedo, Spain), an Omnifit sample injection valve (DropSens Oviedo, Spain) and a Gilson Minipuls-3 peristaltic pump. Cyclic voltammetry experiments (CVs) were performed in a 10 ml thermostated glass cell with a conventional three-electrode configuration. A modified MWCNTs Screen Printed Electrode was used as working electrode, a graphite counter electrode and an Ag/AgCl/Cl⁻ (Metrohm, Switzerland, 198 mV vs NHE) as reference electrode.

5.2.3 Biosensors Preparation

The carbon nanotubes screen printed electrodes were preliminary treated by depositing on the working electrode 10 μ l of 0.5 mol L⁻¹ nitric acid solution in order to obtain the carboxyl functionalisation of their surface.²⁵ *Trametes versicolor* Laccase biosensor (TvL-MWCNTs-SPE and TvL-SWCNTs-SPE) and *Trametes hirsuta* Laccase biosensor (ThL-MWCNTs-SPE and ThL-SWCNTs-SPE) were prepared by spreading 3 μ l of a solution of PAP, containing enzymes, onto the electrodes surface to have a final amount of 0.80 U. To assess the matrix effect on the measurements, a sensor with only PAP (PAP-MWCNTs-SPE) was prepared by spreading 3 μ l of PAP solution onto the surface of the electrode. Then the electrodes were left to dry overnight at room temperature.

²⁵ Kim S. N., Rusling J. F., Papadimitrakopoulos F. *Adv. Mat.* **2007**, *19*, 3214-3228.

Another aspect taken into account was the influence of impurities present in commercial Laccase (TvL). To test the impurities influence, a proper amount of BSA was added to ThL based biosensor and the obtained results were compared with those obtained with TvL based biosensor for polyphenol index.

Biosensors were stored in 0.1 mol L⁻¹ Britton-Robinson buffer, pH 5 at 4°C, when not in use.

5.2.4 Polyphenol Content by Folin-Ciocalteu Method

For comparison purpose, wines were also analysed by the spectrophotometric method involving the use of the Folin-Ciocalteu reagent using a T60U Spectrometer PG Instruments Ltd (Wibtoft Leicestershire, United Kingdom). Briefly, 100 µL of white wine sample, or 20 µL in the case of red wines, were added at 2000 µL of chromogen solution; the same procedure (using the same volume, respectively) was also adopted for the blank (distilled water) and standard (0.6 g L⁻¹ gallic acid for white wines or 3 g L⁻¹ gallic acid for red wines). The obtained solutions were mixed and incubated for about 1 minute at room temperature; then 1000 µL of alkaline buffer was added to every solution and the resulting solutions were mixed and incubated for 30 minutes at room temperature. The absorbances of blank, sample and standard solutions were read at 760 nm against distilled water.

The total polyphenols content was calculated by:

$$\text{Total polyphenols (g L}^{-1}\text{)} = \frac{A_{\text{sample}} - A_{\text{blank}}}{A_{\text{std}} - A_{\text{blank}}} [\text{Std}]$$

Where A_{sample} is the absorbance read for the sample, A_{blank} for the blank, A_{std} for the standard and finally $[\text{Std}]$ is the standard concentration expressed in g L⁻¹ of gallic acid.

This method is specific for the –OH groups of the polyphenolic compounds and the obtained result is referred to the polyphenols concentrations as gallic acid.²⁶

5.2.5 Electrochemical Measurements

Flow experiments were carried out at a fixed potential of -100 mV vs the internal silver pseudoreference electrode with a flow rate of 4 $\mu\text{l s}^{-1}$. The carrier buffer was 0.1 mol L⁻¹ Britton-Robinson, pH 5 and aliquots of 100 μl of gallic acid standard solutions at different concentrations in the same buffer were used to obtain the calibration plot. The same procedure has been followed in the analysis of wine samples appropriately diluted and the resulting signal was referred to that one of gallic acid.

Batch electrochemical experiments, for pharmaceutical compounds were carried out at a fixed potential of -100 mV vs the internal silver pseudoreference electrode. The samples were prepared by dissolving tablets with the 0.1 mol L⁻¹ Britton-Robinson buffer solution, pH 5.5, and the result solution was referred to the calibration plot of the corresponding catecholamine (dopamine and methyldopa).

All the values reported are the average of at least six measurements.

²⁶ Jaroz-Wilkolazka A., Ruzgas T., Gorton L. *Enzyme Microb. Technol.* **2004**, 35, 238-241.

5.3 Results and Discussion

5.3.1 Laccase-Based Biosensor for the Determination of Polyphenols in Wine

To assess the effective catalytic properties of TvL-MWCNTs-SPE and ThL-MWCNTs-SPE biosensors toward gallic acid, CVs experiments were performed.

The cyclic voltammogram of gallic acid is characteristic of an electrochemical irreversible reaction. In presence of immobilised Laccase onto the electrode an increase of the cathodic current was observed. At same time the anodic peak disappeared in accord with a catalytic electrochemical reaction.²⁷ An analogue result was obtained with TvL-MWCNTs-SPE biosensor.

Having established the effective catalytic properties of the biosensors toward gallic acid, the quantity of enzyme to deposit onto the electrode surface has been optimised. In Figure 5.4 the effect on the amperometric response of the ThL loading onto the surface of the electrode is showed, by monitoring the signal obtained for a 4.2 mg L^{-1} gallic acid solution at -100 mV and, on the basis of the obtained results, an amount of Laccase corresponding to an activity of 0.8 U has been considered the optimum.

²⁷ Léger C., Elliott S. J., Hoke K. R., Jeuken L. J. C., Jones A. K., Armstrong F. A. *Biochemistry* **2003**, *42*, 8653-8662.

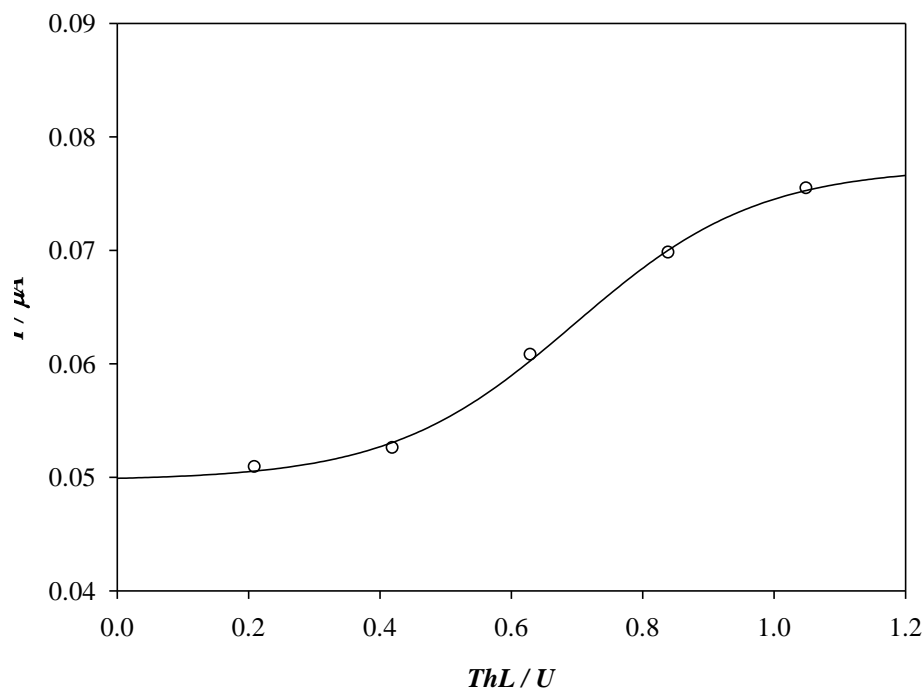


Figure 5.4 Effect of ThL enzyme loading on the amperometric response, of a 4.2 mg L^{-1} gallic acid solution, recorded at a fixed potential of -100 mV vs silver internal pseudoreference electrode.

The TvL-MWCNTs-SPE and ThL-MWCNTs-SPE electrodes, previously described, were bioelectrochemical and analytically characterised, in the presence of gallic acid as substrate, in flow injection conditions.

In Table 5.1 are summarised the main kinetic and analytical characteristics obtained and the reported data show a similar affinity of TvL and ThL toward gallic acid as well as sensitivity.

Table 5.1 Kinetic and analytical characteristics of gallic acid obtained by FIA amperometry in 0.1 mol L^{-1} Britton-Robinson buffer, pH 5 at a fixed potential of -100 mV for TvL-MWCNTs-SPE and ThL-MWCNTs-SPE biosensors.

Laccase	K_M^{app} (mg L^{-1})	I_{max} (μA)	I_{max}/K_M^{app} ($\mu\text{A mg}^{-1} \text{ L}$)	Slope ($\mu\text{A mg}^{-1} \text{ L}$)	Linear range (mg L^{-1})	r^2	LOD (mg L^{-1})
TvL	138.0 ± 15.6	2.6 ± 0.2	0.019	0.009 ± 0.001	0.1-17.0	0.999	0.1
ThL	133.3 ± 17.0	0.8 ± 0.1	0.006	0.007 ± 0.001	0.1-18.0	0.999	0.3

The two biosensors life times have been also estimated, monitoring the slope variation, using gallic acid as standard, day after day. In Figure 5.5 this variation is showed, using the two biosensors, and as it can be seen they have been used for several measurements with only a little loss of their performances, with a repeatability of about 3-4%.

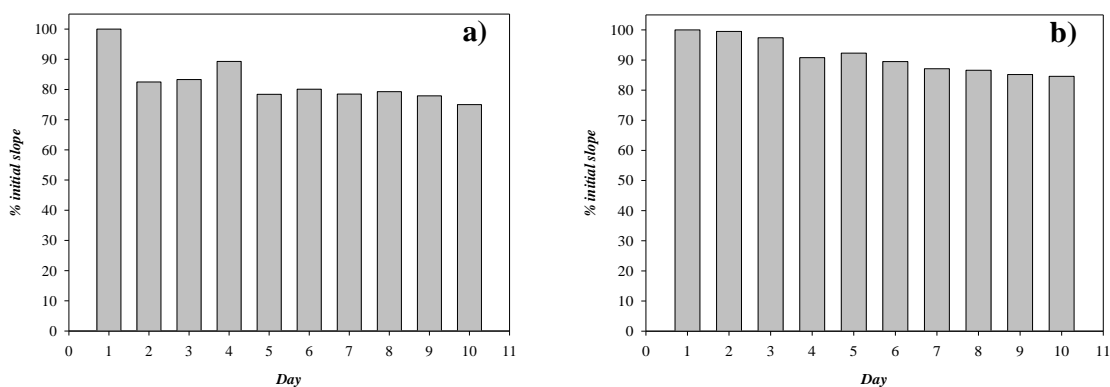


Figure 5.5 Slope variation for TvL-MWCNTs-SPE (a) and ThL-MWCNTs-SPE (b).

The proposed biosensors have been tested in a set of measurements with several Italian wine samples (six white and six red). In Figure 5.6 the amperometric behaviour obtained after the addition of gallic acid, a white wine, a red wine and the corresponding calibration plot constructed by using ThL-MWCNTs-SPE biosensors, is reported.

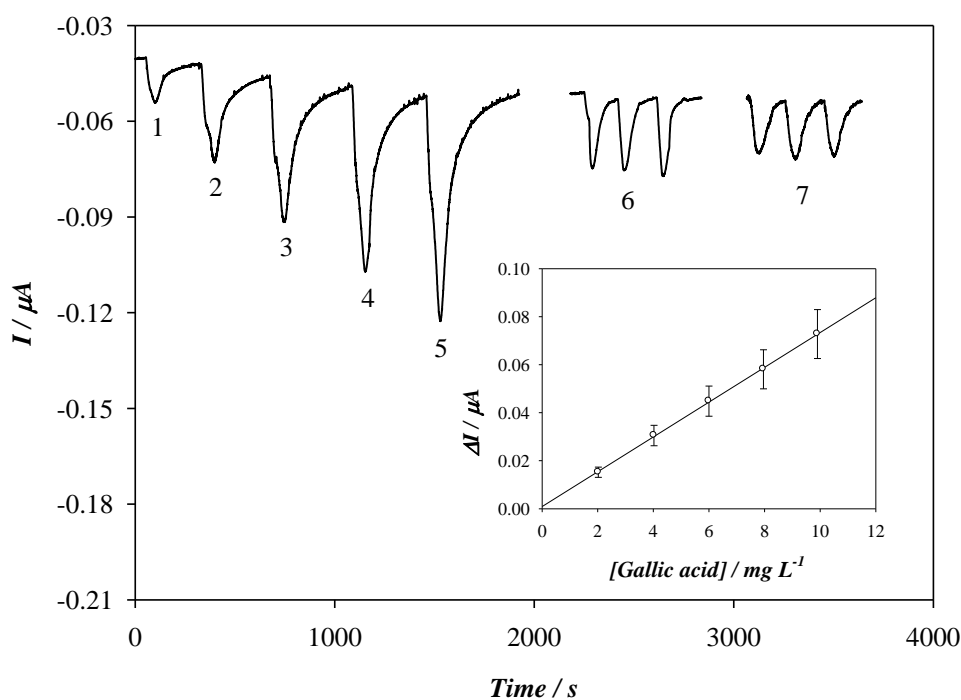


Figure 5.6 Amperometric current response, using ThL-MWCNTs-SPE biosensor under FIA conditions, of gallic acid 2.02 mg L^{-1} (1), 4.02 mg L^{-1} (2), 6.00 mg L^{-1} (3), 7.96 mg L^{-1} (4), 9.90 mg L^{-1} (5), three consecutive injections of white wine sample 6 diluted 50 times (6) and red wine sample 9 diluted 500 times (7). Inset: calibration plot of gallic acid.

As it can be observed, the overall time of analysis of a wine sample is of about 4 minutes, demonstrating the great time sparing of the system, also considering that it is possible to make several measurements during a single run.

The results obtained in the wine analysis are reported in Table 5.2, together to those obtained with the Folin-Ciocalteu reference method as comparison.

Table 5.2 Electrochemical polyphenol index obtained with the use of TvL-MWCNTs-SPE and ThL-MWCNTs-SPE biosensors and comparison with the value obtained using the Folin-Ciocalteu reference method.

Wines		Folin-Ciocalteu (mg L⁻¹)	FA TvL (mg L⁻¹)	Recovery TvL (%)	FA ThL (mg L⁻¹)	Recovery ThL (%)
white wines	sample 1	242 ± 1	142 ± 2	59	261 ± 7	108
	sample 2	199 ± 3	95 ± 9	48	197 ± 17	99
	sample 3	172 ± 4	72 ± 1	42	187 ± 1	109
	sample 4	189 ± 7	87 ± 1	46	185 ± 5	98
	sample 5	273 ± 7	132 ± 9	48	267 ± 11	98
	sample 6	199 ± 1	115 ± 3	42	185 ± 11	93
red wines	sample 7	2132 ± 103	1126 ± 36	53	2077 ± 87	97
	sample 8	2327 ± 38	1355 ± 41	58	2141 ± 86	92
	sample 9	1088 ± 18	609 ± 34	56	1129 ± 49	104
	sample 10	1326 ± 23	924 ± 54	70	1400 ± 25	106
	sample 11	1614 ± 17	1001 ± 94	62	1585 ± 69	98
	sample 12	1835 ± 15	1098 ± 94	60	1714 ± 40	93

As it can be seen in Table 5.2 the values of polyphenol index obtained with TvL-MWCNTs-SPE are lower than those obtained with the Folin-Ciocalteu method, in fact the recovery values ranged from 42% to 70%. On the contrary, the results obtained with ThL-MWCNTs-SPE biosensor are closer to the reference method, with recovery values ranging from 92% to 109%. These differences were unexpected but they may be ascribed to the impurities present in the commercial TvL (this question will be exposed below). However, it is interesting to note that the polyphenol index values obtained with the use of ThL-MWCNTs-SPE are in very good accordance with those obtained using the spectrophotometric reference method.

The same measurements made with MWCNTs-SPE have been carried out using SWCNTs-SPE electrodes, in the same experimental conditions. In Table 5.3 are summarised the main analytic parameters obtained using SWCNTs-SPE electrodes.

Table 5.3 Analytical characteristics of gallic acid obtained by FIA amperometry in 0.1 mol L⁻¹ Britton-Robinson buffer, pH 5 at a fixed potential of -100 mV for TvL-SWCNTs-SPE and ThL-SWCNTs-SPE biosensors.

Laccase	Slope ($\mu\text{A mg}^{-1} \text{L}$)	r^2	<i>LOD</i> (mg L^{-1})
TvL	0.016 ± 0.001	0.998	0.2
ThL	0.004 ± 0.001	0.997	0.6

As it can be seen, the sensitivities of these biosensors is almost 50% the sensitivity of the same biosensors based on MWCNT, this could be explained taking into account the lower electroactive area of SWCNTs.

Preliminary, measurements on two wine samples have been carried and because the obtained results have evidenced that TvL-SWCNTs-SPE biosensor gives similar values to those obtained using MWCNTs (i.e. very low recovery values), the wine samples have been tested only with ThL-SWCNTs-SPE biosensor. The obtained results are reported in Table 5.4 and in this case the values of polyphenol index are lower than those obtained with the Folin-Ciocalteau method of the 4-11% for the white wines and of the 4-8% for the red ones.

Table 5.4 Electrochemical polyphenol index obtained with ThL-SWCNTs-SPE biosensor and comparison with the value obtained using the Folin-Ciocalteu reference method.

Wines	Folin-Ciocalteu (mg L ⁻¹)	FIA ThL (mg L ⁻¹)	Recovery ThL (%)	
white wines	sample 1	242 ± 1	221 ± 14	92
	sample 2	199 ± 3	177 ± 5	89
	sample 3	172 ± 4	163 ± 1	95
	sample 4	198 ± 7	190 ± 2	96
	sample 5	273 ± 7	258 ± 2	95
	sample 6	199 ± 1	187 ± 2	94
red wines	sample 7	2132 ± 103	2005 ± 38	94
	sample 8	2327 ± 38	2219 ± 46	95
	sample 9	1088 ± 18	1006 ± 31	92
	sample 10	1326 ± 23	1250 ± 44	94
	sample 11	1614 ± 17	1518 ± 48	94
	sample 12	1835 ± 15	1757 ± 76	96

These results are very interesting because they are all lower than those obtained with the reference method, that generally leads to an overestimation of the real content of polyphenols in wines.

To better understand the role of other electrochemical species that could interfere with the biosensor response, leading to distorted results, a study of the interferents has been carried out.

The possible interferents present in the wine are sulphur dioxide (SO₂), coming from the reaction of sodium metabisulphite (Na₂S₂O₅) (added as preservative) with wine organic acids, reducing sugars (glucose and fructose) and ascorbic acid. Neither sulphur dioxide nor reducing sugars interfere with electrochemical measurements because the first one is simply eliminated by nitrogen bubbling, as this is a known pretreatment procedure in wine

analysis,²⁸ and the last ones because they are not electroactive species; hence, ascorbic acid is the only compound that could interfere with the electrochemical measurements.

In order to evaluate the ascorbic acid interference, a proper amount (150 mg L⁻¹ is the Italian maximum limit for the addition of ascorbic acid in wines)²⁹ was added to wine sample. Its interference, for biosensors based on MWCNTs, ranges from +8% to +10% for white wines and from +5 to +7% for red ones, while biosensors based on SWCNTs are not affected.

At the same time, these wine samples were analysed by means of colorimetric method and values obtained are the following: ascorbic acid 200 mg L⁻¹ produce an interference of about +10% on the measurements of polyphenol index in white wines and of about +6% in red wines, this is almost the same percentage difference obtained when comparing colorimetric data to those ones obtained by means of ThL-SWCNTs-SPE biosensor. Nevertheless, spectrophotometric interferences reported in literature,^{16,17c} due to ascorbic acid, are higher than those obtained in this work. This difference could be ascribed to the fact that Folin-Ciocalteu is an equilibration method. In the classical procedure, the absorbance is read 1 or 2 hours after the preparation of the solutions, while in our study is carried out 30 minutes after (due to a modification of the Folin-Ciocalteu reagent introduced by the supplier), thus leading to smaller interference.

Finally, in order to evaluate the matrix effect in the electrochemical measurements in wine samples, a set of experiments has been performed with an electrode PAP-MWCNTs-SPE. The obtained results put in evidence the absence of any interferences in the electrochemical measurements of wine samples, due to the low applied potential (-100 mV), in the amperometric measurements.

²⁸ Becchetti R. *Metodo di Analisi dei Vini e delle Bevande Spiritose* (sixth ed., Libertini, Italy) **1999**.

²⁹ *Gazzetta Ufficiale Italiana* **31-08-1998**, n. 202.

In order to explain the different results obtained with TvL and ThL based biosensors, probably due to impurities present at 90% into the commercial TvL, a further experiment was carried out. A certain amount of an inert protein (BSA) was added to ThL to have the same percentage of protein concentration of commercial TvL and the resulting ThL-based biosensor was compared to TvL one in absence of BSA.

Polyphenol index determined by BSA-ThL based biosensor is similar to that obtained by TvL-MWCNTs-SPE and lower than that obtained by the reference method. Data demonstrated that impurities present in commercial Laccase (TvL) creating an obstacle for analytes diffusion towards electrode surface, while *Trametes hirsuta*, with a high level of purity, is more disposed for polyphenols determination in wines.

Finally, in Table 5.5 the main electroanalytical properties of some amperometric biosensors reported in literature and based on different enzymes for the determination of polyphenol compounds in wines are summarised and compared to the results obtained in this research. In particular, type of electrode, immobilisation method, used enzyme, detection potential, recovery and life time of biosensor are reported.

The simplicity of preparation of the biosensors presented in this section and the working potential are comparable with the other proposed systems. Taking into account the recovery, the data presented here are in the range 92-109 % for the system ThL-MWCNTs-SPE and 89-96 % for ThL-SWCNTs-SPE, while values obtained by the other authors cited in Table 5.5 are clearly worse with respect to those obtained here. Considering also the life time the reported values don't exceed 5 days, while the developed biosensors in this work performed acceptably for a period longer than 10 days.

Table 5.5 Amperometric biosensors based on different enzymes for determination of polyphenol index in wines.

Electrode	Immobilisation	Enzyme	Sample	E_{appl} (V)	Recovery (%)	Life time	Ref.
MWCNTs/SWCNTs	PAP	Laccase (ThL)	Wine	-0.1 V vs Ag/AgCl	89-96 ^{b,e}	10 days	
Au	SAM of MPA	HRP	Red wine	0.0 V vs Ag/AgCl	66-83 ^{a,d}	-	30
CPE modified with Ru	Entrapment in the CPE	Tyrosinase	Wine	-0.10 V vs Ag/AgCl	2-6 ^{c,d}	3-4 h	15b
GCE	Cross-linking with glutaraldehyde	Laccase (TvL)	Wine	-0.20 V vs Ag/AgCl	3-5 ^{c,d} 4-7 ^{c,e} 21-61 ^{b,d} 43-94 ^{b,e}	5 days	19b
Pt coupled with a transducer for oxygen	Kappa-carrageenan gel	Tyrosinase	Wine	-0.65 V vs Ag/AgCl	83-122 ^{c,d}	-	31
Graphite SPE modified with ferrocene	Different immobilisations	Laccase (TvL)- Tyrosinase	Wine	0.05 V vs Ag/AgCl	~17 ^{b,e,f}	5 days	32

^a (+)-catechin; ^b gallic acid; ^c caffeic acid; ^d in batch conditions; ^e in flow injection conditions; ^f estimated from figure 6.

5.3.2 Laccase-Based Biosensor for the Determination of Catecholamines in Pharmaceutical Preparations

The catalytic properties of TvL-MWCNTs-SPE and ThL-MWCNTs-SPE biosensors, toward dopamine, have been assessed in Chapter 3 (see Figure 3.9). CVs experiments showed that the voltammetric behaviours of TvL and ThL based biosensor, in the presence of dopamine, are characteristic of electrochemical quasi-reversible reactions. In presence of immobilised enzymes onto the electrode, an increase of the cathodic currents was observed. At same time the anodic peaks disappeared according to catalytic electrochemical reactions.³³

The TvL-MWCNTs-SPE and ThL-MWCNTs-SPE electrodes, previously described for their bioelectrochemical properties, here, have been analytically characterised, in the

³⁰ Imabayashi S., Kong Y.-T., Watanabe M. *Electroanalysis* **2001**, *13*, 408-412.

³¹ Campanella L., Bonanni A., Finotti E., Tomassetti M. *Biosens. Bioelectron.* **2004**, *19*, 641-651.

³² Montareali M. R., Della Seta L., Vastarella W., Pilloton R. *J. Mol. Catal. B: Enzym.* **2010**, *64*, 189-194.

³³ Léger C., Elliott S. J., Hoke K. R., Jeuken L. J. C., Jones A. K., Armstrong F. A. *Biochemistry* **2003**, *42*, 8653-8662.

presence of catecholamines as substrates, in batch conditions. In Figure 5.7, the experimental chronoamperometric response of TvL-PAP-MWCNT biosensor and the corresponding calibration curve, for increasing concentration of dopamine, are reported and in Table 5.6 are summarised the main analytical characteristics obtained.

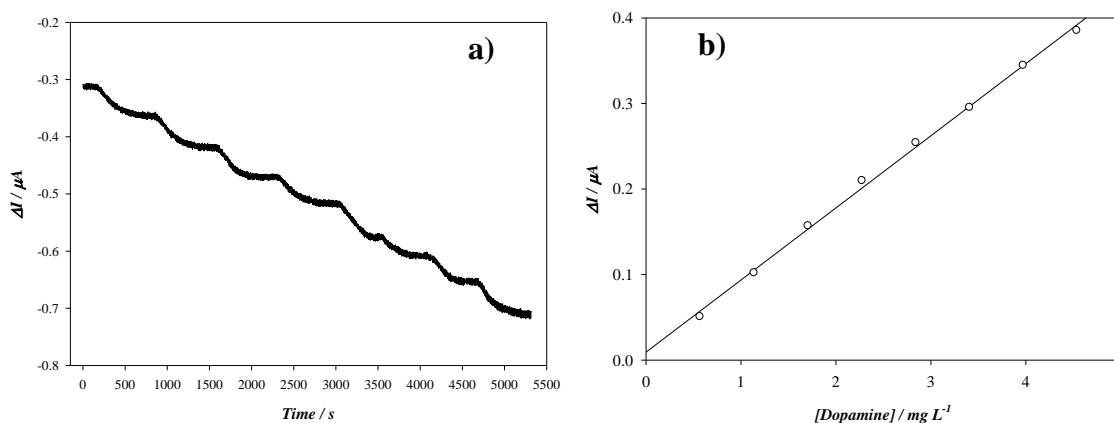


Figure 5.7 Experimental current response (a) and calibration plot (b), obtained with TvL-MWCNTs-SPE biosensor, using dopamine as substrate; measurements carried out in batch condition, in Britton-Robinson buffer pH 5.5, at $E_{\text{appl}} = -100$ mV.

Table 5.6 Analytical characterisation of Laccase-PAP-MWCNT biosensor for each mediator obtained by batch chronoamperometry at fixed potential in stirred solutions.

	Mediator	Linear range (mg L ⁻¹)	Slope ($\mu A \text{ mg}^{-1} \text{ L}$)	r^2	LOD (mg L ⁻¹)
TvL	Dopamine	0.800-4.130	0.0029 ± 0.0002	0.998	0.240
	L-Dopa	1.900-5.900	0.0016 ± 0.0003	0.999	0.570
	Carbidopa	1.100-5.590	0.0038 ± 0.0005	0.999	0.330
	Methyldopa	2.500-4.760	0.0018 ± 0.0001	0.997	0.750
ThL	Dopamine	0.030-6.000	0.710 ± 0.020	0.995	0.010
	L-Dopa	0.070-7.880	0.400 ± 0.100	0.990	0.020
	Carbidopa	1.780-63.280	0.107 ± 0.006	0.990	0.530
	Methyldopa	0.003-0.143	18.000 ± 2.000	0.990	0.001

The functional life time of the Laccase-based biosensors was evaluated by performing repetitive measures for the selected mediators in their concentration range, respectively;

after use, the biosensor was stored at 4 °C. After 6 days, it retained 50% of the original response, which considering the nature of immobilisation provided by PAP,³⁴ can be mainly attributed to the loss of the immobilised enzyme.

The suitability of the proposed system as a biosensor for measurements in real samples, was checked by determining the catecholamines content in drug formulations, using TvL-MWCNTs-SPE biosensor in batch conditions.

Since the selected pharmaceutical formulations are constituted by different catecholamines, the obtained signal was referred to different standard compounds. Obtained results on commercial pharmaceutical formulations are reported in Table 4.

Table 5.7 Analysis of pharmaceutical formulations by TvL-PAP-MWCNT biosensor.

Pharmaceutical preparation	Nominal value for each tablet (mg)	Determined value for each tablet (mg)	Accuracy (%)
Sample 1	25 Carbidopa 250 L-Dopa	172 as total Dopamine	n.a.
Sample 2	250 Methyldopa	247 Methyldopa	-1.2

For sample 1, which is constituted by carbidopa and L-dopa, the catecholamine content was referred to total amount of dopamine; conversely, methyldopa was used as standard for sample 2, taking into account the declared composition. In the latter case a very good agreement to nominal value was observed; in the case of sample 1, the estimation of the accuracy was not possible: anyway, it should be pointed out that the obtained result is consistent with the relative sensitivity of the considered compounds.

³⁴ Frasconi M., Favero G., Di Fusco M., Mazzei F. *Biosens. Bioelectron.* **2009**, *24*, 1424-1430.

5.4 Conclusions

In conclusion the Laccases biosensors proposed are suitable devices for the determination of both polyphenol index in wines and catecholamines in pharmaceutical preparations. In this chapter, regarding to the wines, it has been demonstrated that biosensor performance depends on enzyme adopted, in fact, ThL-based biosensor is to be preferred to TvL one. In particular, values obtained by using *Trametes hirsuta* are close to those determined by Folin-Ciocalteu method, on the contrary polyphenol index measured with *Trametes versicolor* is discordant to reference assay. The influence of the interferences on both spectrophotometric and electrochemical measurements have been carefully evaluated, demonstrating that they do not affect the electrochemical measurements using SWCNTs, but only the spectrophotometric one by a percentage attributable to the interference of ascorbic acid. For these reasons, ThL-SWCNTs-SPE biosensor represents a good and easy method for monitoring polyphenols in real samples.

Finally, it has been demonstrated that TvL-MWCNTs-SPE and ThL-MWCNTs-SPE biosensors are very suitable for the detection of catecholamines; in particular, the former has been tested with two real samples, giving very promising results for further experiments.

Chapter 6

Development of a LSAO-Based Biosensor for the Detection of Biogenic Amines in Real Samples

6.1 Introduction

Biogenic amines (BA) are nitrogen-containing compounds produced during the fermentation, from the decarboxylation of amino acids by yeast and bacteria.¹ The main biogenic amines are tyramine, histamine, putrescine, cadaverine, tryptamine and spermine (from which derives spermidine) synthesised by decarboxylation of the amino acids tyrosine, histidine, ornithine, lysine, tryptophan, phenylalanine and arginine, respectively.

BA have long been recognised as responsible for health problems in humans such as allergic or asthmatic events;² moreover, BA are potential precursors for the formation of carcinogenic *N*-nitroso compounds² and for this reason it is important to detect BA in food and beverages. Under normal conditions the biogenic amines are neutralised by the action of specific enzymes in the gut (e.g. Diamine Oxidase (DAO) metabolises histamine,³ while the Monoamine Oxidase (MAO) metabolises tyramine).⁴ However, some pharmacological substances (MAO and DAO inhibitors) or foods in decomposition, rich of cadaverine and putrescine, may disrupt this mechanism.⁵

BA concentration is higher in fast-perishable foods, especially if fermented and rich in amino acids, such as fish, meat, fruit juices, wine, beer, cocoa, milk and cheese.² In particular, BA may be present in wines and beer at highly variable concentrations. The increase in biogenic amines content

¹ (a) Silla Santos M. H. *Int. J. Food Microb.* **1996**, *29*, 213-231; (b) Halász A., Baráth A., Simon-Sarkadib L., Holzapfel W. *Trends in Food Science & Technol.* **1994**, *5*, 42-49.

² Shalaby A. R. *Food Res. Int.* **1996**, *29*, 675-690.

³ Biegański T., Kusche J., Lorenz W., Hesterberg R., Stahlknecht C.-D., Feussner K.-D. *Bioch. Bioph. Acta* **1983**, *756*, 196-203.

⁴ Hasan F., McCrodden J. M., Kennedy N. P., Tipton K. F. *J. Neur. Trans. Suppl.* **1988**, *26*, 1-9.

⁵ (a) Horwitz D., Lovenberg W., Engelman K., Sjoerdsma A. *J. Am. Med. As.* **1964**, *188*, 1108-1110; (b) Hui J. Y., Taylor S. L. *Toxicol. Appl. Pharmacol.* **1985**, *81*, 241-249; (c) Johnston J. P. *Bioch. Pharmacol.* **1968**, *17*, 1285-1297.

in wines occurs after malolactic fermentation and it is dependent on the bacterial strain used. The content is higher in case of spontaneous malolactic fermentation,⁶ but there are other conditions that increase the content of biogenic amines and therefore must be kept under control. Among these, there are poor hygiene during the fermentation period,⁷ long contact between wine and lees,⁸ high temperature⁹ and high pH.¹⁰ In the beer, putrescine, spermine and spermidine are naturally present because malt is a source of these substances, while tyramine, histamine and cadaverine are formed during fermentation due to the contamination of lactic bacteria.⁷

There are a great number of analytical methods used for the determination of BA for food and beverages samples¹¹ and they are mainly based on gas chromatography (GC),¹² high-performance liquid chromatography (HPLC)¹³ with pre-column¹⁴ or post-column¹⁵ derivatisation, ion-pair chromatography¹⁶ and capillary electrophoresis (CE).¹⁷ For the detection, fluorescence,¹⁸ UV,¹⁹

⁶ (a) Hernández-Orte P., Peña-Gallego A., Ibarz M. J., Cacho J., Ferreira V. *J. Chrom. A* **2006**, *1129*, 160-164; (b) Pramateftaki P. V., Metafa M., Kallithraka S., Lanaridis P. *Let. Appl. Microb.* **2006**, *43*, 155-160; (c) Manfroi L., Silva P. H. A., Rizzon L. A., Sabaini P. S., Glória M. B. A. *Food Chem.* **2009**, *116*, 208-213; (d) Izquierdo-Pulido M., Font-Fábregas J., Vidal-Carou C. *Food Chem.* **1995**, *54*, 51-54; (e) Izquierdo Cañas P. M., Romero E. G., Alonso S. G., González M. F., Palop Herreros M. L. *J. Food Comp. Anal.* **2008**, *21*, 731-735.

⁷ Kalač P., Šavel J., Křížek M., Pelikánová T., Prokopová M. *Food Chem.* **2002**, *79*, 431-434.

⁸ González-Marco A., Ancín-Azpilicueta C. *J. Food Science* **2006**, *71*, C544-C548.

⁹ González Marco A., Ancín Azpilicueta C. *Food Chem.* **2006**, *99*, 680-685.

¹⁰ Lonvaud-Funel A., Joyeux A. *J. Appl. Microb.* **1994**, *77*, 401-407.

¹¹ Önal A. *Food Chem.* **2007**, *103*, 1475-1486.

¹² (a) Karoum F., Cattabeni F., Costa E., Ruthven C. R. *J. Anal. Biochem.* **1972**, *47*, 550-561; (b) Davis B. A., Durden D. A., Boulton A. A. *J. Chrom. B: Biomed. Sciences Appl.* **1986**, *374*, 227-238.

¹³ (a) Landete J. M., Ferrer S., Polo L., Pardo I. *J. Agric. Food Chem.* **2005**, *53*, 1119-1124; (b) Romero R., Sánchez-Viñas M., Gázquez D., Bagur M. G. *J. Agric. Food Chem.* **2002**, *50*, 4713-4717; (c) Kalač P., Hlavatá V., Křížek M. *Food Chem.* **1997**, *58*, 209-214; (d) Torrea D., Ancín C. *J. Agric. Food Chem.* **2002**, *50*, 4895-4899; (e) Loukou Z., Zotou A. *J. Chrom. A* **2003**, *996*, 103-113; (f) Bauza T., Blaise A., Daumas F., Cabanis J. C. *J. Chrom. A* **1995**, *707*, 373-379; (g) Buiatti S., Boschelle O., Mozzon M., Battistutta F. *Food Chem.* **1995**, *52*, 199-202.

¹⁴ (a) García-Villar N., Hernández-Cassou S., Saurina J. *J. Chrom. A* **2009**, *1216*, 6387-6393; (b) García-Villar N., Saurina J., Hernández-Cassou S. *Anal. Chim. Acta* **2006**, *575*, 97-105.

¹⁵ Vidal-Carou M. C., Lahoz-Portolés F., Bover-Cid S., Mariné-Font A. *J. Chrom. A* **2003**, *998*, 235-241.

¹⁶ (a) Hlabangana L., Hernández-Cassou S., Saurina J. *J. Chrom. A* **2006**, *1130*, 130-136; (b) De Borba B. M., Rohrer J. S. *J. Chrom. A* **2007**, *1155*, 22-30.

¹⁷ (a) Jayarajah C. N., Skelley A. M., Fortner A. D., Mathies R. A. *Anal. Chem.* **2007**, *79*, 8162-8169; (b) García-Villar N., Saurina J., Hernández-Cassou S. *Electrophoresis* **2006**, *27*, 474-483; (c) Male K. B., Luong J. H. T. *J. Chrom. A* **2001**, *926*, 309-317; (d) Kovács A., Simon-Sarkadi L., Ganzler K. *J. Chrom. A* **1999**, *836*, 305-313.

¹⁸ (a) Li J.-S., Wang H., Huang K.-J., Zhang H.-S. *Anal. Chim. Acta* **2006**, *575*, 255-261; (b) Cortacero-Ramírez S., Arráez-Román D., Segura-Carretero A., Fernández-Gutiérrez A. *Food Chem.* **2007**, *100*, 383-389; (c) Zhang N., Wang H., Zhang Z.-X., Deng Y.-H., Zhang H.-S. *Talanta* **2008**, *76*, 791-797.

¹⁹ (a) Soufleros E. H., Bouloumpasi E., Zotou A., Loukou Z. *Food Chem.* **2007**, *101*, 704-716; (b) Arce L., Ríos L., Valcárcel M. *J. Chrom. A* **1998**, *803*, 249-260; (c) Mazzucco E., Gosetti F., Bobba M., Marengo E., Robotti E., Gennaro M. C. *J. Agric. Food Chem.* **2010**, *58*, 127-134.

mass-spectrometric²⁰ and electrochemical detectors^{16b} are used. In any of these cases the analysis of BA is not simple being often necessary either a derivatisation step or an extraction procedure or some other sample pretreatment.

Electrochemical biosensors for the determination of BA have attracted much attention in the last years for their simplicity, reproducibility, low cost, short analysis time and low detection limit; moreover they could provide an up front method for BA determination, useful for field analysis in food and beverage industries. They are essentially based on Amine Oxidase,²¹ Diamine Oxidase²² or Monoamine Oxidase²³ and were used to determine BA in food samples.

In this work it has been used Amine Oxidase from *Lathyrus sativus* (LSAO). Amine Oxidases are a class of enzymes that catalyse the oxidation of primary amines in aldehydes, in the presence of molecular oxygen as electrons acceptor, with the formation of ammonia (NH₃) and hydrogen peroxide (H₂O₂). The enzymatic reaction can be followed with amperometric detection by means of electrochemical oxidation of H₂O₂ onto a Au electrode at +600 mV vs the internal silver pseudoreference electrode of a screen printed sensor.

In this work, firstly LSAO was electrokinetically characterised both free in solution and once immobilised with PAP membrane, which was already used for this purpose in other works.²⁴ Then, LSAO was used to develop an electrochemical biosensor whose analytical performances were evaluated; finally it was applied to the determination of the total amount of BA in wine and beer samples. This samples are complex matrices with a lot of potentially interfering compounds. For

²⁰ (a) Santos B., Simonet B. M., Ríos A., Valcárcel M. *Electrophoresis* **2004**, *25*, 3427-3433; (b) Simó C., Moreno-Arribas M. V., Cifuentes A. *J. Chrom. A* **2008**, *1195*, 150-156.

²¹ (a) Niculescu M., Frébort I., Peč P., Galuszka P., Mattiasson B., Csöregi E. *Electroanalysis* **2000**, *12*, 369-375; (b) Wimmerová M., Macholán L. *Biosens. Bioelectron.* **1999**, *14*, 695-702.

²² (a) Bouvrette P., Male K. B., Luong J. H. T., Gibbs B. F. *Enz. Microb. Tech.* **1997**, *20*, 32-38; (b) Male K. B., Bouvrette P., Luong J. H. T., Gibbs B. F. *J. Food Science* **1996**, *61*, 1012-1016; (c) Ching M. K., Abu Bakar F., Abu Bakar S., Lee Y. H., Rahman W., Low S. B. *Food Chem.* **2007**, *105*, 1636-1641; (d) Carelli D., Centonze D., Palermo C., Quinto M., Rotunno T. *Biosens. Bioelectron.* **2007**, *23*, 640-647; (e) Draisci R., Volpe G., Lucentini L., Cecilia A., Federico R., Palleschi G. *Food Chem.* **1998**, *62*, 225-232; (f) Tombelli S., Mascini M. *Anal. Chim. Acta* **1998**, *358*, 277-284; (g) Compagnone D., Isoldi G., Moscone D., Palleschi G. *Anal. Lett.* **2001**, *34*, 841-854.

²³ Alonso-Lomillo M. A., Domínguez-Renedo O., Matos P., Arcos-Martínez M. J. *Anal. Chim. Acta* **2010**, *665*, 26-31.

²⁴ (a) Frasconi M., Favero G., Di Fusco M., Mazzei F. *Biosens. Bioelectron.* **2009**, *24*, 1424-1430; (b) Mazzei F., Botrè F., Montilla S., Pilloton R., Podestà E., Botrè C. *J. Electroanal. Chem.* **2004**, *574*, 95-100; (c) Di Fusco M., Tortolini C., Deriu D., Mazzei F. *Talanta* **2010**, *81*, 235-240; (d) Tortolini C., Di Fusco M., Frasconi M., Favero G., Mazzei F. *Microchem. J.* doi:10.1016/j.microc.2010.05.004.

this reason we have developed an amperometric biosensor which employs a double working electrode connected to a bipotentiostat able to measure two working channels simultaneously. This allows to subtract the sample signal (BA + interference) to the blank one (interference) making possible to determine the total amount of BA in the sample under analysis.

6.2 Experimental Section

6.2.1 Materials

Amine Oxidase from *Lathyrus sativus* (EC 1.4.3.22, activity: 131 U ml⁻¹, concentration: 2 mg ml⁻¹, M_r = 148 kDa). Bovine Serum Albumin (BSA, EC 232-936-2) and 1,4-diaminobutane (putrescine) were purchased from Sigma and used as received. The polymeric film employed for protein entrapping was poly-1-(aminomethyl)-1-{2-[(6-oxysesane)amino]ethyl}-3-hydroxyazetidinium chloride (polyazetidine prepolymer, PAP®), donated by Hercules Inc. Wilmington DE (USA). Other chemicals were all of analytical grade. High purity deionised water (Resistance: 18.2 MΩ × cm at 25 °C; TOC < 10 µg/L) obtained from Millipore (France) has been used to prepare all the solutions.

Different commercial wine and beer samples were acquired from local market. In the samples the appropriate amount of phosphate salts was added to finally have a concentration of 0.1 mol L⁻¹ phosphate and then the pH value was adjusted to 7.4 using NaOH.

6.2.2 Apparatus

Electrochemical experiments were performed by using a µStat 400 bipotentiostat (DropSens, Oviedo, Spain) controlled by means of the DropView 2.0 Software (DropSens). Dual channel Screen Printed Electrodes (DualAu-SPE) (DropSens), constituted by two gold working electrode, gold as counter electrode and silver as pseudoreference one, were used. Flow experiments were carried out using a microliter cell (DropSens Oviedo, Spain), an Omnifit sample injection valve (DropSens Oviedo, Spain) and a Gilson Minipuls-3 peristaltic pump.

GC-MS analyses were performed with an Agilent 6850A gas chromatograph coupled to a 5973N quadrupole mass selective detector (Agilent Technologies, Palo Alto, CA, USA).

Chromatographic separations were carried out with an Agilent HP5ms fused-silica capillary column (30 m × 0.25 mm i.d.) coated with 5%- phenyl-95%-dimethylpolysiloxane (film thickness 0.25 µm) as stationary phase. Injection mode: splitless at a temperature of 260 °C. Column temperature

program: 70 °C (2 min) then to 300 °C at a rate of 15 °C/min and held for 5 min. The carrier gas was helium at a constant flow of 1.0 ml/min. The spectra were obtained in the electron impact mode at 70 eV ionisation energy; ion source 280 °C; ion source vacuum 10^{-5} Torr.

MS analysis was performed simultaneously in TIC (mass range scan from m/z 50 to 800 at a rate of 0.42 scans s⁻¹) and SIM mode. For GC-SIM-MS analysis three characteristic ions were selected for each of the amines analysed.

6.2.3 Biosensor Preparation

LSAO-based Dual Au-SPE biosensors were prepared by spreading 3 µl of a solution, containing 2 µl of enzyme 131 U ml⁻¹ and 1 µl of PAP, onto one gold working electrode surface and a solution, containing 2 µl of BSA and 1 µl of PAP, onto the other gold working electrode surface. The electrodes were left to dry overnight at room temperature and when not in use were stored at 4°C.

6.2.4 Biogenic Amines Content by GC-MS

Amines were analysed according to the method of Paik et al.²⁵ with slight modification. Briefly, 0.5 ml aliquots of wine, spiked with internal standard (IS) 1,6-diaminohexane (300 ng), were added with 0.5 ml 5 mol L⁻¹ NaOH and immediately subjected to sequential *N*-ethoxycarbonylation and *N*-pentafluoropropionylation. *N*-ethoxycarbonylation was performed in one step by adding to the aqueous phase ethyl chloroformate (20 µl), dissolved in dichloromethane (1 ml). After vortex mixing (2 min) the mixture was saturated with NaCl and extracted with diethyl ether (3 ml) and ethyl acetate (2 ml). The organic extracts were combined and dried under reduced pressure. Then, the sample was subjected to the second derivatisation step by adding 20 µl pentafluoropropionyl anhydride (65°C for 60 min).

A stock solution of the seven amines was prepared at concentration of 10 mg ml⁻¹, each in 0,1 mol L⁻¹ HCl. This solution was used to prepare working solutions ranging from 10 ng ml⁻¹ to 100 ng

²⁵ Paik M. J., Lee S., Cho K. H., Kim K. R. *Anal. Chim. Acta* **2006**, 576, 55-60.

ml⁻¹ in HCl 0,1 mol L⁻¹. The internal standard working solution was prepared by dissolving stock solution of 1,6-diaminohexane at 15 ng μl in 0.1 mol L⁻¹ HCl. The calibration samples were prepared at eight different concentrations in the range 25 -20000 ng ml⁻¹.

6.2.5 Electrochemical Measurements

Chronoamperometric experiments were carried out at a fixed potential +600 mV vs the internal silver pseudoreference, whose potential was checked in the chosen experimental conditions using ferrocyanide 1 mM as electrochemical probe and it was determined to be +123 vs Ag/AgCl/Cl⁻. Flow injection experiments were carried out using a flow rate of 4 μl s⁻¹, and 0.1 mol L⁻¹ phosphate solution, pH 7.4, as carrier buffer. Aliquots of 250 μl of putrescine standard solutions at different concentrations in the same buffer were used to obtain the calibration plot. The analysis of wine and beer samples were performed injecting appropriately diluted samples, whose resulting signals were referred to that of putrescine.

6.3 Results and Discussion

The LSAO-biosensor was analytically characterised, using putrescine as standard, either in batch and under flow injection conditions. In order to reduce the influence of matrix effect which could affect the detection of biogenic amines in real samples, a special SPE employing two working electrodes was used as transducer. This dual-working electrodes SPE coupled to the proper multimeter and driven by the DropView™ Software, allows the simultaneous registration of both sample and blank signals and eventually to subtract the latter on the fly. Unfortunately, only a few limited types of dual-SPEs are available so far and among them a dual platinum SPE is still missing. Hence, a dual gold electrode, in place of platinum, was chosen although in the detection of hydrogen peroxide, gold entails a little loss in the sensitivity²⁶ but it is still useful for our purposes. Anyway, using the dual-Au-SPE the following analytical parameters were obtained using putrescine as substrate: sensitivity $7.9 \pm 0.5 \text{ nA mg}^{-1} \text{ L}$ and $11.2 \pm 0.4 \text{ nA mg}^{-1} \text{ L}$, linear range $2.0\text{-}80.5 \text{ mg L}^{-1}$ and $0.7\text{-}20.0 \text{ mg L}^{-1}$, LOD 0.6 mg L^{-1} and 0.2 mg L^{-1} , for the batch and FI systems respectively. The corresponding chronoamperograms obtained and the calibration plots thereof are reported in Figure 6.1.

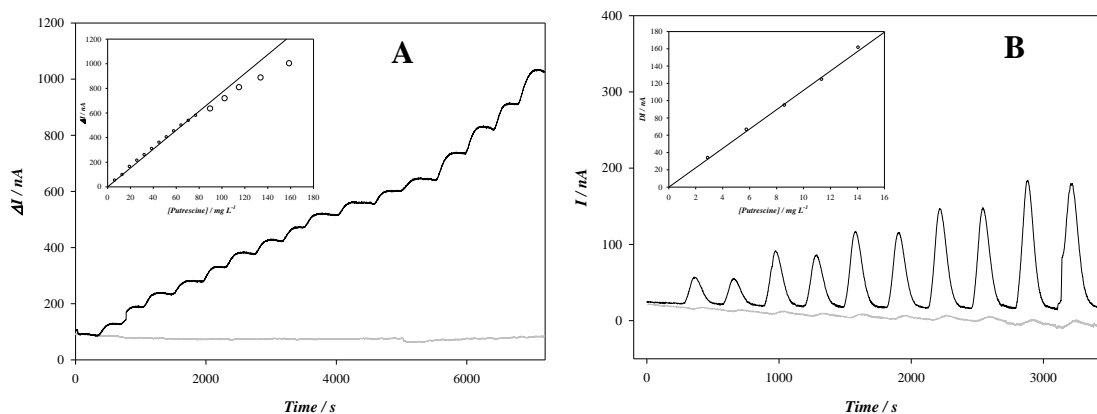


Figure 6.1 Amperometric responses, using DualAu-SPE (black line is LSAO-PAP and gray one is BSA-PAP), for different additions of putrescine in batch (A) and five double additions of putrescine in FI (B). Insets: calibration plots.

²⁶ Carelli D., Centonze D., De Giglio A., Quinto M., Zamboni P. G. *Analytica Chimica Acta* **2006**, 565, 27-35.

The biosensors have been used for 10 consecutive calibration plots without a significant loss of performances for the first 5 plots (Figure 6.2).

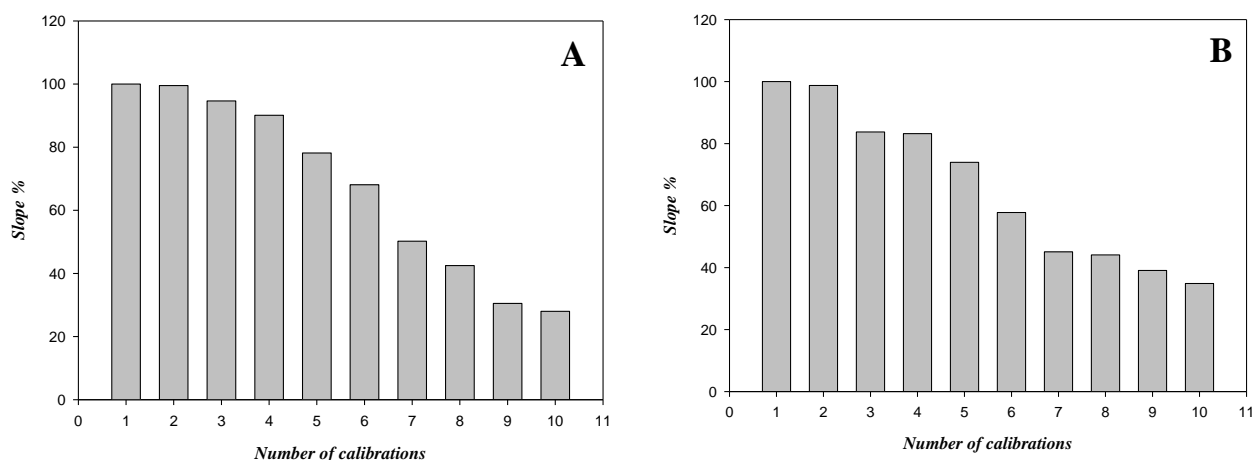


Figure 6.2 Sensitivity loss using DualAu-SPE biosensor in batch (A) and in FI (B) conditions.

In order to reduce any kind of interference, the analysis of real samples was carried out by a differential method employing the dual SPE-based biosensor above described. The measurements were carried out on two white wines, two red wines, two blonde beers and the registered amperometric signals were referred to that one of putrescine thus obtaining the total amount of BA expressed as concentration of putrescine.

In Table 6.1 the results obtained with the different methods in the detection of BA in real samples of wine and beer both using batch and FI systems, are reported and compared to the results obtained by GC-MS as reference method. Also in the case of GC-MS data, the total amount of BA was expressed as putrescine even if this technique provides the concentration of each different amine eventually present in the sample (Table 6.2); in particular, for each real sample the obtained amounts of phenylethylamine, tyramine, cadaverine, histamine, spermidine and spermine were expressed in molar concentration, summed and multiplied by putrescine molecular weight thus obtaining the total amount of BA as putrescine in mg L^{-1} .

Table 6.1 Total amount of BA in wine and beer obtained in flow injection conditions.

Sample	[Total BA as putrescine] (mg L ⁻¹)	
	FIA	GC-MS
White wine 1	15.0 ± 0.8	12.6
White wine 2	6.6 ± 0.7	6.0
Red wine 1	26.5 ± 6.5	21.8
Red wine 2	43.0 ± 5.4	44.9
Blonde beer 1	7.8 ± 2.2	15.1
Blonde beer 2	3.8 ± 0.1	8.1

By comparing the data obtained with the proposed biosensor in flow conditions to those obtained with the reference method, it can be observed that in the case of both white and red wines the data are in a good agreement, conversely in the case of blonde beers data obtained using FI are half as much with respect to GC-MS ones. It must be remembered that the biosensor data are obtained as pool of all the biogenic amines present in the real sample even if they are expressed as total amount of putrescine, hence they are affected by a systematic error due to the different sensitivities of the enzyme chosen to assemble the biosensor towards the different amines (e.g. see Table 6.2); this could explain the poor accuracy of biosensor method for blonde beers. Nevertheless it should be borne in mind that biosensors are often accounted as up front methods whose results have a significance as “alarm signals” useful to locate those real samples that should be analysed by a reference method. In this respect, since the maximum content of BA allowed in most European countries is 15 mg L⁻¹, our proposed biosensor is in every case able to discriminate if a wine is safe or not according to the current law.

Table 6.2 Total amount of BA in wine and beer obtained with GC-MS.

Sample	phenylethylamine (ng ml ⁻¹)	tyramine (ng ml ⁻¹)	putrescine (ng ml ⁻¹)	cadaverine (ng ml ⁻¹)	histamine (ng ml ⁻¹)	spermidine (ng ml ⁻¹)	spermine (ng ml ⁻¹)
White wine 1	655,44	901,67	3430,08	80,42	182,00	67,93	-
White wine 2	80,82	624,53	1382,55	40,95	612,00	60,37	38,69
Red wine 1	135,64	2074,53	5872,06	213,75	1962,00	119,15	41,69
Red wine 2	448,34	6545,96	11022,06	457,61	1862,00	153,29	41,15
Blonde beer 1	61,53	1598,81	3546,13	441,82	412,00	877,68	401,15
Blonde beer 2	33,11	565,96	2694,28	178,67	-	287,44	193,46

6.4 Conclusions

In this research a biosensor based on Amine Oxidase from *Lathyrus sativus* (LSAO) was analytically characterised, using putrescine as substrate either in batch and in flow conditions, and employed for the analysis in flow conditions of the amine content in real samples of alcoholic beverages. In order to reduce interferences, a double Au electrode was used as electrochemical transducer thus allowing to analyse wines and beers without any chemical pretreatment apart from a proper dilution. The proposed LSAO biosensor proven to be very promising in estimating the total amount of amines considering the good agreement to data obtained with a classical GC-MS method used for comparison. In particular, the LSAO biosensor described herein could be a cheap and fast alternative to classical chromatographic methods for assessing the quality of wines considering its ability to estimate reliably the maximum content of BA allowed in most European countries (15 mg L⁻¹).

Chapter 7

Soft Landed Modified Electrodes

7.1 Introduction

The ion soft landing is an interesting technique that provides the deposition, at low kinetic energies, of specific molecular ions on solid surfaces, using a modified mass spectrometer. In fact, with the use of a quadrupole, it is possible to select an ion and make it collide with a solid surface or assembled molecules (SAM).¹

Nowadays, there is an increasing interest for low energy collisions (kinetic energies between 1 and 100 eV) because they can be used to attach organic or biological molecules, such as fragments of DNA² and proteins,³ to surfaces. In this contest, it has been demonstrated that a protein, at first attached to a surface with the use of soft landing and then removed by the surface itself, do not lose its catalytic properties.⁴ Moreover, inelastic collisions can cause the excitation of the projectile ion, leading to its the fragmentation, this can occur for instance at the target surface, generating a process known as surface induced dissociation. This allows to obtain structural information about the ion and to characterise the surface from a physical-chemical point of view.⁵ Therefore, such reactions can be used both for chemical modification and analysis of a surface.

¹ (a) Kleyn A. W. *Science* **1997**, 275, 1440-1441; (b) Miller S. A., Luo H., Pachuta S. J., Cooks R. G. *Science* **1997**, 275, 1447-1450; (c) Gologan B., Green J. R., Alvarez J., Laskin J., Cooks R. G. *Phys. Chem. Chem. Phys.* **2005**, 7, 1490-1500.

² Feng B., Wunschel D. S., Masselon C. D., Pasa-Tolic L., Smith R. D. *J. Am. Chem. Soc.* **1999**, 121, 8961-8962.

³ (a) Blake T. A., Ouyang Z., Wiseman J. M., Takáts Z., Guymon A. J., Kothari S., Cooks R. G. *Anal. Chem.* **2004**, 76, 6293-6305; (b) Volny M., Elam W. T., Ratner B. D., F. Turecek *Anal. Chem.* **2005**, 77, 4378-4384.

⁴ (a) Gologan B., Takáts Z., Alvarez J., Wiseman J. M., Talaty N., Ouyang Z., Cooks R. G. *J. Am. Mass. Spectrom.* **2004**, 15, 1874-1880; (b) Laskin J., Bailey T. H., Futrell J. H. *J. Am. Chem. Soc.* **2003**, 125, 1625-1631.

⁵ Gologan B., Green J. R., Alvarez J., Laskin J., Cooks R. G. *Phys. Chem. Chem. Phys.* **2005**, 7, 1490-1500.

With the soft landing technique, working at low translational energies, the projectile ion is deposited intact on the surface in its neutral or charged form and the linkage between the surface and the ion can be either electrostatic or covalent.^{1b,6}

The coupling of the soft landing technique with voltammetry has given rise to a new technique, called soft landed protein voltammetry (SLPV) (Figure 7.1), which allows to functionalise an electrodic surface with biologically active molecules, opening in this way new perspectives in the development of biosensors.⁷

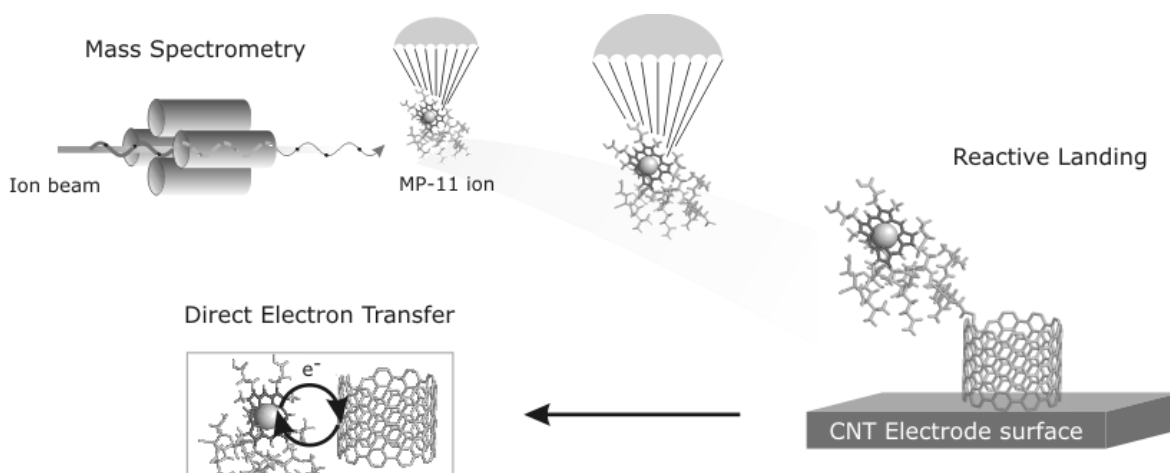


Figure 7.1 Schematic illustration of SLPV: the molecular ion of a protein is selected by a quadrupole, is sent at low kinetic energy to an electrodic surface and finally is detected by means of voltammetric analysis.

SLPV can be used to assess the yield of protein deposition on a surface and the retention of both its native structure and biocatalytic properties, without removing it from the surface. Moreover, informations on the nature of the linkage between the surface and the deposited material, can also be obtained. The study of this new technique has been conducted recently in my laboratory with a little heme protein, the microperoxidase-11 (MP-11), showing interesting properties (Figure 5.2).⁷

⁶ Grill V., Shen J., Evans C., Cooks R. G. *Rev. Sci. Instrum.* **2001**, *72*, 3149-3172.

⁷ Pepi F., Ricci A., Tata A., Favero G., Frasconi M., Delle Noci S., Mazzei F. *Chem. Commun.* **2007**, *33*, 3494-3496.

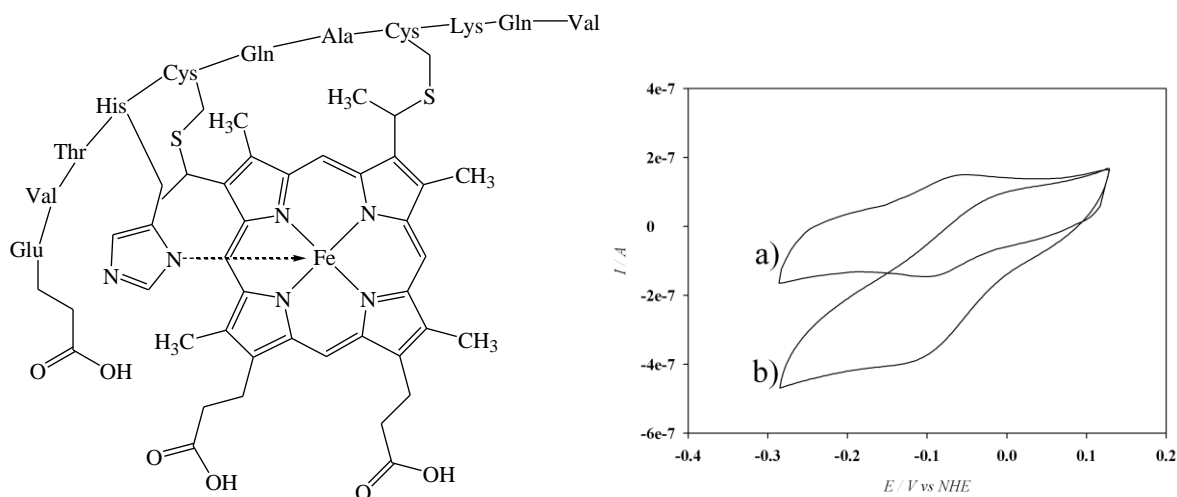


Figure 5.2 Chemical structure of MP-11 (on the left) and CVs (on the right), recorded with a MP-11 soft landing modified electrode, in absence (a) and in presence (b) of H_2O_2 .

The soft landing technique allows to functionalise surfaces with biologically active molecules and this is a very important prerogative in the field of molecular nanotechnology. In addition, mass spectrometry can easily separate specific molecules from complex samples leading to a simplification in the procedures for sample preparation and, especially, for the purification of the protein to be immobilised. This is one of the most important aspects of this technique because the purification of proteins is a very time consuming process and requires resources that can be avoided with the use of this technique, leading to results even better than those current in the immobilisation of proteins on electrode surfaces. This method provides a unique selectivity and specificity in modified surfaces preparation by removing the solvent effects, possible contaminants in the sample and a reduction in the cost of the process.

The soft landing represents an alternative technique to current approaches regarding the modification of surfaces and it has been shown that the presence of particular functional groups, both on the solid supports and projectile ions, allows the efficient formation of a

covalent bond between them.⁸ For example, it has been highlighted the formation of an amide bond depositing a lysine-containing peptide both on a self-assembled monolayer with terminal *N*-hydroxysuccinimidyl ester functions (NHS-SAM)⁹ and on MWCNTs electrodes functionalised with carboxylic groups (MWCNTs-COOH).¹⁰

In this section, the soft landing of simple redox molecules containing terminal amino groups, such as aminoferrocene and various ω -ferrocenyl-1-aminoalkanes (Figure 7.3), on functionalised electrodes of multi-walled carbon nanotubes (MWCNTs-COOH) has been considered. This kind of application led to the born of a new type of modified electrodes by soft landing technique, developed in my research laboratory, named Soft Landed Modified Electrodes (SLaME).

The aminoferrocene is commercially available, while the ω -ferrocenyl-1-aminoalkanes ($\omega = 3, 6, 11, 16$) were synthesised according to literature procedures.

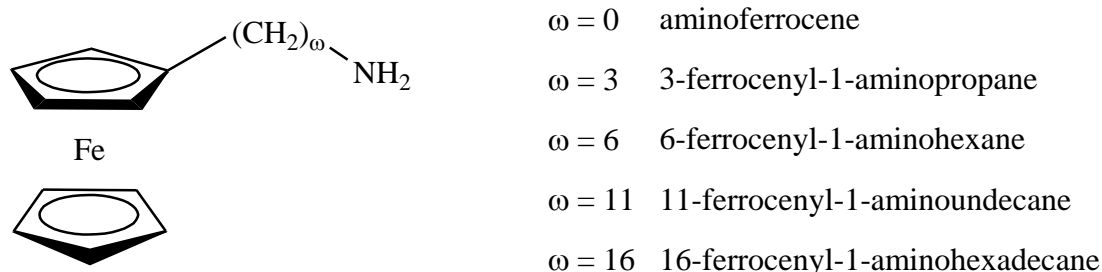


Figure 7.3 Chemical structures of the ferrocene derivatives used in this work.

The protonated aminoferrocene $[\text{NH}_2\text{-Fc}]^+\text{H}^+$, and ω -ferrocenyl-1-aminoalkanes $[\text{NH}_2\text{-(CH}_2\text{)}_\omega\text{-Fc}]^+\text{H}^+$, were generated by ionising the parent compounds with an

⁸ (a) Pradeep T., Feng B., Ast T., Patrick J. S., Cooks R. G., Pachuta S. J. *J. Am. Soc. Mass. Spectrom.* **1995**, *6*, 187-194; (b) Shen J. W., Grill V., Evans C., Cooks R. G. *J. Mass. Spectrom.* **1999**, *34*, 354-363; (c) Wade N., Pradeep T., Shen J. W., Cooks R. G. *Rapid Commun. Mass. Spectrom.* **1999**, *13*, 986-993; (d) Wade N., Gologan B., Vincze A., Cooks R. G., Sullivan D. M., Muening M. L. *Langmuir* **2002**, *18*, 4799-4808; (e) Evans C., Wade N., Pepi F., Strossman G., Schuerlein T., Cooks R. G. *Anal. Chem.* **2002**, *74*, 317-323; (f) Volny M., Elam W. T., Branca A., Ratner B. D., Turecek F. *Anal. Chem.* **2005**, *77*, 4890-4896.

⁹ (a) Wang P., Hadjar O., Laskin J. *J. Am. Chem. Soc.* **2007**, *129*, 8682-8683; (b) Wang P., Hadjar O., Gassman P. L., Laskin J. *X Phys. Chem. Chem. Phys.* **2007**, *10*, 1512-1522; (c) Wang P., Laskin J. *Angew. Chem. Int. Ed.* **2008**, *47*, 6678-6680.

¹⁰ Mazzei F., Favero G., Frasconi M., Tata A., Pepi F. *Chem. Eur. J.* **2009**, *15*, 7359-7367.

electrospray source (ESI) or chemical ionisation (CI) of a modified triple quadrupole mass spectrometer.⁷ These compounds have been used as a model to try to explain for the first time the mechanism of reactive landing.

7.2 Experimental Section

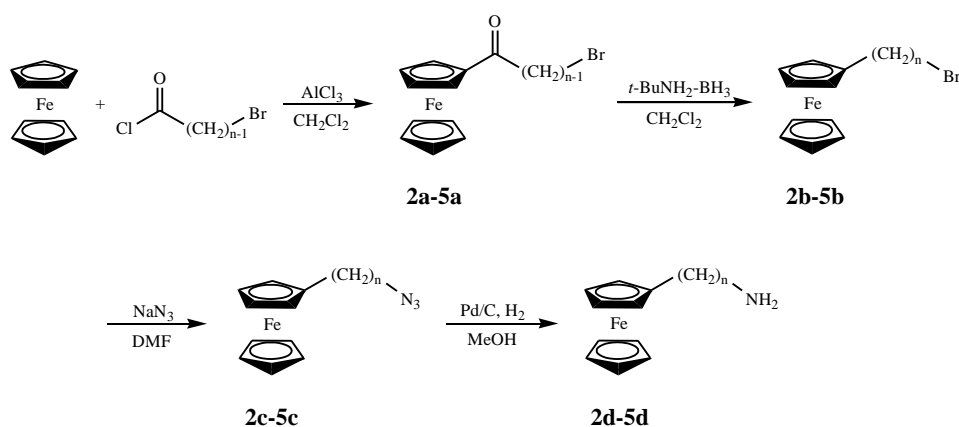
7.2.1 Materials

Aminoferrocene was purchased from TCI Europe nv (Belgium) and used as received. Laccase from *Trametes versicolor* was supplied by Fluka (EC 1.10.3.2, activity: 30.6 U mg⁻¹). Ferrocene derivatives 3-ferrocenyl-1-aminopropane, 6-ferrocenyl-1-aminohexane, 11-ferrocenyl-1-aminoundecane and 16-ferrocenyl-1-aminohexadecane were synthesised as reported below.

Other chemicals were all of analytical grade. High purity deionised water (Resistance: 18.2 MΩ × cm at 25 °C; TOC < 10 µg L⁻¹) obtained from Millipore (France) has been used to prepare all the solutions.

7.2.2 Synthesis of Ferrocene Derivatives

Ferrocene derivatives **2d-5d** were synthesised according to the following reaction scheme (Scheme 7.1).



Scheme 7.1 Synthesis of the ferrocene derivatives 2d-5d

The first step of the synthesis was a Friedel-Crafts acylation of ferrocene¹¹ with the appropriate acyclic chlorides to obtain the ferrocenyl bromoalkyl ketones **2a-5a** (yield 52-71%). The lower value of the medium yield depend on the fact that the acyclic chloride for the synthesis of **4a** and **5a** are not commercially available and were synthesised from the corresponding acids with the use of oxalyl chloride.¹² Therefore, the yields of **4a** and **5a** include the two steps. The compounds **2a-5a** were reduced at the carbonyl site¹¹ to obtain **2b-5b** (yield 95-96%), then the latter ones were transformed in **2c-5c** by means of a S_N2 reaction with sodium azide (yield 97-99%)¹³ and, finally, were obtained the desired compounds **2d-5d** with a catalytic reduction of the azide groups (95-97%).¹³

Below are reported the NMR and IR characterisations of the compounds **2d-5d**:

2d ¹H NMR (CDCl₃): δ 1.76 (qu, 2H), 2.36 (t, 2H), 2.66 (t, 2H), 4.03 (s, 4H), 4.08 (s, 5H).

¹³C NMR (CDCl₃): δ 30.65, 31.09, 49.43, 67.41, 68.26, 68.72, 88.54.

IR (CHCl₃): 3390-3220 (stretching N-H), 2930 (stretching C-H) cm⁻¹.

3d ¹H NMR (CDCl₃): δ 1.34 (m, 4H), 1.52 (m, 4H), 2.29-2.34 (t, 2H), 2.63 (m, 2H), 4.04 (s, 4H), 4.09 (s, 5H).

¹³C NMR (CDCl₃): δ 27.49, 29.74, 29.76, 29.92, 31.29, 50.06, 67.21, 68.27, 68.66, 89.61.

IR (CHCl₃): 3365-3255 (stretching N-H), 2940, 2760 (stretching C-H) cm⁻¹.

4d ¹H NMR (CDCl₃): δ 1.26 (m, 16H), 1.46-1.51 (m, 2H), 1.76-1.86 (br., 2H), 2.28-2.33 (t, 2H), 2.87-2.92 (m, 2H), 4.02-4.05 (m, 4H), 4.08 (s, 5H).

¹³C NMR (CDCl₃): δ 26.09, 26.82, 27.12, 29.27, 29.33, 29.65-29.88 (overlapping), 31.34, 47.79, 67.18, 68.26, 68.65, 89.76.

¹¹ (a) Méta y E., Duclos M. C., Pellet-Rostaing S., Lemaire M., Schulz J., Kannappan R., Bucher C., Saint-Aman E., Chaix C. *Eur. J. Org. Chem.* **2008**, 25, 4304-4312; (b) Kumar J., Purohit C. S., Verma S. *Chem. Comm.* **2008**, 22, 2526-2528.

¹² Lee H., He Z., Hussey C. L., Mattern D. L. *Chem. Mat.* **1998**, 10, 4148-4153.

¹³ Scriven E. F. V., Turnbull K. *Chem. Rev.* **1988**, 88, 297-368.

IR (CHCl₃): 3350-3210 (stretching N-H), 2985, 2960 (stretching C-H) cm⁻¹.

5d ¹H NMR (CDCl₃): δ 1.25 (m, 26H), 1.49 (m, 2H), 1.75e 1.87 (br, 2H), 2.31 (t, 2H), 2.90 (t, 2H), 4.03-4.04 (d, 4H), 4.09 (s, 5H).

¹³C NMR (CDCl₃): δ 26.17, 27.15, 29.35, 29.72-29.91 (overlapping), 31.34, 68.24, 68.64, 89.81.

IR (CHCl₃): 3320-3200 (stretching N-H), 2990-2755 (stretching C-H) cm⁻¹.

7.2.3 Apparatus

Cyclic voltammetry experiments (CVs) experiments were performed by using a μ-Autolab type III potentiostat (Eco Chemie) controlled by means of the GPES Manager program (Eco Chemie) in a 10 ml thermostated glass cell with a conventional three-electrode configuration. Modified MWCNTs Screen Printed Electrodes (DropSens Oviedo, Spain, diameter 4 mm) were used as working electrodes, a graphite counter electrode and an Ag/AgCl/Cl⁻ (Metrohm, Switzerland, 198 mV vs NHE) as reference electrode. The MWCNTs-SPEs were preliminary treated by depositing on the working electrode 10 μl of 0.5 mol L⁻¹ nitric acid solution in order to obtain the carboxyl functionalisation of their surface.¹⁴

Soft landing experiments were carried out with the use of a modified triple quadrupole mass spectrometer TSQ700 (Thermo Finnigan Ltd., UK). The modification of the mass spectrometer provided the insertion of a probe, on which is fixed the electrode, between the third quadrupole and the detector.

¹H NMR and ¹³C NMR spectra were acquired by means of a VARIAN-XL 300 Mercury (300 MHz), and IR spectra were recorded with a double ray spectrophotometer SHIMADZU IR 470.

¹⁴ Kim S. N., Rusling J. F., Papadimitrakopoulos F. *Adv. Mat.* **2007**, *19*, 3214-3228.

7.2.4 Soft Landing Experiments

The ionisation of the ferrocene derivatives was carried out on 0.1 mol L⁻¹ solutions in H₂O/CH₃OH = 1/1 (v/v) with 1% of CH₃COOH, in the following experimental conditions: needle potential 4.0 kV, flow rate 20 µl min⁻¹, temperature of the capillary 423 K, hexapole potential -0.8 V, capillary exit and skimmer cone potentials 40 and 90 V, respectively.

7.2.5 Electrochemical Measurements

CVs experiments were carried out in phosphate buffer solution 0,01 mol L⁻¹, pH 7.0, with the addition of KCl 0.1 mol L⁻¹ as supporting electrolyte. All the measuring solutions were deoxygenated before every measurement with N₂ and the gas flow was maintained constant during the experiment time.

The electroactive area (*A*) of MWCNTs-SPE was measured before every experiment by CV, using a 1.1 mmol L⁻¹ of K₃[Fe(CN)₆] solution in KCl 0.1 mol L⁻¹ (under this conditions, the diffusion coefficient of Fe(CN)₆³⁻ is 7.6 10⁻⁶ cm² s⁻¹).¹⁵ Plotting the peak current vs the scan rate, *A* was obtained using the equation $i_p = (2.69 \cdot 10^5) n^{3/2} A D^{1/2} v^{1/2} C$. The redox formal potential, *E*^o, was taken as the average between the anodic and cathodic peak potentials, (*E*_{pa} + *E*_{pc})/2, whereas the peak separation, ΔE , was taken as (*E*_{pa} - *E*_{pc}).

The superficial coverage *I*^{*} was calculated integrating the voltammetric peaks to obtain the charge quantity of the process *Q* and then using the relation $I^* = Q/nFA$.

Finally, the electron transfer rate constant were measured using the method of Laviron.¹⁶

¹⁵ Von Stackelberg M. V., Pilgram M. Z. *Elektrochem.* **1953**, 57, 342-350.

¹⁶ Zhang Z., Rusling J. F. *Biophys. Chem.* **1997**, 63, 133-146.

7.3 Results and Discussion

As introduced earlier, in this section has been taken into account the deposition, on functionalised MWCNTs electrodes, of simple redox molecules, such aminoferrocene and ω -ferrocenyl-1-aminoalkanes ($\omega = 3, 6, 11$ and 16). The choice of a particular class of compounds (ferrocene derivatives with amino groups) was dictated by previous experiments that have been clearly shown that compounds containing amino groups bind covalently to carboxyl groups present on solid surfaces in reactive soft landing experiments. Moreover, the ferrocene derivatives are electroactive substances with characteristic voltammetric profiles, useful to monitor the progress of the deposition.

The examined compounds show characteristic dissociations to the mass spectrometer, so the collision activated by dissociation (CAD), at low energy, has been used to characterise at first the structure of the protonated ions $[\text{NH}_2-(\text{CH}_2)_\omega\text{Fc}]^+\text{H}^+$ generated by ESI and CI. The relative intensities of the fragmentation observed is given in Table 7.1.

Table 7.1 Characterisation of the protonated ions by means of CAD spectra.

Parent ion	Fragment ions relative intensities (the neutral loss is indicated)						
	NH ₃	C ₅ H ₆	NH ₂ Cp	C ₅ H ₅ Fe	CH ₃ (CH ₂) _{n-2} NH ₂	(CH ₂) _{n-2} NH ₂	
[H ₂ N-Fc]H ⁺	CH ₄ /Cl	33.5	29.0	30.0	7.5		
	NH ₃ /Cl	33.1	35.0	26.9	5.0		
	ESI	8.1	38.6	46.2	7.1		
[H ₂ N(CH ₂) ₃ Fc]H ⁺	CH ₄ /Cl	6.0	66.1			24.9	3.0
	NH ₃ /Cl	10.0	73.2			13.8	3.0
	ESI	6.4	65.8			23.9	3.9
[H ₂ N(CH ₂) ₆ Fc]H ⁺	CH ₄ /Cl	16.2	38.3			37.4	8.1
	NH ₃ /Cl	14.0	40.7			45.3	-
	ESI	9.5	32.1			47.3	11.1
[H ₂ N(CH ₂) ₁₁ Fc]H ⁺	CH ₄ /Cl	7.8	70.0			14.6	7.6
	NH ₃ /Cl	0.9	82.1			17.0	-
	ESI	5.1	77.5			10.8	6.6
[H ₂ N(CH ₂) ₁₆ Fc]H ⁺	CH ₄ /Cl	4.8	76.2			15.2	3.8
	NH ₃ /Cl	3.2	87.1			6.5	3.2
	ESI	4.4	73.5			15.0	7.1

The gas phase protonation of ferrocene has been widely studied in the past years by different techniques and mass spectrometry has shown that the protonation can occur either on the metal centre or the cyclopentadienyl ring.¹⁷ The ionic form resulting from the protonation on the metal centre is more stable than that resulting from the cyclopentadienyl ring protonation, but the intense exchange of proton between the two rings indicates that the predominant structure of ferrocene in the ionic population is that arising from the global interaction between metal centre, rings and proton. In the case of the ferrocene derivatives, object of this study, the amino group is another site of protonation.

Observing the data reported in Table 7.1, the loss of NH₃ may indicate that the protonation occurs on the amino group, while the fragmentation leading to the loss of the cyclopentadienyl ring could indicate the protonation of the ring itself or metal centre. By

¹⁷ (a) Foster M. S., Beauchamp J. L. *J. Am. Chem. Soc.* **1975**, *97*, 4814-4819; (b) Ikonomou M. G., Sunner J., Kebarle P. *J. Phys. Chem.* **1988**, *92*, 6308-6312; (c) Hop C. E. C. A., McMahon T. B. *J. Am. Soc. Mass. Spectrom.* **1994**, *5*, 274-281; (d) Mayor-Lopez M. J., Luthi H. P., Koch H., Morgantini P. Y., Weber J. *J. Chem. Phys.* **2000**, *113*, 8009-8014; (e) Borisov Y. A., Ustynyuk N. A. *Russ. Chem. Bull. Int. Ed.* **2002**, *51*, 1900-1908.

the first consideration, assuming that the dissociation energy of the bond between carbon and quaternary nitrogen is the same for all the ions $[\text{NH}_2-(\text{CH}_2)_o\text{Fc}]^+\text{H}^+$, is evident that the amino-protonated species is more abundant in the case of 6-ferrocenyl-1-aminohexane, while is less abundant in the case of 11-ferrocenyl-1-aminoundecane and 16-ferrocenyl-1-aminohexadecane. This is unusual because, generally, the proton affinity of the NH_2 group is expected to increase with the lengthening of the alkyl chain. This can be explained assuming a greater probability of interaction between the lone pair of nitrogen and the metal centre of the amino derivatives characterised by a longer alkyl chain. The interaction of the metal centre with the nitrogen lone pair could be highlighted with the largest loss of cyclopentadienyl ring, in CAD spectrum, by 11-ferrocenyl-1-aminoundecane and 16-ferrocenyl-1-aminohexadecane. In fact, the coordination bond between cyclopentadienyl rings and iron could be made more weak by the interaction between nitrogen lone pair and the metal centre, given the presence of a longer and more flexible chain.

In the experiments of soft landing, the entire unresolved isotopic pattern, corresponding to the generated $[\text{NH}_2-(\text{CH}_2)_o\text{Fc}]^+\text{H}^+$ ions, was selected with the first quadrupole and sent for two hours at the screen-printed working electrode, consisting of functionalised multi-walled carbon nanotubes (MWCNTs-COOH). The kinetic energy of the ion beam leaving the third quadrupole, measured by the cut-off potential, can be estimated within 10-12 eV. In order to drive the ions towards the electrode surface, an additional acceleration potential, between 0 and -100 V was applied to the working electrode of the screen-printed sensor. In this context, it was noted that the optimum deposition potential are different and depend on the ionisation method used: -10 V using CH_4/Cl , -20 V using NH_3/Cl , and -50 V in the ESI procedure. No deposition was observed when the acceleration potential was not applied.

The analysis of MWCNTs modified electrodes was carried out by cyclic voltammetry. The voltammogram obtained after the deposition of the ferrocene derivatives ions through soft landing are shown in Figure 7.4.

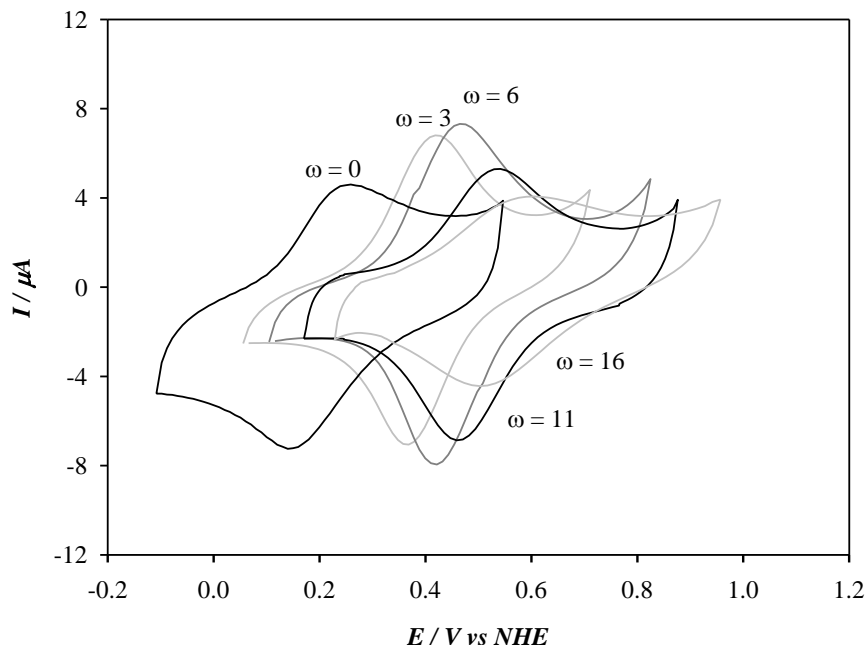


Figure 7.4 Cyclic voltammograms obtained with the different soft landing modified MWCNTs-SPE. Experimental conditions: phosphate buffer 0.01 M at pH = 7, KCl 0.1 M, N₂ atmosphere, 25°C, scan rate of 100 mV s⁻¹.

As it can be seen, the CVs of the ferrocene-modified electrodes show the characteristic shapes of the ferrocene/ferricinium redox couple, that are highly symmetrical and reversible. In fact, the ratio between the anodic peak currents and the cathodic ones are close to unity, as expected by a reversible system.

From the voltammograms recorded after deposition, some parameters, that assess unequivocally the successful immobilisation, can be derived. For example, it was found that scan rate and current intensity are directly proportional, as expected for an immobilised redox species.¹⁸ In fact, for a species free to diffuse in solution, the current intensity is directly proportional to the square root of scan rate. Another evidence of the

¹⁸ Savéant J. M. *Elements of Molecular and Biomolecular Electrochemistry* 2006 (Hoboken: Wiley Interscience).

occurred immobilisation derived from the integration of the current peaks (both anodic and cathodic) of the CVs recorded at different scan rates. The obtained values of charge exchanged with the electrode (Q) remained almost constant and for a non-immobilised system Q must necessarily vary with the variation of scan rate. The coulometric analysis of the voltammograms indicated that the superficial coverages (Γ^*), obtained with the different ferrocene derivatives, vary between $9.9 \pm 0.3 \text{ nmol cm}^{-2}$ and $4.4 \pm 0.3 \text{ nmol cm}^{-2}$. In Table 7.2 are summarised the Γ^* values, such as the formal redox potentials (E^0) and the peak separations (ΔE).

Table 7.2 Electrochemical parameters measured at a scan rate of 100 mV s^{-1} obtained with the ferrocenes-modified MWCNTs-SPEs.

ω	E^0 (mV vs NHE)	ΔE (mV)	Γ^* (nmol cm ⁻²)
0	201 ± 10	71 ± 5	8.2 ± 0.4
3	392 ± 7	31 ± 3	9.5 ± 0.3
6	441 ± 4	38 ± 6	9.9 ± 0.5
11	495 ± 9	59 ± 7	8.1 ± 0.4
16	518 ± 6	96 ± 9	4.5 ± 0.2

It is interesting to observe (Figure 7.5) the dependence of the surface coverage (Γ^*) of the immobilised ferrocene derivatives on the number of methylenic groups in the alkyl chain (ω).

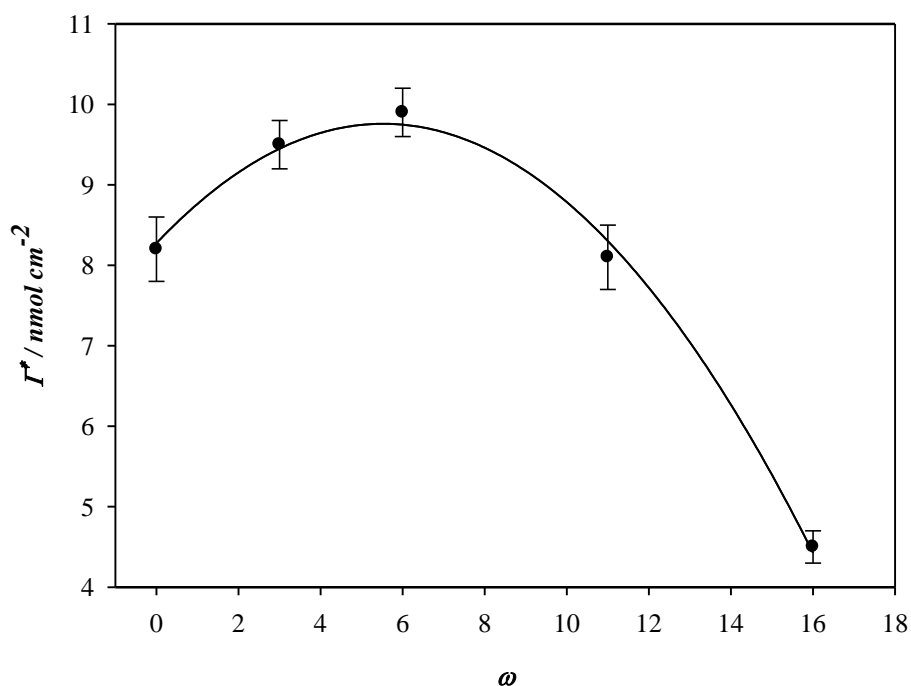


Figure 7.5 Dependence of the surface coverage (Γ^*) of the immobilised ferrocene derivatives on the number of methylenic groups in the alkyl chain (ω).

The maximum coverage of the surface was measured for 6-ferrocenyl-1-aminohexane, while the amount of deposited substance undergoes a marked decrease for 11-ferrocenyl-1-aminoundecane and 16-ferrocenyl-1-aminohexadecane. This behaviour is closely related to the protonation of the amino group highlighted by the CAD spectra, given the reduced availability of nitrogen lone pair of C₁₁ and C₁₆ derivatives. The aminoferrocene, although characterised by a high protonation on the NH₂ group, has a lower reactivity with respect to the C₃ and C₆ derivatives, due probably to the delocalisation of the nitrogen lone pair in the cyclopentadienyl ring.

As it can be observed from Figure 7.4, there is a progressive increase of the formal redox potential (E^0) for the ferrocene derivatives according to the length of the alkyl chain. This is a clear indication that the electron transfer occurs through a simple mechanism. The increase of E^0 is due to the oxidation process that becomes progressively more complicated because of the increased distance of the electroactive centre (iron) from the electrode

surface. Another possible explanation could be that the oxidation process involves a transfer of counter-ions to balance the incipient charge of the ferricinium ion and the approach of these ions to ferrocene derivative becomes increasingly difficult with increasing the hydrophobic alkyl chain length.¹⁹

By voltammetric measurements was also possible to obtain the electronic exchange constants (k_0) for the heterogeneous electron exchange of the ferrocene derivatives with the electrode surface, using the method of Laviron (Table 7.3).

Table 7.3 Kinetic parameters for the heterogeneous electron Exchange between ferrocene derivatives and the electrode.

ω	k_0 (s ⁻¹)	α
0	511 ± 89	0.55
3	492 ± 92	0.53
6	338 ± 54	0.47
11	15 ± 3	0.52
16	0.14 ± 0.08	0.51

Increasing the scan rate in the experiments of cyclic voltammetry, the separation between anodic and cathodic peak increases; this behaviour is predictable on the basis of theory of Marcus. For an unpaired electron transfer, i.e. in the absence of limiting factors such as the exchange of protons, the peak separation (ΔE) varies symmetrically in relation to the standard potential (E^0), resulting in the trend known as trumpet plot (Figure 7.6).²⁰

¹⁹ Liu J., Paddon-Row M. N., Gooding J. J. *J. Phys. Chem. B* **2004**, *108*, 8460-8466.

²⁰ Marcus R. A., Sutin N. *Biochim. Biophys. Acta* **1985**, *811*, 265-322.

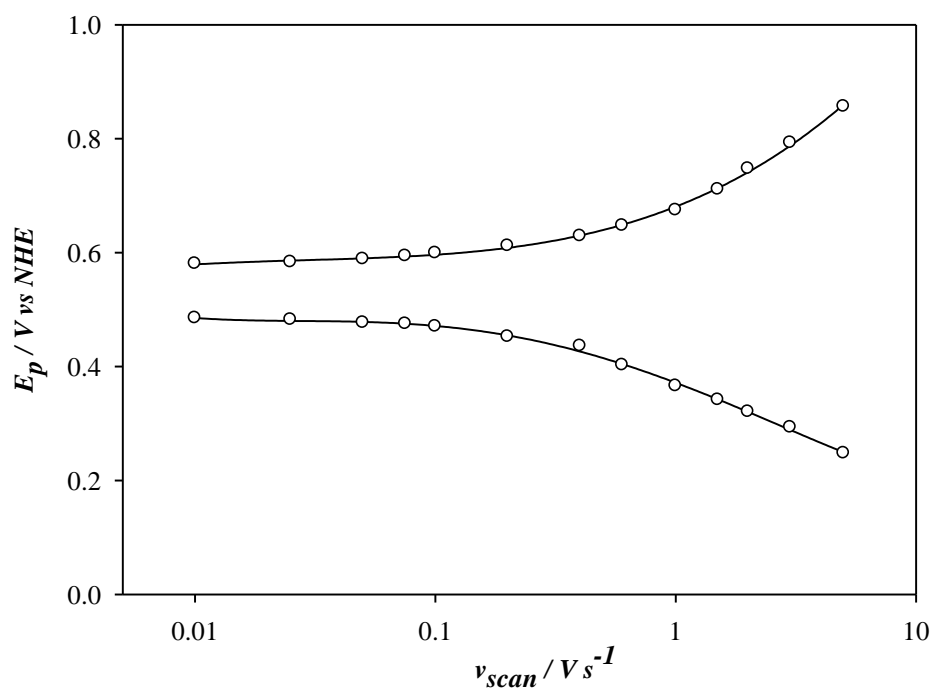


Figure 7.6 Trumpet plot obtained for the ferrocene derivative 16-ferrocenyl-1-aminohexadecane, deposited by means of soft landing on MWCNTs.

In the experimental conditions used (pH and ionic strength), no coupling phenomena were observed (e.g. with protons or hydroxyl ions). Otherwise, in fact, it should be observed a distortion of the graph in different regions. The data reported in Table 3 show that k_0 values decrease with increasing of methylenic groups present in the ferrocene derivatives. This decrease, however, is not linear, as shown in Figure 7.7.

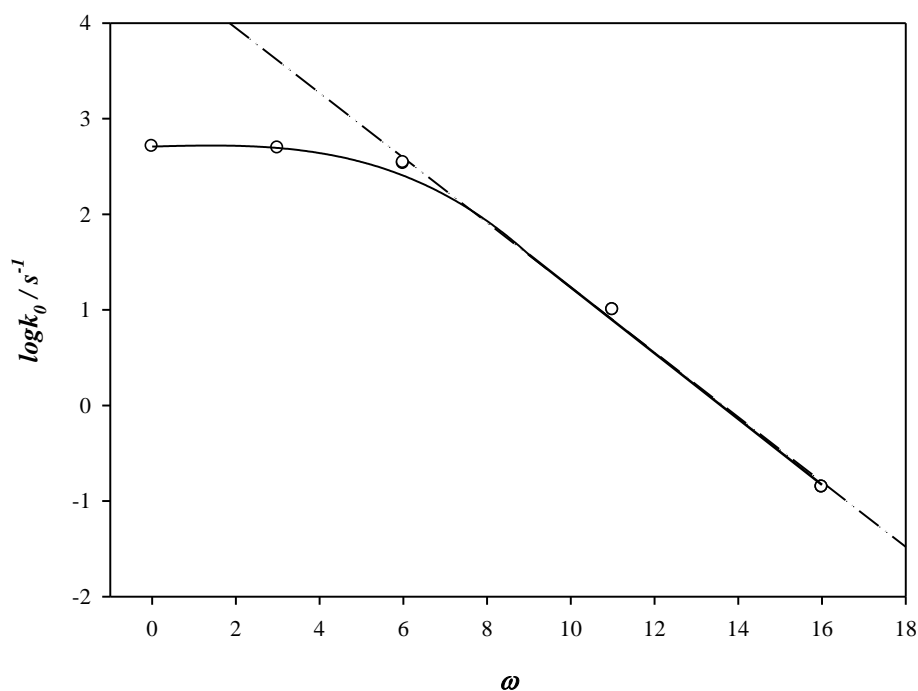


Figure 7.7 Logarithmic plot of k_0 vs ω .

As it can be noticed from Figure 7.7, for the first three compounds ($\omega = 0, 3, 6$) there is a minimum variation of the electronic exchange constant, that in logarithmic terms is negligible, while for the other two ($\omega = 11, 16$) there is a dramatic decrease. On one hand, the derivative 6-ferrocenyl-1-aminohexane is in a situation for which the electron exchange constant varies little with respect to aminoferrocene. On the other hand, the data reported in Table 7.2 show that this compound have the maximum obtained surface coverage. The combination of these two properties makes this compound the best one for the deposition of redox mediators by means of soft landing.

In addition, the ferrocene derivatives were used to determine whether once immobilised they retain their ability to act as redox mediators in an enzymatic reaction. In this regard, electrodes modified by soft landing with the ω -ferrocenyl-1-aminoalkanes were used in the presence and absence of a Laccase type enzyme (*Trametes versicolor*) to see if the presence of the redox mediator provokes a catalytic current. In Figure 7.8 are showed the

CVs of 6-ferrocenyl-1-aminohexane both in absence and in presence of Laccase, such as the dependence of the observed catalytic current from the alkyl chain length of the tested compounds.

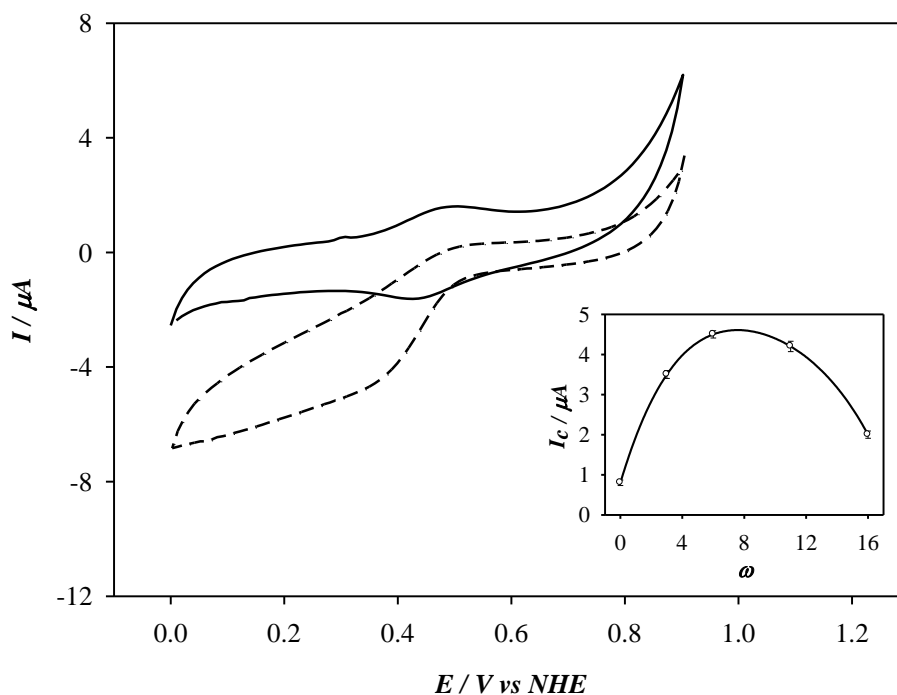


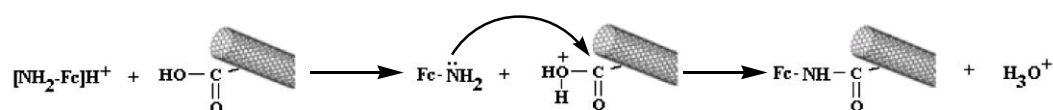
Figure 7.8 CVs of 6-ferrocenyl-1-aminohexane in absence (solid line) and in presence (dashed line) of Laccase from *Trametes versicolor*. Experimental conditions: citrate buffer 0.1 mol L^{-1} (pH 5.0), $T = 25 \text{ }^\circ\text{C}$, scan rate of 10 mV s^{-1} . Inset: catalytic current vs ω .

As it can be seen from Figure 7.8, in the presence of enzyme a current due to the catalytic oxidation of the ferrocene derivative by Laccase, is observed, which subsequently regenerates its active site by reaction with molecular oxygen and therefore can initiate a new cycle.

So far, the study carried out with the soft landing technique, using the aminoferrocene derivatives, has demonstrated that small molecules can be immobilised on electrode surfaces. Now, it will be tempting to hypothesise for the first time a possible mechanism with which the reactive landing between projectile ion and surface takes place. Any attempt to attach a ferrocene derivative on the electrode surface by soft landing, generating

the molecular ions in atmosphere of N₂, have failed as at the same time failed also every experiment carried out by colliding protonated ions on untreated MWCNTs electrodes (i.e. without carboxyl functionalisations). In these cases, the cyclic voltammetry analysis of the MWCNTs-SPEs showed only a low current during the first voltammetric scans, which disappeared quickly. This clearly shows that ions are deposited on the electrode surface but they are not covalently bind when soft landed in the absence of either protons in gas phase and carboxyl groups present on the nanotubes.

These data allow to hypothesise a general outline for the mechanism of an acid catalysed reactive landing that led to the formation of an amide bond when protonated amine compounds are sent to surfaces functionalised with carboxylic groups in vacuum (Scheme 7.1).



Scheme 7.1 Hypothesised mechanism for reactive landing

The first step of the reaction could be an endothermic proton transfer from the amino group of the projectile molecule (more basic) to a carboxyl function on the surface of nanotubes. The excited ion, generated under the conditions of chemical ionisation, requires a smaller contribution of translational energy to overcome this barrier, while more kinetic energy is needed to the ion produced by electrospray ionisation. The protonated carboxyl group, generated in the first step, now is activated and could undergo a nucleophilic attack by the nitrogen lone pair to form an amide bond, with the concomitant release of a water molecule.

7.4 Conclusions

The technique of ion soft landing is an excellent means for proteins immobilisation on solid surfaces functionalised with carboxylic groups, such as SAM-COOH or activated carbon nanotubes. The use of this procedure allows to avoid any type of protein purification.

In this work the technique of ion soft landing has been applied to small redox molecules, i.e. ω -ferrocenyl-1-aminoalkanes, to highlight certain aspects: i) the validity of the assumption that an amino group must necessarily be in the projectile molecule, ii) the ability of these compounds to mediate an enzymatic reaction after immobilisation and iii) to try to hypothesise the mechanism of reactive landing. The success that was achieved in the immobilisation of these substances suggests that there is really need of an amino group in the projectile molecule to react with a COOH-covered surface. Moreover, the experimental data, discussed above, allowed to formulate a possible mechanistic scheme for the reactive landing. This proposed mechanism, which at first seems to be obvious, it is far from be so, because this reaction occurs in the gas phase under reduced pressure and in such conditions the projectile molecule has a translational energy capable of giving rise to a new bond without any catalyst. However, experiments conducted in absence of the protonated amino group did not produce any results, therefore it is reasonable to think that the acid catalysis plays a key role in this surface-molecule reaction.

Finally, experiments carried out with ferrocene-modified electrodes in the presence of Laccases from *Trametes versicolor* have shown that these compounds are able to mediate an enzymatic reaction after being immobilised by soft landing.